

STATUS OF THESIS

Title of thesis

**Development of Analytical Tool for Energy Audit of
Cogeneration plant (ATEAC)**

I PHILIP WADEN AUGUSTINO YONGO

hereby allow my thesis to be placed at the Information Resources Center (IRC) of
Universiti Teknologi PETRONAS (UTP) with the following conditions:

1. The thesis becomes the property of UTP
2. The IRC of UTP may make copies of the thesis for academic purposes only.
3. This thesis is classified as

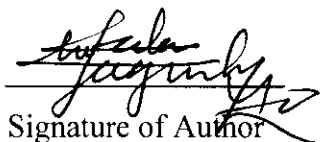
Confidential

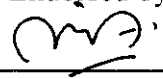
Non - confidential

If this thesis is confidential, please state the reason:

The contents of this thesis will remain confidential for _____ years.

Remarks on disclosure:


Signature of Author

Endorsed by

Signature of Supervisor

Permanent Address

Juba/Sudan

Name of supervisor

Dr. Zainal Ambri Bin Abdul Karim

Date: 20 May 2010

Date: 20 may 2010

ABSTRACT

Energy audit and management of a plant can be considered as a systematic approach to maintain the performance of a plant at high efficiency. The tedious task of energy audit of a cogeneration plant can be undertaken by aid of the analytical method which represents the working principles of the respective equipment used in a plant. The performance of the plant can be inefficient due to energy misusage and energy lost and hence, identifying the operating parameters that cause energy losses and misusage can be the technique for management of a cogeneration plant. This research discusses an analytical method for energy audit of an existing cogeneration plant in Universiti Teknologi PETRONAS (UTP). The analytical models were developed for the gas turbine engine, heat recovery steam generator, steam absorption chiller, air cooled chiller, cooling tower, and thermal energy storage. The study involves the investigation of the energy lost and imbalances within the systems which degrade the performance of the cogeneration plant. The models were defined based on the principles of thermodynamics, mass and energy balance. The analytical models were implemented using Matlab7.1 and the results were validated to that of the actual operating data.

The results show that the analytical models developed are able to represent the operating principles of all the systems in the plant. It was found that the performance of the plant is not at optimum operation due to losses in the components of the plant. The energy loss in the sub-systems of the cogeneration plant is found to be 35.23%. The energy loss in the components of steam absorption chiller is 77.15% of the total energy lost inside the components. The energy loss in air cooled chiller is found to be 70.6% of the total energy loss. The energy losses in the cooling tower due to evaporated mass and convection heat transfer are 5.41% and 94.6% respectively. The

energy losses in the thermal energy storage are found to be 5-22.4% of the total energy lost in thermal energy storage. The analytical models also enable strategies for optimization of the plant. Reduction in the amount of losses can be observed when selected operating parameters are changed. It was found that by decreasing the inlet temperature to the air compressor by 1-1.5 K, the net work of the turbine increases by 0.11-0.2%. In the air cooled chiller condenser, the energy loss can be decreased by 5.74-7.3% when the inlet air temperature is decreased by 1-1.5 K. In the cooling tower, the energy lost by evaporated mass can be decreased by 1.01-1.5% at the same inlet air temperature.

The analytical model can be used as a tool for energy audit and management of the cogeneration plant. The energy conservation can be identified by quantifying the percentages of energy losses in each component. The performance of the cogeneration plant can be maintained at optimum by monitoring the operating parameters at optimum levels.

ABSTRAK

Audit dan pengurusan tenaga sesebuah loji boleh diistilahkan sebagai satu pendekatan sistematik untuk mengekalkan prestasi sebuah loji pada kecekapan yang tinggi. Kesukaran dalam pelaksanaan audit tenaga di loji penjanaan bersama boleh dipermudahkan dengan bantuan kaedah analisis yang mewakili prinsip kerja bagi peralatan masing-masing yang digunakan dalam sebuah loji. Prestasi loji itu boleh menjadi tidak cekap oleh kerana penyalahgunaan dan kehilangan tenaga. Maka, operasi mengenalpasti sebab-sebab kehilangan tenaga dan salahguna boleh menjadi teknik untuk pengurusan satu loji penjanaan bersama. Penyelidikan ini membincangkan tentang kaedah menganalisis audit tenaga bagi loji penjanaan bersama yang sedia ada di Universiti Teknologi Petronas (UTP). Model-model analisis dibangunkan untuk enjin gas turbin, penjana stim pemulihan haba, pendingin penyerapan stim, pendingin pengudaraan sejuk, menara pendingin, dan alat penyimpanan tenaga haba. Kajian ini melibatkan siasatan keatas kehilangan tenaga dan ketidakseimbangan didalam sistem-sistem yang mengurangkan prestasi loji penjanaan bersama. Model-model ini dilaksanakan menggunakan pengaturcaraan matlab and keputusan yang diperolehi telah disahkan melalui perbandingan dengan data operasi sebenar daripada loji berkenaan.

Keputusan menunjukkan bahawa prinsip operasi alatan didalam loji dapat diwakili oleh model-model analisis yang dibangunkan. Adalah di dapati, prestasi sesebuah loji tidak berada pada tahap optimum disebabkan oleh kehilangan tenaga dalam komponen-komponen loji tersebut. Kehilangan tenaga didalam subsistem di sesebuah loji penjanaan bersama telah dijumpai menjadi 35.23%. Kehilangan tenaga didalam komponen sistem pendingin penyerapan stim adalah 77.15% daripada jumlah kehilanagn tenaga loji manakala bagi pendingin pengudaraan sejuk, kehilanagn tenaga

dijumpai sebanyak 70.6% daripada jumlah kehilangan tenaga. Kehilangan tenaga bagi menara pendingin yang disebabkan oleh penguapan jisim dan penghantaran pemanasan haba adalah 5.41% dan 94.6% masing-masing. Kehilangan tenaga bagi alat simpanan tenaga haba dijumpai sebanyak 5-22,4% daripada jumlah kehilangan tenaga di dalam komponen tersebut. Analisis model juga membenarkan strategi untuk kenaikan tarafan sesebuah loji. Pengurang dari segi jumlah kehilangan tenaga boleh diperhatikan apabila sesuatu parameter operasi berubah. Adalah juga didapati, penurunan suhu masukan pemampat udara dari 1-1.5 K, meningkat kerja bersih pada engine turbin sebanyak 0.11%-0.2%. Kehilangan tenaga pada pemeluwapan pengudaraan sejuk berkurangan sebanyak 5.74-7.3% apabila suhu udara masukan dikurangkan sebanyak 1-1.5 K. Di dalam menara pendingin, kehilangan tenaga disebabkan oleh jisim pemeluwapan, boleh dikurangkan sebanyak 1.01%-1.5% pada suhu udara masukan yang sama.

Analisis model boleh digunakan sebagai alat untuk audit tenaga dan pengurusan di loji penjanaan bersama. Pemeliharaan tenaga boleh di kenal pasti dengan mengukur peratusan kehilangan tenaga untuk setiap komponen. Prestasi untuk loji penjanaan bersama boleh dikekalkan pada tahap optimum dengan mengawasi selia parameter operasi pada tahap optimum.

In compliance with the terms of the copyright Act 1987 and the IP policy of the University, the copyright of this thesis has been reassigned by the author to the legal entity of the University,

Institute of technology PETRONAS Sdn Bhd.

Due to acknowledgement shall always be made of the use of any material contained in, or derived from, this thesis.

© PHILIP WADEN AUGUSTINO YONGO, 2010

Institute of Technology PETRONAS Sdn Bhd.

All rights reserved.

TABLE OF CONTENTS

STATUS OF THESIS.....	i
APPROVAL PAGE.....	ii
TITLE PAGE.....	iii
DECLARATION OF THESIS.....	iv
ACKNOWLEDGEMENT.....	v
ABSTRACT.....	vi
ABSTRAK.....	viii
COPYRIGHT.....	x
TABLE OF CONTENTS.....	xi
LIST OF TABLES.....	xv
LIST OF FIGURES.....	xvi
PREFACE.....	xx
NOMENCLATURES.....	xxii

CHAPTER

1. INTRODUCTION.....	1
1.1 Energy audit.....	1
1.2 Analytical tool for energy audit of cogeneration..... plant (ATEAC).....	2
1.3 Problem statement.....	4
1.4 Objectives of the research.....	4
1.5 Scope of study.....	4
1.6 Thesis overview.....	5
2. LITERATURE REVIEW.....	6
2.1 Energy audit and management.....	7
2.2 Checklist in Energy Audit.....	8

2.3	Energy quantities.....	8
2.4	Bandwidth analysis.....	9
2.5	Accountability of energy in a cogeneration plant.....	9
2.6	Energy model.....	10
2.7	Sustainability of energy management program.....	10
2.8	Tools for energy measurements.....	11
2.9	Researches on analytical model of a cogeneration plant.....	12
2.10	Researches on modeling and simulations of a..... cogeneration plant.....	15
2.11	Researches on parametric studies of a cogeneration..... plant.....	18
3.	SYSTEMS ENERGY MODELS.....	24
3.1	Introduction.....	24
3.2	Gas district cooling plant (GDC).....	24
3.3	Gas turbine engine (GTE).....	25
3.3.1	Air compressor energy model.....	28
3.3.2	Combustion chamber energy model.....	29
3.3.3	<i>Turbine energy model</i>	31
3.4	Heat recovery steam generator (HRSG).....	34
3.4.1	HRSG evaporator energy model.....	36
3.4.2	HRSG economizer energy model.....	37
3.5	Steam absorption chiller (SAC).....	39
3.5.1	Steam absorption chiller (SAC) model.....	42
3.5.2	Absorber energy model.....	42
3.5.3	High temperature generator (HTG) energy model....	43
3.5.4	Condenser energy model.....	43
3.5.5	Evaporator energy model.....	43
3.6	Air cooled chiller (ACC).....	46
3.6.1	Air cooled condenser model.....	47
3.6.2	Air cooled chiller evaporator model.....	48

3.6.3	<i>Screw compressor model</i>	48
3.7	Cooling tower.....	50
3.7.1	Cooling tower energy model.....	52
3.8	Thermal energy storage (TES) model.....	57
3.9	The simulation of the cogeneration plant.....	60
4.	RESULTS AND VALIDATION OF THE MODELS.....	62
4.1	Validation of the models.....	62
4.2	Results from gas turbine engine model analysis.....	65
4.2.1	Energy lost in air compressor.....	68
4.2.2	Energy lost in combustion chamber.....	69
4.2.3	Heat energy lost in turbine.....	70
4.2.4	Net work and part load ratio.....	71
4.3	Results from heat recovery steam generator (HRSG).....	
	model analysis.....	72
4.3.1	Heat lost in HRSG evaporator.....	75
4.3.2	Heat lost in HRSG economizer.....	75
4.3.3	<i>Energy quantities in HRSG</i>	76
4.4	Results from steam absorption chiller (SAC) model.....	
	analysis.....	77
4.4.1	Heat lost in SAC components.....	78
4.5	Results from air cooled chiller (ACC) model analysis.....	82
4.5.1	Heat lost in ACC components.....	83
4.5.2	Heat lost in ACC condenser.....	84
4.5.3	<i>ACC evaporator performance and heat losses</i>	85
4.6	Results from cooling tower model analysis.....	88
4.7	Results from thermal energy storage (TES) model.....	
	analysis.....	92
4.7.1	Cooling load lost in TES.....	93
4.7.2	Effect of returned chilled water on discharge.....	
	load in TES.....	94

4.8	The overall analysis of GDC plant.....	95
5	CONCLUSIONS AND FUTURE WORK.....	101
5.1	Conclusions.....	101
5.2	Gas turbine engine and HRSG.....	101
5.3	Steam absorption chiller (SAC).....	102
5.4	Air cooled chiller (ACC).....	103
5.5	Cooling tower.....	103
5.6	Thermal energy storage (TES).....	104
5.7	Future work.....	104
	APPENDIX.....	105
	REFERENCES.....	107

LIST OF TABLES

Table 3-1:	Operating and nominal parameters of the gas turbine.....	
	Engine.....	27
Table 3-2:	Operating and nominal parameters of HRSG.....	35
Table 3-3:	Operating and nominal parameters of steam absorption chiller (SAC).....	41
Table 3-4:	Operating and nominal parameters of air cooled chiller (ACC).....	47
Table 3-5:	Design and operating parameters of the cooling tower.....	52
Table 3-6:	Design and operating parameters of TES.....	57
Table 4-1:	Calculated parameters and actual operating parameters of the TES.....	65
Table A-1:	Operating parameters of the gas turbine engine.....	105
Table A-2:	Calculated and operating parameters of the gas turbine engine.....	106

LIST OF FIGURES

Figure 2.1:	Bandwidth analysis of air compressor work (kJ/s) at inlet ... temperature (K).....	9
Figure 3.1:	The schematic cycle of gas district cooling plant (GDC).....	25
Figure 3.2:	Gas turbine engine	26
Figure 3.3:	Schematic diagram of the gas turbine engine.....	27
Figure 3.4:	Schematic diagram of air compressor.....	28
Figure 3.5:	Schematic diagram of the combustion chamber.....	30
Figure 3.6:	Schematic diagram of the turbine	31
Figure 3.7:	Computer diagram flow chart for gas turbine system.....	33
Figure 3.8:	Heat recovery steam generator system (HRSG).....	34
Figure 3.9:	Schematic system of HRSG	35
Figure 3.10:	Schematic diagram of HRSG evaporator.....	36
Figure 3.11:	Schematic diagram of HRSG economizer.....	37
Figure 3.12:	Heat recovery steam generator computer flow chart.....	39
Figure 3.13:	Double-effect direct-fired steam absorption chiller.....	40
Figure 3.14:	Schematic diagram of double-effect parallel flow SAC.....	41
Figure 3.15:	SAC computer program flow chart.....	45
Figure 3.16:	Schematic cycle of air cooled chiller.....	47
Figure 3.17:	Air cooled chiller computer program flow chart.....	50
Figure 3.18:	Schematic diagram of an induced draft, wet counter	
	flow cooling Tower.....	51
Figure 3.19:	Schematic diagram of induced draft cooling tower.....	52
Figure 3.20:	Cooling tower computer program flow chart.....	56
Figure 3.21:	Cross-sectional side of TES.....	58
Figure 3.22:	Thermal energy storage computer program flow chart.....	60
Figure 3.23:	Schematic diagram for systems in GDC.....	61
Figure 4.1:	Net work (kW) against part load ratio	62

Figure 4.2:	Steam mass flow rate (kg/s) against heat gained by steam (kJ/s).....	63
Figure 4.3:	Actual and calculated COP against cooling load (kJ/s).....	64
Figure 4.4:	Cooling load (kJ/s) against mass flow rate of steam (kg/s)....	64
Figure 4.5:	Power (kW) against fuel flow rate (kg/s).....	66
Figure 4.6:	Actual power (kW) against the air inlet temperature (K).....	67
Figure 4.7:	Calculated power (kW) against the air inlet temperature (K).....	67
Figure 4.8:	Heat energy lost (%) against gas turbine components.....	68
Figure 4.9:	Heat energy lost (%) in air compressor against air inlet temperature (K).....	69
Figure 4.10:	Heat energy lost in combustion chamber (%) against air mass flow rate (kg/s).....	70
Figure 4.11:	Heat energy(kJ/s) entering turbine against turbine energy lost (kJ/s).....	71
Figure 4.12:	Net work (kW/s) against part load ratio	72
Figure 4.13:	Heat energy lost (%) against heat quantity in..... HRSG Components.....	73
Figure 4.14:	Heat energy (%) against mass of the steam (kg/s)	73
Figure 4.15:	Heat energy (%) against mass of warm water	74
Figure 4.16:	Heat energy lost in evaporator (%) against heat gained	75
Figure 4.17:	Heat energy lost in economizer (%) against heat gained by ... warm water (kJ/s).....	76
Figure 4.18:	Heat energy quantities in the HRSG.....	77
Figure 4.19:	Heat energy lost (%) against the components of SAC	79
Figure 4.20:	Heat rejected by condenser and absorber (kJ/s) against	80
	cooling load (kJ/s).....	

Figure 4.21:	Heat energy lost (kJ/s) in condenser and absorber against heat imbalance in SAC system (kJ/s).....	80
Figure 4.22:	Heat energy lost (kJ/s) against mass flow rate of the..... refrigerant (kg/s).....	81
Figure 4.23:	Heat energy lost (%) against heat imbalance in SAC (kJ/s)....	82
Figure 4.24:	Heat energy lost (%) against COP.....	83
Figure 4.25:	Heat energy lost (%) in air cooled condenser against air inlet temperature (K).....	84
Figure 4.26:	Heat energy lost in air cooled condenser (kJ/s) against heat... removed (kJ/s).....	85
Figure 4.27:	Cooling load (kJ/s) against COP.....	86
Figure 4.28:	Heat energy lost (kJ/s) in ACC evaporator against COP.....	87
Figure 4.29:	Heat energy lost (kJ/s) in ACC evaporator against..... cooling load.....	87
Figure 4.30:	Heat energy lost (J/s) against air mass flow rate (kg/s).....	89
Figure 4.31:	Convection heat lost (J/s) against air mass flow rate (kg/s)....	89
Figure 4.32:	Heat energy lost by evaporation (J/s) against evaporated mass (kg/s).....	90
Figure 4.33:	Heat energy lost by evaporated mass against evaporated mass (kg/s).....	91
Figure 4.34:	Convection heat lost (J/s) against air mass flow rate (kg/s)....	92
Figure 4.35:	Actual cooling load of TES (kJ/s) against time (hr).....	93
Figure 4.36:	Cooling load lost (%/hr) against Figure of Merit (FoM).....	94
Figure 4.37:	Discharge load (kJ/s) against return chilled water temperature (K).....	94
Figure 4.38:	Heat energy lost (kW) in GTE against turbine inlet temperature (K).....	95
Figure 4.39:	Heat gain by the steam in HRSG (kW) against turbine inlet temperature (K).....	96
Figure 4.40:	Mass flow rate of steam in HRSG (kg/s) against turbine inlet temperature (K).....	97

Figure 4.41:	Cooling load in steam absorption chiller (kW) against mass..... flow rate of steam (kg/s).....	98
Figure 4.42:	Air inlet temperature (kg/s) against un-rejected heat in air cooled condenser (%).....	98
Figure 4.43:	TES charging load (kW) against chilled water mass flow rate (kg/s).....	99
Figure 4.44:	Warm water temperature (K) against rejected heat by cooling tower (Watt).....	100

PREFACE

The aim of this research is to present a methodology for energy audit of a cogeneration plant, thus, energy audit can provide a substantial improvement in operation of a cogeneration plant, i.e. energy losses can be investigated by the methodology presented and the outcome can results into upgrading the performance of the cogeneration plant. Cogeneration plant shows a significant performance due to its sufficient usage of energy, as energy from the exhaust turbine engine been use as source of energy to the heat recovery steam generator (HRSG). The proper usage of energy in the systems attributed to a cogeneration plant shows the fact that; a cogeneration plant is system that works under the concept of energy audit and management.

Energy audit is valuable in energy engineering because of its utmost importance of finding the means of upgrading the engineering systems at low cost. The application of energy audit concept is been carried out traditionally for decades, where energy in the components of a system is measured during the preliminary audit. And detail energy audit is carried out after the preliminary audit results. Based on the concept of energy audit an analytical tool for energy audit of a cogeneration plant is proposed in this research and is applied in an existing cogeneration plant. The concept of the tool is basically accomplished based on the first law of thermodynamics, where mass and energy balance in the systems of a cogeneration plant is derived and implemented on a written scripts file in computer program Matlab 7.1. The analytical tool presented shows a significant role in monitoring the mass and energy balance in a cogeneration plant. Energy losses in the components of a cogeneration plant is revealed and discussed accordingly. The energy losses degrade the performance of a cogeneration plant; hence, the main aim of cogeneration plant cannot be accomplished as energy losses occur in the components of the plant.

The analytical tool presented can be of significance to a cogeneration plant energy analysis due to a lacked of a proper analytical tool for detail energy audit of a cogeneration plant. Energy audit and management of an industrial sector has been

carried out by application of a traditional energy audit for decades. Some tools for energy management of industrial sectors have been presented. However, an analytical tool for energy audit of a cogeneration plant has not been developed before, thus, prior to develop an analytical tool for energy audit of a cogeneration plant, where the aim of a cogeneration plant can be maintained.

NOMENCLATURES

C_p	specific heat capacity (kJ/kg K)
COP	coefficient of performance
EC	economizer
EV	evaporator
h	specific enthalpy (kJ/kg)
h_c	coefficient of heat transfer by convection
h_m	coefficient of mass transfer
HRSG	heat recovery steam generator
HEX	high temperature heat exchanger
LEX	low temperature heat exchanger
LHV	low heating value (kJ/kg K)
\dot{m}	mass flow rate (kg/s)
n	polytropic expansion index
P	pressure (bar)
PLR	part load ratio
\dot{Q}	heat flow rate (kJ/s)
r_c	compression ratio of gas turbine
S	solution
SAC	steam absorption chiller
T	temperature (K)
TET	turbine exhaust temperature (K)
V_{eff}	volumetric efficiency
V_d	volumetric displacement
\dot{w}_t	turbine work (kW)
\dot{w}_{net}	net work of the gas turbine (kW)

GREEK SYMBOLS

η_c	isentropic efficiency of air compressor
η_{cc}	efficiency of combustion chamber
η_t	isentropic efficiency of turbine
γ	specific heat ratio
η_{mc}	mechanical efficiency of screw compressor
η_m	efficiency of motor in screw compressor

SUBSCRIPTS

a	air
ab, cw	absorber cooling water
ab, r	absorber refrigerant
ab, los	absorber lost
a, o	air out
c	air compressor
cc	combustion chamber
$cdcw$	condenser cooling water
$cdlos$	condenser lost
cdr	condenser refrigerant
chw	chilled water
$comp$	refrigerant compressor
csa	concentrated solution absorber
$cs hg$	concentrated solution high temperature generator
$cs lg$	concentrated solution low temperature generator
cwo	cooling water out let
d	drain
ec	economizer
ev	evaporator

<i>evchw</i>	evaporator chilled water
<i>evlos</i>	evaporator lost
<i>f</i>	fuel
<i>fg</i>	flue gases
<i>g</i>	hot gases
<i>GTE</i>	gas turbine engine
<i>hgd</i>	high generator drain
<i>hglos</i>	high generator lost
<i>hgr</i>	high generator refrigerant
<i>i</i>	inlet
<i>lc</i>	cooling load
<i>ls</i>	diluted solution
<i>r</i>	refrigerant
<i>s</i>	supply
<i>sw</i>	saturated water
<i>t</i>	turbine
<i>v</i>	vapor
<i>v_{hg}</i>	vapor high temperature generator
<i>v_{lg}</i>	vapor low temperature generator
<i>w, i</i>	water inlet
<i>w, o</i>	water out
<i>ws</i>	water solution
<i>ww</i>	warm water
a, b, c,.....	State points at ACC
1, 2, 3.....	state points at SAC

CHAPTER 1

INTRODUCTION

1.1 Energy audit

Energy audit is defined as the quantification of energy losses and energy misuse for identification of energy conservation in a utility [1]. The purpose of accomplishing this research is to develop a methodology that can be used as an analytical tool in energy audit and management of a cogeneration plant. The methodology proposed and implemented in this study is known as analytical tool for energy audit of cogeneration plant (ATEAC). Undertaking energy audit and management of a plant enables the operator to maintain optimum performance of the plant and hence, reduce the misuse of energy that can be wasted unnecessarily.

The levels of undertaking energy audit can be categorized as preliminary audit, detail audit and feasibility audit [2]. *Preliminary audit* is an initial start of energy audit, where data collection and specification of energy conservation can be pinpointed. The collected data during preliminary audit is used in energy detail audit. *Detail audit* is the analysis of the measured data from the specific utility to be audited and after the data analysis, the area of energy conservation can be identified and energy management can be established. *Feasibility audit* is the economical measures that can be accomplished after the preliminary and detail audit. It is the economical evaluation of the energy consumption, where unnecessarily energy consumption can be managed and components that are malfunctioning or consuming high energy rate can be replaced with optimum components.

After carrying out energy audit of a utility, appropriate measures can be implemented to reduce energy consumption to a feasible cost. Although energy audit has been carried out in many utilities, the methodology of undertaking energy audit is not unified; hence the energy audit is always the same. Most of the thermal systems that operate in a utility are not analyzed based on detail energy audit concept.

However, the application of energy models can be a technique for monitoring the performance of thermal systems to operate at optimum levels. Without detail analysis of a system the energy management program cannot be established. The challenges that the energy auditor face during energy audit of a utility are as follow:

1. Formulation of equations for energy calculation and computation method
2. Identification of energy conservation area in a component
3. Time consumption during energy audit
4. Complexity of a utility

The challenges mentioned above can be overcome by

1. An analytical tool for energy analysis
2. Identification of specific parameters that show effect on energy variation
3. Clear description of the utility
4. Prescription of certain areas in a system to focus for energy conservation

For these reasons, the research is undertaken to design a detail energy audit by developing an analytical tool using an existing cogeneration plant in UTP as a source of operating data. The detail energy analysis of a cogeneration plant carried out gives the baseline for energy audit and management of the components in the system of a cogeneration plant. The energy management of a cogeneration plant can be achieved by controlling the input parameters that show effect on energy consumption. This analytical tool can resolve the challenges that are faced in energy analysis and management of a cogeneration plant.

1.2 Analytical tool for energy audit of cogeneration plant (ATEAC)

ATEAC can be used for identifying detail energy quantities for a given process in a component. The energy quantities can be as follow;

1. Energy input to the component for a given process
2. Energy lost in the waste
3. Energy recovery from the exhaust gases
4. Energy consumed for production

The analytical tool consists of energy models for measuring energy quantities in the components of a cogeneration plant. The analytical tool is developed based on the principle of thermodynamics energy and mass balance. The energy losses occur in the cogeneration plant are due to imbalances in energy quantities and variations of the operating parameters in various components of the systems. By representing these components' performances with energy and mass balance equations, the imbalances of energy in each component can be identified. Mismanagement of energy quantities such as fuel flow rate can increase the economical cost. Hence energy quantity must be controlled to minimize the cost. The analytical tool can be used as a technique for monitoring the energy quantities, where an opportunity for energy conservation can be acquired. The component energy models are implemented by a written script files in a matlab program. The results are then compared to the operating data of gas district cooling (GDC) plant. Since energy management is an initial approach to minimize energy cost in a utility, implementing energy management, results to the benefits listed below;

1. Optimizing energy usage and reducing cost of energy
2. Guiding the performance of the plant at optimum operation
3. Energy conservation can be pinpointed

One of the utmost requirements for vital implementation and operation of energy management is commitment to develop a top management program. Otherwise the developed program will not reach its aims. Energy manager is the one responsible for the absolute implementation of the developed program.

1.3 Problem statement

Plants such as a cogeneration experience continuous energy losses during operation due to several reasons. The investigation of these causes requires huge resources such as time and man hours. Energy audit of the plant can be eased by developing an analytical tool for energy audit and management of cogeneration plant. The analytical tool would enable real-time monitoring of the components performance and implementation of corrective measures in order to operate the plant at its optimum performance.

1.4 Objectives of the research

1. To develop an analytical method for investigation of energy losses in a cogeneration plant
2. To identify the effective parameters that can be used to control energy consumption in a cogeneration plant
3. To develop a computer program for energy auditing of a cogeneration plant

1.5 Scope of study

The scope of this research is to develop an analytical tool which can be used for energy audit and management of a cogeneration plant which exists in UTP. The analytical tool is accomplished in a computer program which is written in a matlab program. Computer script files are written based on the corresponding component energy model derived from the energy and mass balance equations. The systems in the cogeneration plant that is analyzed by the analytical tool include the gas turbine engine, heat recovery steam generator, steam absorption chiller, air cooled chiller, cooling tower and thermal energy storage tank. The analytical tool is validated by the collected data records from the cogeneration plant, where the actual data is correlated with the computed results from the computer program. The performance optimization of the cogeneration plant is clarified by the analytical tool developed.

1.6 Thesis overview

In the introduction chapter the energy audit and management are introduced including the analytical tool that is developed and its application in energy audit of cogeneration plant. Importances of the analytical tool are clarified and the usefulness of the tool is also highlighted. The objectives of the research and the scope of study are also outlined in this chapter.

The background of cogeneration plant and the related literature review is described in the second chapter. In chapter three, development of energy models are explained in details for all the components. Various assumptions and simplifications that were considered in writing the equations are stated. Flow charts for development of the computer program of each component are also drawn. The systems are all represented in schematic diagrams where the mass and energy equations are accomplished.

The results are discussed in chapter four and the effects of energy quantities on components performance are graphed. The effect of air, water, and steam mass flow rate are shown in the performance of the systems. Graphs which show validation of the energy component models are shown. The performance of the gas turbine engine is shown based on actual data collected. Energy losses in the components are discussed based on percentages.

In chapter five, the conclusions are drawn based on the results obtained by the analytical model developed. The analytical model showed its utmost importance in energy audit and management of cogeneration plant. The analytical models enable to identify energy quantities, such as energy losses, energy input and output. Iteration of some operating parameters during analysis identified some parameters which show their effect on performance of the components. The application of the analytical tool developed can be useful for real-time energy audit and management of a cogeneration plant. Hence, it can be the means for optimization of a cogeneration plant.

CHAPTER 2

LITERATURE REVIEW

Numerous researches had been worked on cogeneration plants, combined cycles, and power plants can be found in the literature. The objectives are to enhance the performance of the cogeneration plant or combined cycle plant. Although the methodologies used by researchers in cogeneration analysis are not absolutely energy audit level applications, the method they used can be a guideline to energy auditors. Cogeneration technique of simultaneous production of power and heat or chilled water can be seen as energy audit concept, where complete usefulness of fuel is attained and heat energy is recovered. The refrigeration systems which are installed in GDC plant are operated to produce chilled water that is used in cooling purposes in the buildings. Heat recovery steam generator (HRSG) supply steam as the source of heat energy for chilled water production in steam absorption chiller (SAC).

Energy analysis of refrigeration systems is a technique for finding improvement of the performance in the system. Researches on refrigeration systems aim to optimize the systems and to provide guidelines in designing them. Two types of refrigeration systems that produce chilled water for space cooling considered here are (SAC) and air cooled chiller (ACC).

The purpose of cooling tower is for cooling purposes of the circulating water of absorption chiller. The performance of cooling tower is characterized by range, approach temperature difference and thermal efficiency [3]. Many research on cooling tower has been accomplished, however there is still scope for research on cooling tower. The most important of all the researches is on the maintenance and operation management of the cooling tower.

Chilled water is stored in the thermal energy storage (TES) by the air cooled chiller during the off peak period. This process of storing the chilled water is known as charging load. Chilled water at on-peak will be delivered for air conditioning purposes to the buildings in UTP campus during the discharging process. The capacity management of the TES is one of the main tasks to be monitored so that energy misusage can be minimized.

2.1 Energy audit and management

Energy audit and management is one of the techniques for maintaining the performance of the thermal systems at optimum performance [4]. The quantification of energy losses and energy misusage, for identification of energy conservation in a utility is the technique for accomplishing energy audit [5, 6]. Researches done on energy audit and management are neither widely available nor accessible in thermal engineering systems. Several work are presented on optimization of cogeneration plant, where the target is on the efforts of changing the operating parameters.

Energy audit and management became utmost important in facilities to address the misuse and losses of energy which result in poor performance of the plant. Checklist and guidelines, though been the tools for achieving energy conservation in utilities, their application is time consuming and expensive. Several analytical tools have been proposed and implemented on thermal systems. Robert [2] developed a tool for manufacturing process management and named it as exergy ratio diagnostic tool (ERDT). While Bhatt [7, 8] developed an analytical method for steam systems and air conditioning systems. Although analytical tools are presented on guidelines for energy audit implementation, it still requires knowledge on engineering thermodynamics. Checklist on the other hand is more straight forward and could be used as an alternative to the analytical tool.

2.2 Checklist in energy audit

Energy audit by checklist is accomplished by visiting the utility to be audited, where operating components are identified and components are classified by the energy quantities from least to the maximum energy consumption of each component. Identification of obvious energy losses in steam and hot gases piping, and leakages of air, fuel and coolant are the preliminary audit of the facility. After the preliminary audit is done, the second level carried out is the detail energy audit. It is done by determining the major operating parameters that shows their effect on energy consumption for overall energy usage in a certain area. Identification of the operating parameters which show their effect on energy usage are accounted for and used for energy conservation where total energy consumption in a given component can be reduced.

2.3 Energy quantities

Energy input is the amount of energy supplied to the component to produce work or other forms of energy. In most instances, energy inputs are not completely used due to losses in the components or devices. *Energy loss* is the amount of energy which is not used during component work. Energy loss occurs due to incomplete heat exchange between the working fluid and the gases in the components. The work of the component increases as the energy losses decrease, which can lead to increase of performance of the component. Awareness in energy quantity for a given component can be the guideline for energy management in the component.

Energy balance is the amount of energy supplied to the component which is equal to the energy output, energy gain, and energy lost in the component. Identification of energy quantities in components by ATEAC can be the method for regulating the performance of the component in a given system.

The Significances of energy auditing that can overcome energy challenges in energy field based on energy cost and environmental point of view is as follows [2].

1. Energy cost can be decreased

2. Facility performance can operate at optimum
3. Economical feasibility can be attained in a facility
4. Environmental pollution due to exhaust gases can be reduced

2.4 Bandwidth analysis

Bandwidth analysis is a technique where two different utilizations of energy are compared and the difference is analyzed for improvement of the system or components. The concept of bandwidth can be applied for example, in air compressor performance [2]. The air compressor work is compared at two different inlet temperatures where the rate of energy consumption in air compressor is varies at different temperatures as shown in the Figure 3.25. At two different work attained in the air compressor, its optimum performance can be managed based on the bandwidth identified and its obvious optimum operation range. The comparison of the component's performance by implementing bandwidth technique is one of the methods in energy audit and management of the system.

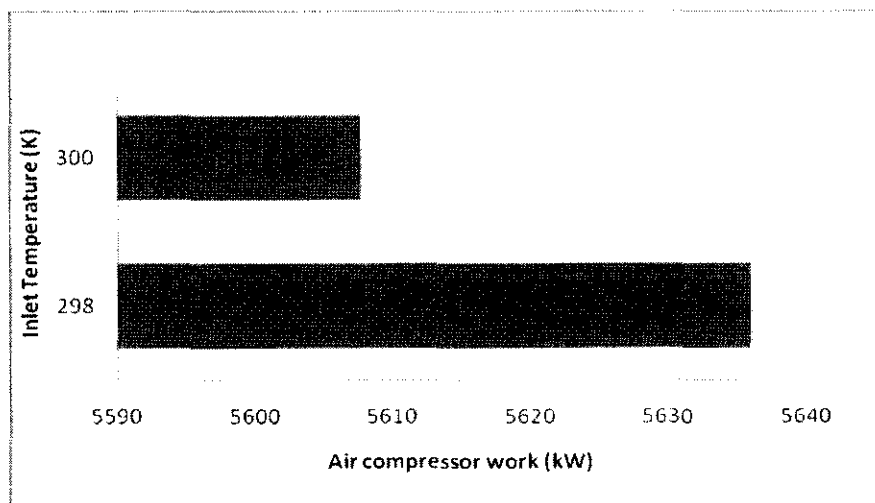


Figure 2.1: Bandwidth analysis of air compressor work (kJ/s) at inlet temperature (K) [2]

2.5 Accountability of energy in a cogeneration plant

Vital approaches in energy management and conservation is the measuring and accounting of energy consumption. Energy accounting is the technique used to trace the level of energy consumption and costs [4]. Energy accountability is utmost

important for the energy audit of a utility. The accountability can be accomplished by a written computer program. Accounting of energy flow in a system is the method to monitor energy variation in a system and thus energy management of the components.

The economical feasibility of a given thermal system can be achieved by the engineering model developed for energy quantification. The accountability of the energy quantity in HRSG is calculated by ATEAC. Energy accounted in the components of the plant varies from one component to other based on the quantity of energy consumption, losses and the complexity of the component. The correlation of the systems that can be developed usually varies between the rates of energy conservation that can be attained in a given system. The energy accountability can be done based on comparison of the data; usually the data obtained from the model is compared to the recorded data of the operating system.

2.6 Energy model

Energy model in a thermal system is a correlation developed to quantify energy in each component of the system, where the model can be used as a track for sustaining energy level at optimum performance in a system. Energy model developed in, ATEAC which is implemented in a cogeneration energy analysis, is accomplished based on computation of energy and mass balance concept of the related component. Energy model is advantageous as it can be used as a tool for identification of energy losses and misuse of energy in a system where accuracy and monitoring levels of energy consumption at optimum can be obtained [9].

2.7 Sustainability of energy management program

Energy management program requires a constant and continuous monitoring of the energy utilization in facility. It is therefore important for a plant to assign person who can be responsible for monitoring the program. If no single person is being assigned the responsibility of handling the energy program, it can be found out that the energy management program is given less importance than the rest of the job in a utility. Hence, the plant can be operated at high cost due to lack of energy optimization.

The success of energy management can be acquired by the following aspects.

1. A successful development of energy management tool
2. Commitment of the managers for energy management program
3. Visibility of the program

2.8 Tools for energy measurements

During energy audit of a facility, measuring devices are used to record important parameters of the system. After the measurement of energy consumption in the equipments, the detail analysis can be carried out [10]. The devices which are being used for energy audit of a facility are as follows.

1. *Voltmeter*: Used for measuring operating voltages on electrical equipments
2. *Wattmeter*: It is used for measuring power consumption and power factor for equipments such as motor and other devices
3. *Combustion analyzer*: This device is used for the analysis of combustion chamber efficiency for thermal systems such as gas turbine combustion chamber, furnace, boiler etc.
4. *Ultrasonic leak detector*: It is used for detecting air leakage through the hissing sound
5. *Airflow measurement device*: It is used for measuring airflow in pipes, ducts of air conditioner, the device includes velometer and anometer
6. *Blower door attachment*: This device is used in buildings, offices for detecting air leakage in to the building or air change per hour in the facility
7. *Smoke generator*: This device is used for detecting air filtration in buildings, offices, air leaking through the doors, windows, ducts etc, should be checked for any contaminants

8. *Tape measure*: It is used for determining the dimensions of the wall, ceiling, doors and windows and distances between the equipments where the pipe length of the energy transfer from equipment to another can be measured
9. *Thermometer*: This device is used for measuring temperature in offices and operating equipment
10. *Light meter*: It is used for measuring the illumination levels in a facility

2.9 Researches on analytical model of a cogeneration plant

Silveira and Tuna [11] presented an analytical model on thermo-economic analysis of cogeneration plant, based on minimization of operating cost such as exergetic production cost (EPC). They concluded EPC is a powerful tool of optimization in cogeneration context. The methodology of their work is almost the same the method used in this research.

Casarosa et al. [12] made analytical and numerical mathematical methods for optimization of HRSG, in a combined plant. The combined cycle efficiency is close to 60% when the HRSG is optimized as shown by the tool developed. Kong et al. [13] presented an energy optimization model for a combine cooling, heating, and power production (CCHP). They stated that the available engineering and statistical tools for energy problem of the CCHP cannot provide sufficient solutions. They came up with a linear programming model of the CCHP, to determine the optimal strategies that minimize the overall cost of energy of the system. They have shown that the optimal operation of the system depends on the cooling, heating, and electrical loads to be satisfied.

Bassily [14] presented an article on modeling, numerical optimization and irreversibility reduction in dual pressure reheat combined cycle. He described the constraint sets for pinch points and approach at minimum temperature difference. Other parameters considered are pressures and steam turbine inlet temperature. It is found that the optimized combined cycle increased by 1% in efficiency than the reduced-irreversibility combined cycle which increase by 2.5% in efficiency than the

regularly designed combine cycle. Yu and Chan [15] investigated an air cooled chiller for improving the performance of air condenser for more energy efficiency. They developed an analytical model to investigate how the COP changes with various set points of condensing temperature. They revealed that the optimum set point for maximum COP is a fraction of outdoor temperature and chiller load. They found that COP could increase by 12.1-110.4% when the variable speed condenser fans and optimum set point condensing temperature were applied to the air cooled screw chillers.

Chan and Yu [16] introduced a thermodynamic behavior model for air cooled screw chillers. They found that the chiller's COP can increase by up to 115% when the set point condensing temperature is adjusted, based on any given outdoor temperature. Yu and Chan [17] modeled air cooled chiller with variable speed condenser fans. They revealed that the chiller COP would increase by 4-127.5% when condenser temperature control and variable speed condenser fans are used together in the air cooled screw chiller. The annual electricity consumption can be reduced by 12.2-44 kWh/m². Sessaiah et al. [18] proposed a mathematical modeling of the working cycle of oil rejected rotary screw compressor. They found that heat transfer coefficient between gas and oil has been determined from experimental observation in which volumetric efficiency decreases with increase of inlet temperature.

Khan et al. [19] presented a model for a comprehensive design and performance evaluation study of counter flow wet cooling towers, and it is reported that the effectiveness of cooling tower degrades significantly with time indicating that for a low risk level there is about 6.0% decrease in effectiveness for their given fouling model. Jin et al. [20] made a simplified modeling of a mechanical cooling tower, for controlling and optimizing heating ventilation and air conditioning (HVAC) systems. They reported that the performance varies with time due to different operation and their model was able to accommodate changes by parameters tuning.

Facao and Oliveira [21] presented a correlation for heat and mass transfer for design of small indirect contact cooling tower. They found that their correlation lead to mass and heat transfer coefficients that are lower than the ones published for large

indirect contact cooling towers. They extended the model to evaluate the effect of the error associated to those coefficients on tower efficiency. Zalewski and Gryglaszewski [22] presented a mathematical model of heat and mass transfer processes in evaporative fluid coolers. The model was tested for Reynolds number of air $Re_p=5500-12000$ and Reynolds number of cooled liquid $Re_f=4000-10,000$ and spray density $G=0.01-0.021 \text{ kgm}^{-1}\text{s}^{-1}$.

Soylemez [23] proposed a model for optimum performance of forced draft counter flow cooling towers. They set optimum points for the performance of the cooling tower and they stated that the cooling tower must be operated close to the optimum set points. The model may be helpful for cooling tower designers, manufacturers, and users.

Stabat and Marchio [24] presented a simplified model for indirect contact evaporative cooling tower. The model can be used for estimation of energy and water consumptions under different operating conditions such as variable wet bulb temperatures. They compared their model with manufacturer catalogue data. The error in heat transfer is less than 10%. The standard deviation in heat transfer is 3.4% and the standard deviation in temperature is 0.17°C . Naphon [25] studied the characteristic of heat transfer in an evaporative cooling tower. They developed a mathematical model based on the conservation equations of mass and energy and solved by an iteration method to determine the heat transfer characteristic of the cooling tower. They observed that the mass ratio of water/dry air and the number of transfer unit increases moderately as the temperature ratio increase and rapidly as the temperature ratio reaches over 0.18.

Williamson et al. [26] presented a numerical simulation in a natural draft wet cooling tower. They found that a largely uniform velocity profile across the tower radius with the greatest non-uniformity occurs at the outer edge of the tower. The water outlet temperature was found to vary by 6K (~40%) between the tower center and exterior under reference tower conditions. This is largely due to the rise in air temperature and humidity through the rain zone. It is concluded that the model can predict the performance of the real time operating cooling tower. Lee and Jones [27] developed a model for analysis of ice storage tank. They reported that the external

heat transfer coefficient and return water temperature have significant effect on the bulk water temperature.

Chaichana et al. [28] made a computer model for ice thermal storage and they reported that application of the full ice thermal storage can reduce the electric energy consumption by 55% per month, and the total energy consumption by 5% for the selected building. Yimer and Adami [29] developed an analytical model to study and evaluate the parameters of phase change TES. They have shown that the charging rate and stored energy increase as the initial system temperature decreases, but penetration of the melting front is slower. The stored energy, charging rate, and melting front depth increase with increasing effective thermal conductivity of the melted medium caused by acceleration forces. The effect of liquid effective thermal conductivity is significant during the discharging mode. Energy storage and melting front depth increase with the tube diameter or outer shell diameter. It is also shown that fins application increases the heat stored and the melting front penetration.

MacPhee and Dincer [30] developed an analytical model for a packed bed TES for charging condition, and reported that at inlet temperature 269.7 K (84.3%) and 270.7 K (87.9%), a maximum flow exergy was found. The variation of exergy is 48% to 88% and energy efficiency varies from 90% to 99%. Badescu [31] developed a model for a stratified TES unit by means of three partial differential equations governing the time and space dependence of various temperature involved. They have shown that the performance indicator adopted is the minimum exergy destruction. They stated that the dependence of the exergy destruction number on the operation time in case of fully mixed TES units shows rather similar qualitative features as in the case of stratified storage tanks. They found that the overall heat transfer coefficient for the stratified TES units depends on time and space.

2.10 Researches on modeling and simulations of a cogeneration plant

Mostafavi et al. [32] presented on modeling and simulation of combined cycles and they revealed that there is sufficient amount of energy in the exhaust gases for pre-cooling purposes. The energy can be introduced to an absorption unit to produce

chilled water for space cooling in buildings. One technique being used to increase the performance of the gas turbine is the air inlet cooling. The air entering the air compressor of gas turbine engine, when cooled, will reduce the compressor work, as the compressor work is delivered from the turbine. Chacartegui et al. [33] studied inlet air cooling and reported that this technique can save fuel, reduces CO₂, NO_x and improve the efficiency of the cogeneration plant. Alhazmy and Najjar [34] investigated the effects of cooling inlet air of two different types of air coolers, namely water spraying system and cooling coil. They found that spraying cooler is capable of cooling the air by 3-15% with corresponding increase in power by 1-7% and improvement in efficiency by 3%. Cooling coil on the other hand, reduces the overall plant performance due to the large demand for input power.

Khurana et al. [35] investigated a thermal system and found that 35% of energy is lost by the waste heat streams in a cement plant. A heat recovery steam generator is selected to recover the energy lost by the waste heat. It is estimated that 4.4 MW of electricity can be generated. The recovery represents 30% of electricity required by the plant and 10% increase in primary energy efficiency of the plant. Manuel and Jose [36] presented a technique for optimization of the HRSG, based on application of influence coefficient. Their optimization technique permits a better understanding on the effects of the modification in the variables of the thermal systems. They found that application of influence coefficient in the calculation gives obvious support to the optimization works.

Butcher and Reddy [37] analyzed a waste heat recovery which is used for cooling, heating and power (CHP) plant. They found that the cooling load ratio of the unit varies between 10%-55% during the experimental investigation. And below 30% of cooling load ratio the operational stability of the device was limit. Zaporawski and Szczerbowski [38] made a modeling and simulation on a natural gas fired combined heat and power plants, base on energy quantification. They revealed that the most effective use of natural gas in term of energy can be found in systems with back-pressure heat and steam turbine power. Gas-steam combined heat-and power plants with extraction-condensing heat and power turbines allow one to achieve higher efficiencies of electric energy generation. The plant can also operate during summer

season producing warm water in the HRSG, and with high efficiency, electric energy. Natural-gas fired-steam combined heat-and-power plants not only have high energy efficiency, but also considerably decrease harmful impacts on the environment.

Kim et al. [39] simulated HRSG and investigated the thermal stress evolution in steam drum during start up of a HRSG. They found that the highest thermal stress occurs at the drum lines surface, where the temperature gradient is the greatest. Estimating the maximum thermal stress makes it possible to schedule the bypass damper operation. The peak stress for the steady gas turbine exhaust condition is much higher than the allowable limit. Bypassing part of the gas flow during the initial stage of the start up lowers the peak stress. Boonnasa et al. [40] studied the performance improvement of combined cycle power plant by using intake air cooling scheme. They proposed a steam absorption chiller to cool the intake air to the desired temperature level. They found that the application of the steam absorption chiller for air cooling could increase the power output of a gas turbine by about 10.6%. The economic analysis shows that the payback period will be about 3.81 years, with an internal rate of return of 40%. Sanjay et al. [41] analyzed energy and exergy of reheat gas-steam combined cycle using cooling techniques namely, steam cooling and air film cooling. They reported that steam cooling is superior to air film cooling. Closed loop steam cooling enhances thermal efficiency around 62%. Closed-loop steam cooling of plant efficiency, reaches an optimum value in higher range of compressor pressure ratio as compared to that in film air cooling. Closed loop steam cooling shows the maximum exergy loss to be, in combustion chamber around 30%.

Yousef et al. [42] investigated the performance of combine gas turbine system under three different blade cooling schemes. The three different blade cooling schemes were, air cooling, open circuit steam cooling (OCSC) and closed loop steam cooling (CLSC). They found that the combined system with CLSC is better than OCSC system in specific power and overall efficiency. Under the given conditions the power of the lower steam cycle with CLSC is increased by 6% accompanied by 19% rise in cycle efficiency relative to OCSC at similar conditions. The CLSC results in 11% enhancement in power and 3.2% in efficiency relative to air cooling.

Wang and Chiou [43] investigated a gas turbine generation system integrated with two cooling schemes; steam injection and inlet air cooling. They found that by implementing both steam injection and inlet air cooling the power can be boosted more than 70% and 20.4% improvement in heat rate occurs. Tong and Sung [44] investigated the effect of control modes and turbine cooling in the gas turbine cogeneration system. They found that when the coolant remains constant as the design values, both the variable and constant air flow represent similar gas turbine part load efficiency. The part load efficiency of gas turbine is always improved for both air flow control methods by varying the coolant fraction thus maintaining blade temperature as high as possible. Abker and Sanjeev [45] studied a heat recovery steam generator for option capabilities and selection criterion for a combined cycle. They showed the influence of parameters by the type of circulation in HRSG and how to select the HRSG for combined cycle.

Reddy et al. [46] carried out analysis of a waste heat recovery steam generator. They have formulated a general equation for entropy generation number for a waste heat recovery steam generator. They observed that a particular non-dimensional inlet gas temperature difference and for other fixed parameters, entropy generation number is minimum at particular number of transfer unit. The entropy generation number increases with increase in non-dimensional hot flue gas inlet temperature difference ratio due to higher temperature difference between stream to steam (flue gas and water/steam) which increases total irreversibility.

2.11 Researches on parametric studies of a cogeneration plant

Bassily [47] analyzed the effect of turbine inlet temperature (TIT), ambient temperature and relative humidity on the performance of recuperated gas turbine cycle. They found that as TIT increases the optimum pressure ratio increases by 0.45 per 100 K for regular recuperated cycle and 1.4 per 100 K for recuperated cycle with evaporative after-cooling. The evaporative cooling of inlet air could boost the efficiency by up to 3.2% and that evaporative after-cooling could increase the power by up to about 110% and cycle efficiency by up to 16%. Franco and Russo [48]

revealed the optimization of HRSG operating parameters to increase the combined cycle plant efficiency. They found that thermodynamics analysis provides zero pinch-points. They mentioned that by their method it is possible to reach overall combined cycle efficiencies near to 60% on existing plants, just by optimizing the heat recovery and the steam cycle, and modifying the gas turbine characteristics.

Zhang and Ruixian [49] analyzed a single shaft gas turbine and they found that the relative steam flow rate and work/heat ratio are almost not influenced by the gas turbine design values. They emphasized that the approach temperature difference is likely to be negative at low-load condition. However, they also noted that many HRSG cannot operate safely with negative approach temperature difference. Omar [50] studied the improvement of parameters concerned with performance of gas turbine. They revealed that the inlet temperature of air to the compressor depends on ambient conditions. The thermal efficiency of the cycle improves as inlet air temperature decreases. An increase in the compressor efficiency will decrease the work of compression and increase the work of expansion. These will improve the performance of a gas turbine by increasing the net work output, which can result in a lower energy cost.

Bedecarrats and Strub [51] studied the performance of gas turbine by applying an air cooler supplied by phase change energy storage. They found that the climate in France is unfavorable due to its hotness and wetness, which penalizes the turbine operation. Xu et al. [52], [53] analyzed a double effect parallel flow type and series flow type absorption chiller for optimization strategy. They carried out the analysis thermodynamically to study the effect of design parameters on the performance of absorption chiller. They found that COP increases with an increasing heat recovery ratio in the high temperature heat exchanger and the low temperature heat exchanger, with a decreasing solution circulation ratio. The total heat transfer area decreases slightly with an increasing heat recovery ratio. The solution concentration increases the COP when the total heat transfer area decreased. It is found that the optimum results of the series flow type are similar to that of the parallel flow, though the parameters at various state point and components are different.

Tozer et al. [54] presented an extended temperature–entropy diagram for aqueous lithium bromide (LiBr) absorption refrigeration cycle. They described the use of the T-S diagram of water extended with additional curves to represent real and ideal LiBr/water absorption cycles. They found that the T-S diagram has the unique characteristic of being able to represent both the first and second laws of thermodynamics. Arun et al. [55] made comparison of parallel and series flow absorption chiller and found that parallel flow type has higher performance than series flow type absorption chiller.

Fluorides et al. [56] presented a design and construction of a LiBr/water absorption machine. They constructed a methodology to evaluate the characteristic and performance of a single stage LiBr/water absorption machine. Their analysis shows that the greater the difference between the absorber LiBr inlet and outlet percentage ratio, the smaller the mass circulating in the absorber. It is found that at a solution strength effectiveness for a constant difference of 6% between the absorber inlet LiBr percentage ratio and absorber outlet ratio. A reasonable temperature exit of the absorber would be around 30°C, which results in an absorber outlet LiBr/water percentage above 58%. Chua et al. [57] studied thermodynamic properties of LiBr solution. They derived a thermodynamic consistent set of specific enthalpy, entropy, and heat capacity fields of LiBr/water solution. The temperature range is 0-190°C and the concentrations range is 0-75%.

Yu and Chan [58] carried out a research on improved condenser design and condenser fan operation for air cooled chillers. They found that the chiller's COP can be maximized by adjusting the set point based on any given chiller load and wet bulb temperature of the outdoor air. A 5.6-113.4% increase in chiller COP can be achieved for the new condenser design and condenser fan operation. Chan and Yu [59] studied the operating efficiency of air cooled chillers by applying an advanced control of condensing temperature. Their experimental findings confirm that maintaining a fixed degree of superheat will still be a valid control of refrigerant flow if condensing temperature control is applied. Depending on operating conditions, compressor power can be saved by 8.6-40.2% under condenser temperature control in relation to head pressure control.

Yu and Chan [60] investigated air cooled chiller by considering the control of condensing temperature of the chiller. They stated that by applying condensing temperature control technique, the chiller consumption can be maintained below 2 kW/TR throughout the entire range of outdoor temperature and part load conditions giving an average efficiency of 1.08 kW/TR. They found that the potential energy savings of 18.2-29% in the annual chiller consumption are achievable by applying their mode. Yu and Chan [61] studied the performance of air cooled centrifugal chillers. They improved the energy performance by optimizing the control of condensing temperature and varying the evaporator's chilled water flow rate which enable the COP to increase by 0.8-191%, depending on the load and ambient conditions. The electricity could be reduced by 16.3-21% in the annual electricity consumption of the building's chiller plant in another study Yu and Chan [62] presented on optimization of condenser fan control for air cooled centrifugal chillers. They found that by optimizing the condenser fan control for the air cooled chiller, the COP could increase by 11.4-237.2% depending on the operating conditions. The increase in COP results in a reduction of up to 14.1 kWh/m² or 23% in the annual electricity consumption per unit air conditioning floor area of chillers.

Kloppers and Kroger [63] investigated the effect of heat and mass transfer analysis of a counter flow wet-cooling tower. The governing equations according to Poppe, Merkel, and *e-NTU* methods were derived and presented. The difference between the Merkel and Poppe methods of analysis of evaporative cooling is explained by enthalpy diagrams and psychrometric charts which leads to a better understanding of the implications of the assumptions made by Merkel. The Merkel and *e-NTU* methods of analysis give approximately the same results as it is based on the simplifying assumptions.

Maiya [64] analyzed a modified counter flow cooling tower. The counter flow cooling tower is modified by introducing a heat exchanger. Air at the tower inlet is pre-cooled to reduce its wet bulb temperature. Their study shows that the modified cooling tower with pre-cooling by tower exit air is always better than the one with pre-cooling by circulating water. The modified cooling towers are capable of delivering negative approaches, and when operated with number of transfer unit

(NTU) of more than 2 cooling tower range of less than 4 can deliver approaches of about 1-2°C less than that achievable by the conventional cooling tower with the same operating parameters.

Khan et al. [65] investigated the performance characteristic of counter flow wet cooling towers. They have shown that the predominant mode of heat transfer is evaporation. Evaporation contributes about 62.5% of the total rate of heat transfer at the bottom of the tower and almost 90% at the top of the tower. Bosnjakovic and Knoche [66] analyzed a pinch for cooling tower. Pinch analysis with respect to heat and mass transfer has been applied to find the optimum mass flow rate for the cooling tower. They stated that the condition pinch at the top reduces the losses of irreversible heat transfer in the condenser, due to the temperature difference between the condensing vapor and the cooling water assume the smallest values compared with other pinch conditions.

Kloppers and Kroger [67] investigated the Lewis factor and its influence on the performance prediction of wet-cooling towers. They found that if the values of the Lewis factor are applied in the full test analysis and in the subsequent cooling tower performance analysis, the water outlet temperature will be accurately predicted. The amount of water that evaporates is a function of the actual value of the Lewis factor. If the inlet ambient air temperature is relatively high, the influence of the Lewis factor on tower performance diminishes. Lemouari et al. [68] investigated the thermal performance of a wet cooling tower. They found that the tower characteristic decreases with an increase of water/dry air mass ratio. They observed the increase in water flow rate is accompanied by an increase in the water hold up in the cells of the packing and this might cause a decrease in the evaporative rates of water into the air stream. The cooling water range increases gradually with an increase in the air flow rate.

Maungnoi et al. [69] analyzed a counter flow wet cooling tower based on exergy performance. They revealed that water exergy decreases continuously from the top to the bottom. Exergy of air via convection heat transfer initially losses at inlet and slightly recovers along the flow before leaving the tower. They have shown that the

cooling processes due to thermodynamics irreversibility perform poorly at bottom and gradually improve along the height of the tower. The lowest exergy destruction is found at the top of the tower.

Domanski and Fellah [70] presented an analysis of sensible heat on TES. They developed analytical models for the analysis, and their application show how advantageous the models could be adopted in the design and operations of TES. They found that for a given number of transfer units (NTU), the charging temperature would increase irreversibility due to the temperature difference between the working fluid and the storage medium. The results showed that by having NTU of 5.6 and second law efficiency of 0.2663 with the charging time of 0.86 (dimensionless) and corresponding first law efficiency of 0.5768, the operation of the analyzed TES is optimum. Alawadhi [71] made a numerical analysis of cool-thermal storage with a thermal conductivity enhancer. They have shown that the aspect ratio of the rectangular fin has a significant effect on the melting process of water; and cooling rate increases for aspect ratio greater or less than 0.75.

SYSTEMS ENERGY MODELS

3.1 Introduction

The analytical tool for energy audit of cogeneration plant (ATEAC) is developed based on the principle of first law of thermodynamic; mass and energy balance models. The analytical method formulated for the systems include the gas turbine engine (GTE), heat recovery steam generator (HRSG), steam absorption chiller (SAC), air cooled chiller (ACC), cooling tower and thermal energy storage (TES). The analytical models for all the system components are written in a script file in the matlab program. Specifications of the components were obtained from the manufacturer of the component.

The validation of the models was done based on the actual data collected from the gas district cooling plant in UTP (GDC). The results from the model are compared with the actual data for each of the sub-systems. The results are displayed to indicate the variation shows the imbalance when the plant operates at the local condition. These information provide the efficiencies of the sub-systems and the overall performance of the plant. The program enables intervention by the operator to take corrective measures to optimize the sub-system in the plant. The governing equations for the various components models are described in the following sections.

3.2 Gas district cooling plant (GDC)

The GDC plant is a cogeneration plant which produces both electric power and chilled water for space cooling in UTP. It consists of gas turbine engine, heat recovery steam generator, steam absorption chiller, air cooled chiller, cooling tower, and thermal energy storage. The gas turbine engine drives the electric generator for production of electrical power. The exhaust heat from the gas turbine is utilized for

steam production which is needed for heating in the steam absorption chiller. The chilled water produced from the steam absorption chiller is used for air conditioning of the buildings in UTP. The air cooled chiller also produces chilled water and is used for space cooling in UTP. The cooling tower is part of the plant because it is cooling the recycling water of the steam absorption chiller. TES in the plant acts as a storage tank for chilled water that is used during peak period. Cogeneration is a form of energy conservation process [72], because of the heat energy recovery that can be lost from the gas turbine exhaust. The layout of the whole GDC is shown in the Figure 3.1. The following paragraphs describe the main components of a cogeneration plant.

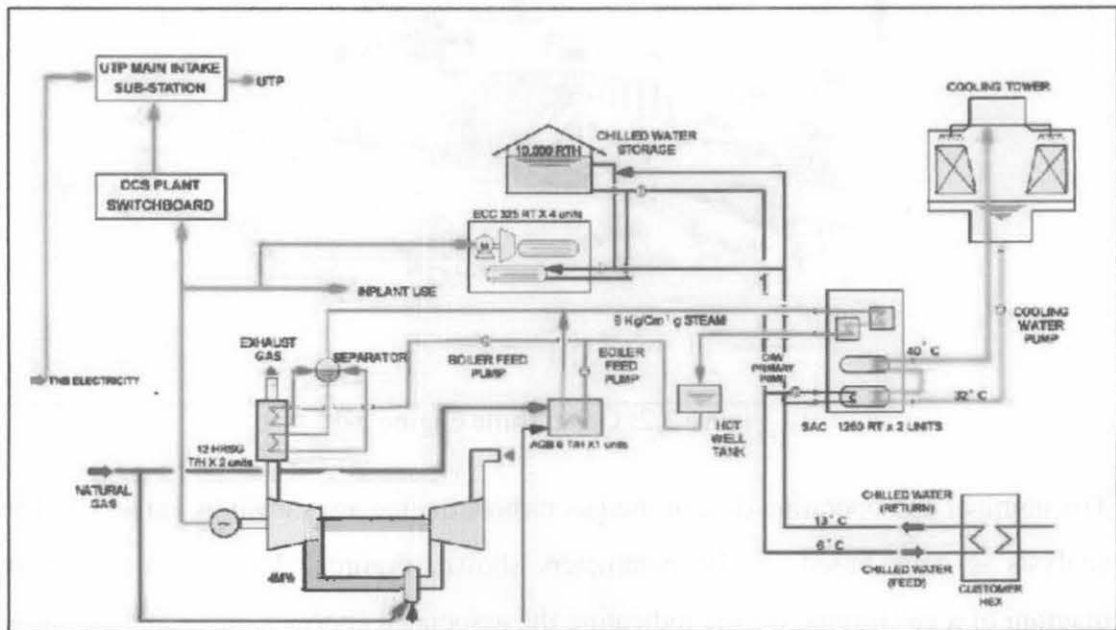


Figure 3.1: Schematic cycle of gas district cooling plant (GDC)

3.3 Gas turbine engine (GTE)

Gas turbine engine consists of air compressor, combustion chamber, and turbine. The air compressor is used to compress the air entering the combustion chamber, the temperature and pressure of compressed air increase and therefore the combustion process is enhanced. The air compressor consists of one or more blade wheels named stages. The stages are built in air compressor to increase the pressure of the air compressed [72]. The air is directed to the combustion chamber where fuel is burned with the compressed air. The burned fuel produces hot gases which expand in the

turbine section. The temperature of hot gases decreases as their thermal energy is converted to mechanical work, which drives the electric generator. Turbine is composed of stationary and rotating blade wheels usually arranged with one or more rows which are known as stages [73]. The stages which are built in the turbine are to decrease the pressure of the working fluid. Gas turbine engine is shown in Figure 3.2.

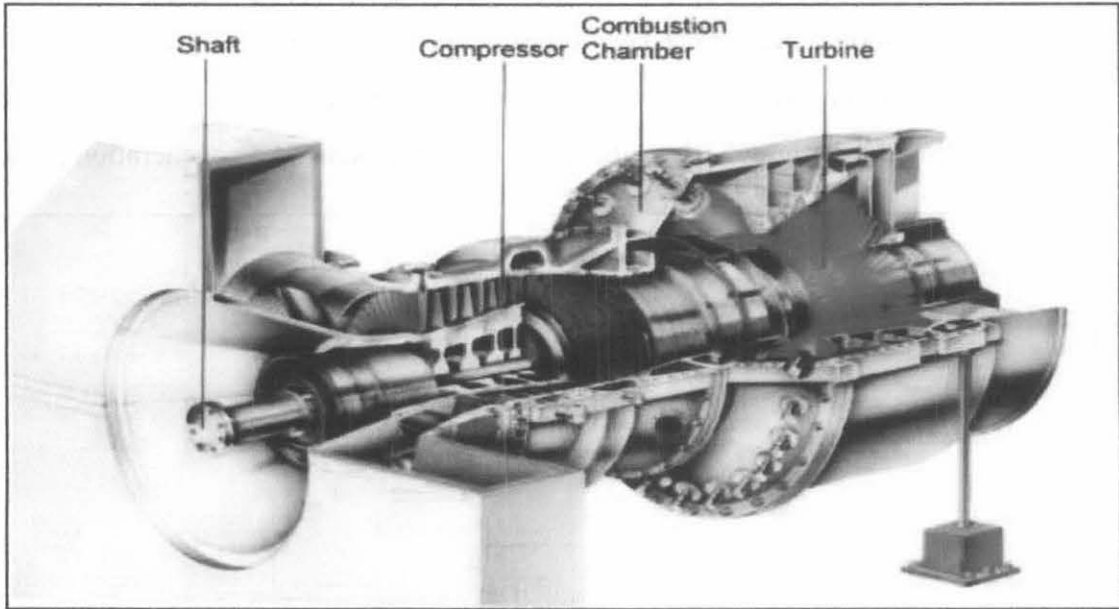


Figure 3.2: Gas turbine engine [4]

The nominal and operating data of the gas turbine engine are shown in Table 3.3. The analysis is done based on the parameters shown. Figure 3.3 shows a schematic diagram of a gas turbine engine indicating the associated energies, input and output to each of the sub-system. The models are formulated based on practical operation performance of the cogeneration plant [73]-[75]. The assumption made here are as follow:

1. The turbine engine is at steady state
2. Air is an ideal gas
3. The pressure ratio is constant both in compressor and turbine

The (GTE) model consists of three sub-systems, i.e. air compressor, combustion chamber, and the turbine.

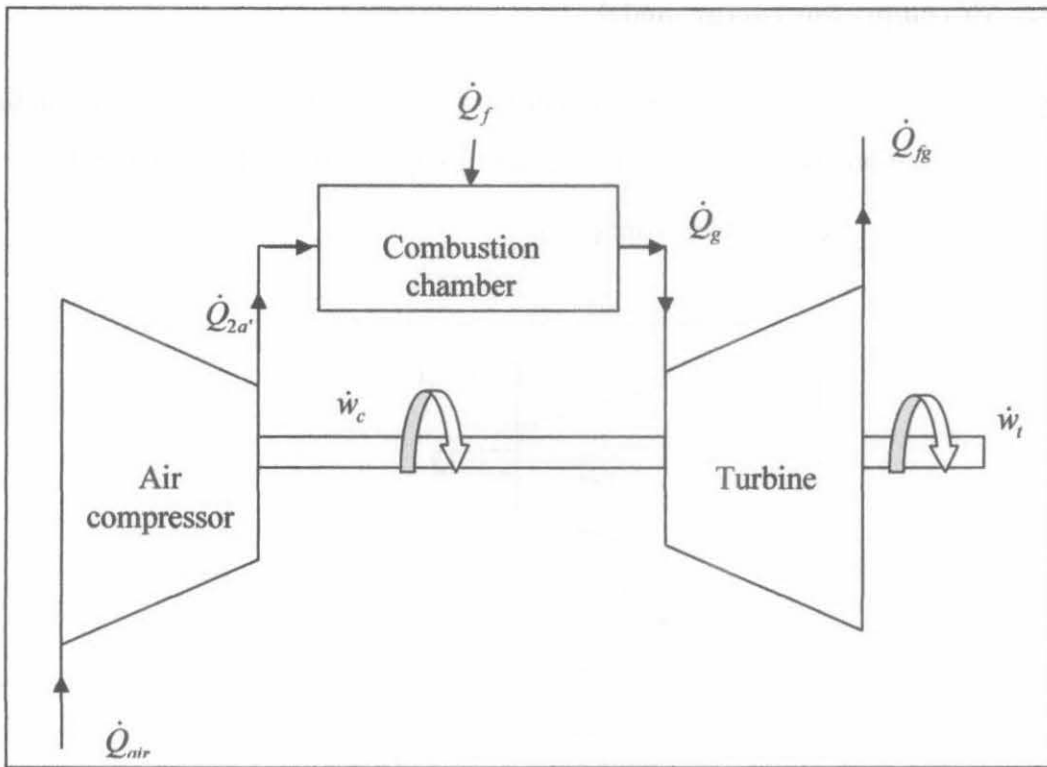


Figure 3.3: Schematic diagram of the gas turbine engine

Table 3-1: Operating and nominal parameters of the gas turbine engine

Component	Nominal value	Operating range
Air compressor		
\dot{m}_a	19 kg/s	14-19 kg/s
T_a	<305 K	300-308 K
r_c	11.7	
Combustion chamber		
\dot{m}_f	0.26 kg/s	0.26-0.3
LHV	41000 kJ/kg K	
Turbine		
T_g	923K	903-923 K
\dot{W}_{net}	4.2 MW	2.44-3.26
MW		
TET	723 K	719-723 K

3.3.1 Air compressor energy model

Figure 3.4 shows the schematic diagram of the air compressor. The parameters in the air compressor are, namely, inlet air temperature (T_a), air mass flow rate (\dot{m}_a), specific heat (c_p), compressor work (\dot{w}_c).

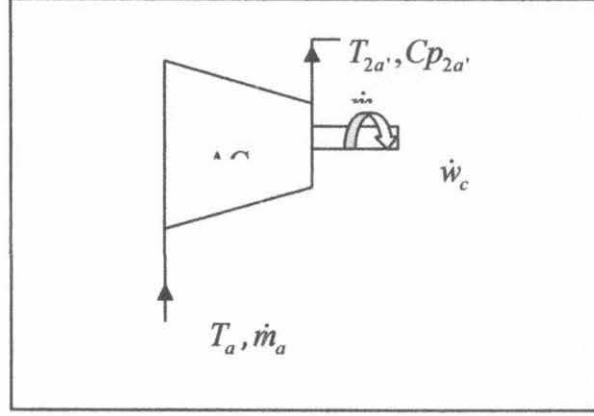


Figure 3.4: Schematic diagram of the air compressor

The specific heat of inlet air at ambient temperature and compressed temperature after compressor are respectively calculated from the correlation below [34]:

Specific heat of air at temperature $200\text{ K} < T < 800\text{ K}$

$$Cp_a = 1.0189134 \times 10^3 - 1.3783636 \times 10^{-1} T_a + 1.9843397 \times 10^{-4} T_a^2 + 4.2399242 \times 10^{-7} T_a^3 \quad (3.1)$$

Specific heat of air at compressed temperature $800\text{ K} < T < 2200\text{ K}$

$$Cp_{2a'} = 7.9865509 \times 10^2 + 5.3392159 \times 10^{-1} T_{2a'} - 2.2881694 \times 10^{-4} T_{2a'}^2 + 3.7420857 \times 10^{-8} \times T_{2a'}^3 \quad (3.2)$$

Isentropic efficiency η_c can be calculated by the correlation given in Alhazmy [34] as,

$$\eta_c = 1 - \left(0.04 + \frac{r_c - 1}{150} \right) \quad (3.3)$$

Compressor work can be determined from first law of thermodynamics as below;

$$\dot{Q} - \dot{W}_c = \dot{m}_a \left[(h_{2a'} - h_a) + \frac{v_{2a'}^2 - v_a^2}{2} + g(z_{2a'} - z_a) \right] \quad (3.4)$$

\dot{Q} is the heat energy released by the air compressor and \dot{W}_c is the work done by the air compressor.

where h, v, g, z are the enthalpy, kinetic velocity, distance, and potential energy respectively.

At steady state the kinetic and potential energy can be ignored.

The compressor work can be obtained by;

$$\dot{w}_c = \dot{m}_a (Cp_{2a'} T_{2a'} - Cp_a T_a) \quad (3.5)$$

where $T_{2a'}$ is the temperature leaving the air compressor which is calculated by;

$$T_{2a'} = T_a + \frac{T_a}{\eta_c} \left(r_c^{\frac{\gamma-1}{\gamma}} - 1 \right) \quad (3.6)$$

where r_c, γ are compression ratio and specific ratio respectively.

Knowing the input parameters of \dot{m}_a, T_a, r_c , the program for the GTE model will compute values $\eta_c, T_{2a'}, Cp_{2a'}, Cp_a$ and finally \dot{w}_c . These provide the energy required to compress the air.

3.3.2 Combustion chamber energy model

The combustion chamber is supplied with energy of the compressed air and energy of the fuel which would produce combustion of the mixture. The energy balance equation requires that this energy equals the energy of the output hot gases. The difference between the inlet and outlet total energy would indicate the losses in the component. Some of the losses could be due to heat transfer; friction etc. Assuming that the combustion of fuel is complete and the product of combustion are CO_2, H_2O, N_2, O_2 only. Figure 3.5 shows the schematic diagram for energy flow in the combustion chamber.

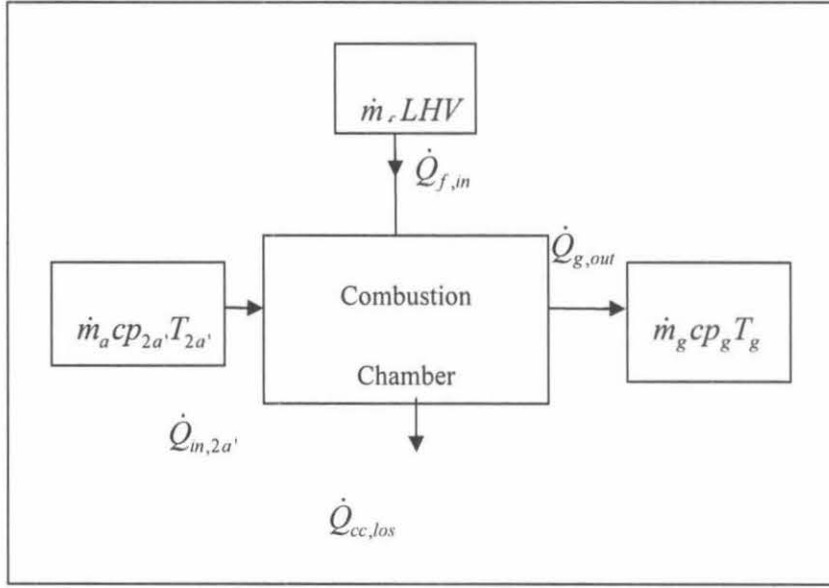


Figure 3.5: Schematic diagram of combustion chamber

Energy input to combustion chamber by the compressed air is calculated from;

$$\dot{Q}_{in,2a'} = \dot{m}_a cp_{2a'} T_{2a'} \quad (3.7)$$

Energy input to combustion chamber is calculated by;

$$\dot{Q}_{in,f} = \dot{m}_f LHV \quad (3.8)$$

where \dot{m}_f and LHV are fuel mass flow rate and low heating value of fuel respectively;

Temperature of hot gas entering turbine is estimated by

$$T_g = \frac{\dot{m}_f LHV \eta_{cc} + \dot{m}_a Cp_{2a'} T_{2a'}}{\dot{m}_g Cp_g} \quad (3.9)$$

where η_{cc} is the combustion chamber efficiency

Specific heat of hot gases is calculated by;

$$Cp_g = a + bT_g + cT_g^2 + dT_g^3 \quad (3.10)$$

The constants a, b, c, d are obtained from Cengel [86]

The mass balance is;

$$\sum \dot{m}_{in} = \sum \dot{m}_{out} \quad (3.11)$$

$$\dot{m}_a + \dot{m}_f = \dot{m}_g \quad (3.12)$$

Knowing the gas temperature at the outlet of the combustion chamber, exit energy of the combustion chamber can be determined by;

$$\dot{Q}_{g,out} = \dot{m}_g C p_g T_g \quad (3.13)$$

Hence energy lost in combustion chamber is calculated by;

$$\dot{Q}_{cc,los} = \dot{m}_a C p_{2a} T_{2a} + \dot{m}_f LHV - \dot{m}_g C p_g T_g \quad (3.14)$$

3.3.3 Turbine energy model

The energy input to the turbine is supplied by the hot gases from combustion chamber, to convert thermal energy to mechanical energy in the form of work. However, not all of the thermal energy is utilized and subsequently some of the energy is lost and escape with the hot flue gases. A portion of the work produced by the turbine is used to drive the air compressor. Thus, the difference between the turbine work output and air compressor work input is known as the net work. Figure 3.6 shows the schematic diagram for energy flow in the turbine. The parameters shown in the turbine are the heat energy entering turbine, network, and exhaust heat energy leaving the turbine.

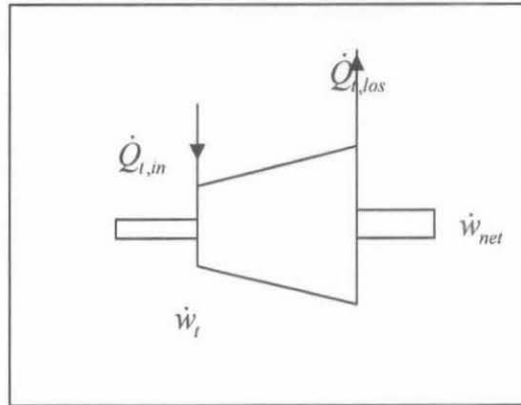


Figure 3.6: Schematic diagram of the turbine

Energy input to the turbine is the same energy which exits the combustion chamber and is calculated by;

$$\dot{Q}_{g,out} = \dot{m}_g C p_g T_g \quad (3.15)$$

Energy of the turbine exhaust gases is considered as energy lost from the turbine is calculated by;

$$\dot{Q}_{t,los} = \dot{m}_g C_{p_{gTET}} T_{TET} \quad (3.16)$$

Turbine work is calculated by;

$$\dot{w}_t = \dot{m}_g (C_{p_g} T_g - C_{p_{gTET}} T_{TET}) \quad (3.17)$$

where $C_{p_{gTET}}$, T_{TET} are the specific heat and turbine exhaust temperature, respectively

The specific heat of flue gases is calculated by;

$$C_{p_g} = a + bTET_g + cTET_g^2 + dTET_g^3 \quad (3.18)$$

The turbine exhaust temperature (TET) can be determined from the polytropic relations for ideal gases as,

$$TET = T_g + \eta_t T_g \left(\left(\frac{1}{r_c} \right)^{\frac{\gamma-1}{\gamma}} - 1 \right) \quad (3.19)$$

where the isentropic efficiency of the turbine η_t is estimated using correlation given in Alhazmy [34]

$$\eta_t = 1 - \left(0.03 + \frac{r_c - 1}{180} \right) \quad (3.20)$$

The net work of the gas turbine engine is the difference between the turbine work and the air compressor work. It is calculated by;

$$\dot{w}_{net} = \dot{w}_t - \dot{w}_c \quad (3.21)$$

Total energy lost in gas turbine engine system is the sum of the energy losses in the three sub-systems, calculated by;

$$\dot{Q}_{GTE,los} = \dot{Q}_{cc,los} + \dot{Q}_{t,los} + \dot{w}_{c,los} \quad (3.22)$$

where $\dot{w}_{c,los}$ is the energy lost in the air compressor

Figure 3.7 shows a computer program flow chart for the gas turbine engine. The input parameters are, mass flow rate of air \dot{m}_a , mass flow rate of fuel \dot{m}_f , compression ratio r_c , and inlet air temperature T_a , these are the operating parameters recorded during operation of the gas turbine engine. Based on the variety of the parameters the calculation is done in the computer program. The parameters which are calculated are isentropic efficiencies for air compressor and turbine, turbine exhaust temperature, hot gases temperature, specific heat, and air compressor work. The energy balance in

combustion chamber is then calculated after the air compressor work is calculated. The net work produced from the turbine is calculated and compared to the actual net work. If the net work is approximately equal to the actual then the energy losses is calculated. If the net work is not approximately equal to the actual value then there must be a mistake which need to be checked in the equations or the input parameters. The variation of the parameters affect the energy balance as can be observed in the output results; hence the energy losses and the imbalance of the energy are determined in the components of the gas turbine engine.

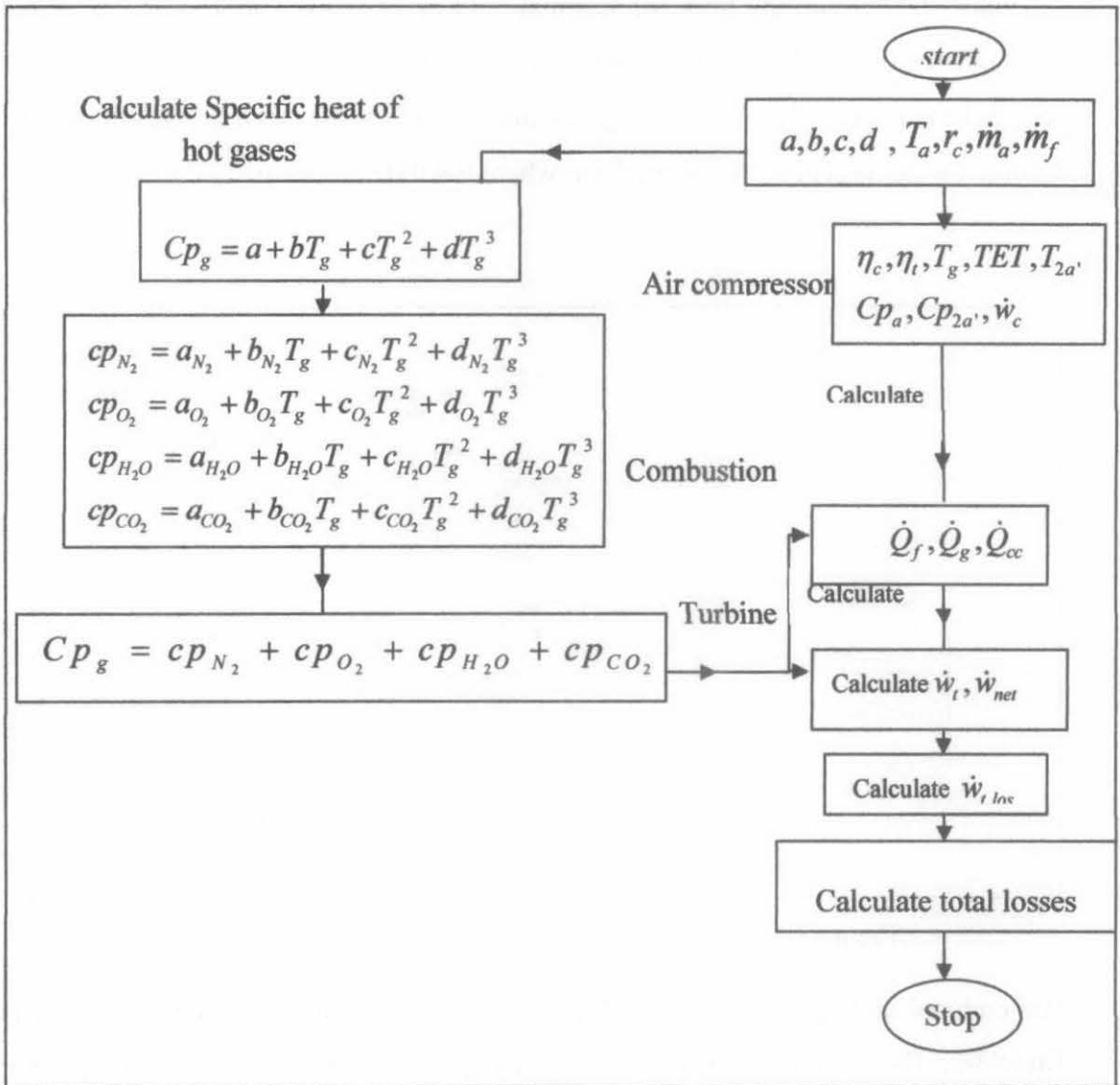


Figure 3.7: Computer program flow chart for gas turbine system

3.4 Heat recovery steam generator (HRSG)

HRSG is a thermal system that recovers heat from the exhaust hot gases for steam generation. The HRSG discussed here, consists of evaporator and economizer and is shown in Figure 3.8 The exhaust hot gases from the gas turbine enter the evaporator and steam is produced at temperature of 180°C and at the rate of 12t/hr nominal state. Steam produced is used as heat source for steam absorption chiller (SAC). The hot gases leaving the evaporator enter the economizer.

Warm water returning from the steam absorption chiller is sent to economizer and heat transfer occurs between the hot gases and the warm water. The warm water gained heat energy from the hot gases and reach its saturated temperature. The saturated water is sent to the steam drum where it will be delivered to the evaporator.

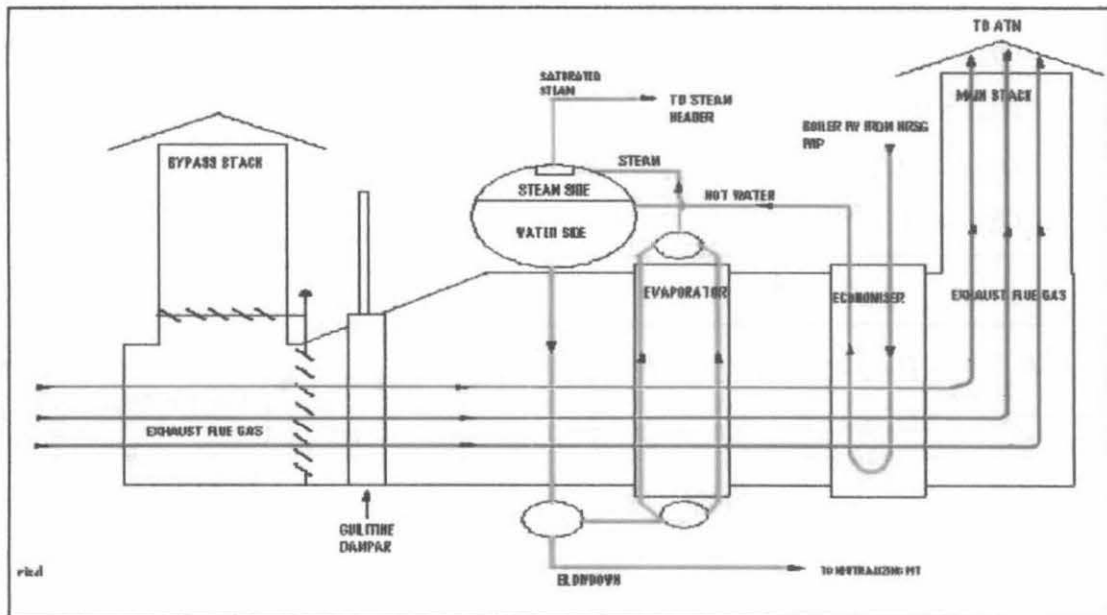


Figure 3.8: Heat recovery steam generator system (HRSG)

The nominal and operating data of the heat recovery steam generator are shown in Table 3-2. The system of HRSG consists of other sub-systems, including evaporator (EV), economizer (EC), and steam drum. Returning water from the SAC flows through the EC, and exit as warm water used as the boiler feed water. Hot flue gas from the GTE flows through HRSG section before exhausted to the atmosphere. The energy from the hot gas is firstly recovered by the EV, and then the hot gas from the

EV is used to warm the water in the EC, as shown in Figure 3.9. The assumptions made for the HRSG are as follows:

1. The pressure variations in components are neglected.
2. The system is at steady state
3. There is no leakage of hot gases and steam

Table 3-2: Nominal and operating parameters of HRSG

Component	nominal value	operating value
<i>Evaporator</i>		
\dot{m}_{steam}	3.3kg/s	1.2-5 kg/s
T_{steam}	458 K	
$T_{ev,exit}$	<823	
<i>Economizer</i>		
\dot{m}_{ww}	4.2 kg/s	1.2-5 kg/s
T_{ww}	358 K	358-366 K
T_{fg}		403-408 K

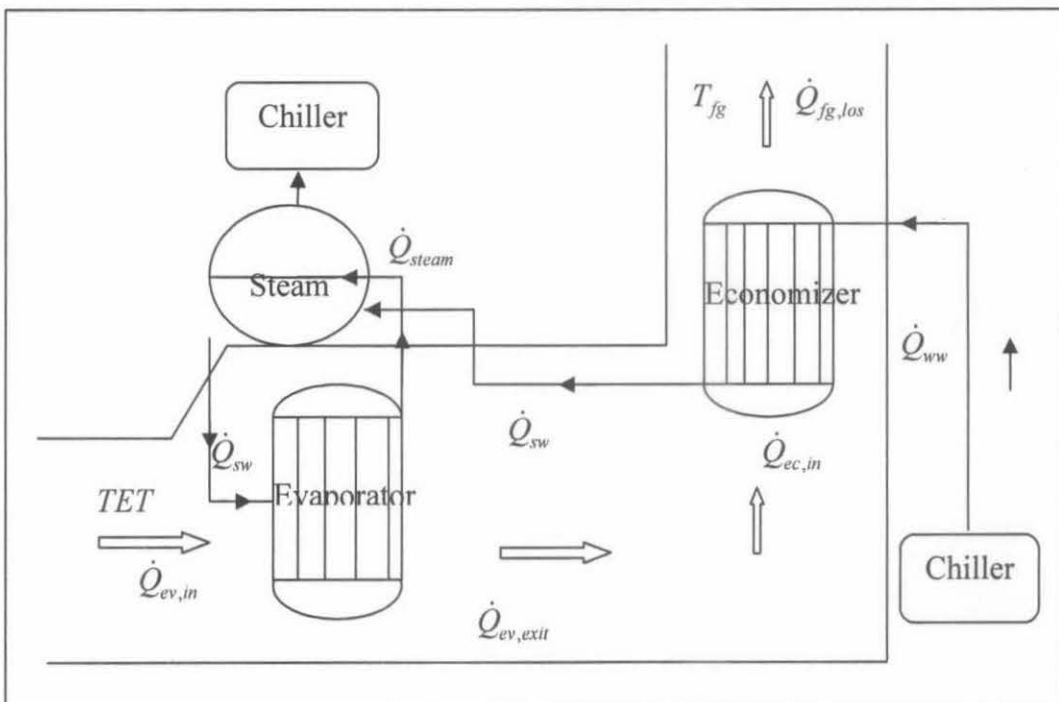


Figure 3.9: Schematic system of HRSG

3.4.1 HRSG evaporator energy model

The energy balance in the evaporator is the heat energy supplied by the flue gases which must be equal to energy gained by the steam plus energy leaving the evaporator and the energy losses in the evaporator. Figure 3.10 shows the schematic diagram for energy flow in the HRSG evaporator. The energy flow in the evaporator are, heat energy of saturated water from the steam drum \dot{Q}_{sw} , heat energy from the turbine exhaust $\dot{Q}_{ev,in}$, heat energy gain by the steam \dot{Q}_{steam} , heat energy leaving the evaporator $\dot{Q}_{ev,exit}$.

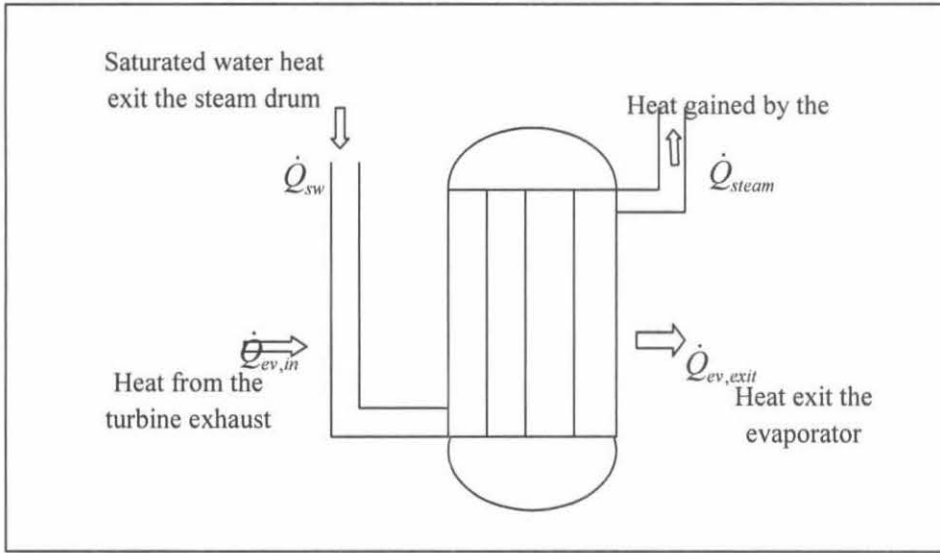


Figure 3.10: Schematic diagram of HRSG evaporator

Energy entering HRSG from gas turbine engine is calculated by;

$$\dot{Q}_{HRSG} = \dot{m}_g c_{p_{gTET}} TET \quad (3.22)$$

Energy supplied by hot gases in evaporator

$$\dot{Q}_{ev,s} = \dot{Q}_{ev,in} - \dot{Q}_{ev,exit} = \dot{m}_g (h_{ev,in} - h_{ev,exit}) \quad (3.23)$$

Heat energy in saturated water is calculated by

$$\dot{Q}_{sw} = \dot{m}_{sw} c_{p_{sw}} T_{sw} \quad (3.24)$$

Energy gained by the steam in evaporator

$$\dot{Q}_{steam,g} = \dot{Q}_{steam} - \dot{Q}_{sw} = \dot{m}_{steam} (h_{steam} - h_{sw}) \quad (3.25)$$

The energy different between the EV, inlet and EV, exit theoretically should be equal to the energy given by the water. Any inequality would be considered as energy lost in the evaporator, thus;

$$Q_{ev,los} = (\dot{Q}_{ev,in} - \dot{Q}_{ev,exit}) - (\dot{Q}_{steam} - \dot{Q}_{sw}) \quad (3.26)$$

3.4.2 HRSG economizer energy model

The flue gas from the evaporator continuous to flow through the economizer, the heat exchange occurs between the flue gas and the warm water from the SAC. Energy exchange in the economizer must be the energy supplied by hot gases from the evaporator, should be equal to the energy gained by the warm water supplied to the economizer. Due to energy inequality in the economizer, the energy supplied by the flue gas would not be equal to the energy gained by the warm water; hence some energy would be lost. The flue gas exiting the economizer carries some energy which would be lost in the atmosphere. Figure 3.11 shows the schematic diagram for energy flow in HRSG economizer. The energy flow in the economizer are, heat energy entering the economizer $\dot{Q}_{ec,in}$, heat energy gain by the saturated water \dot{Q}_{sw} , heat energy lost by the flue gases $\dot{Q}_{fg,los}$, heat energy in the warm water \dot{Q}_{ww} .

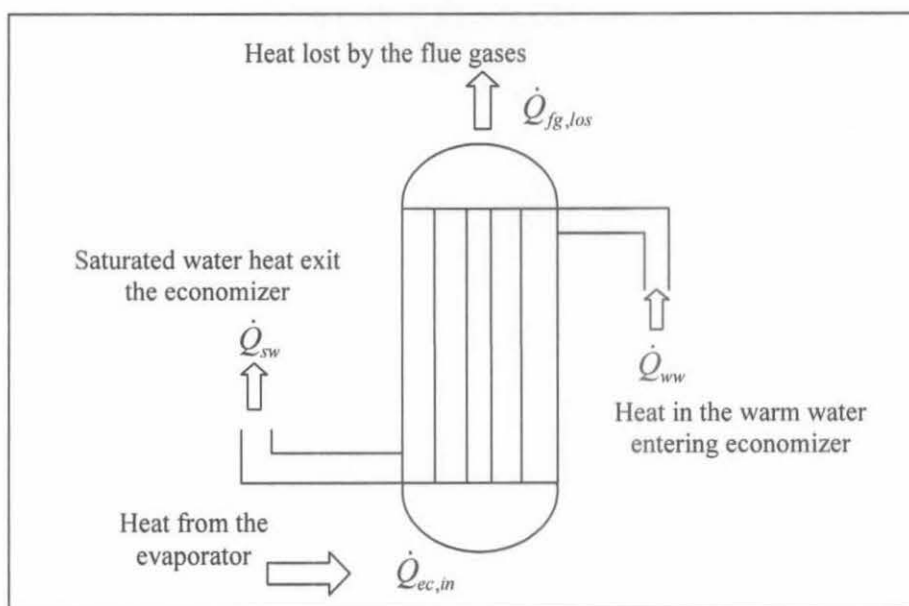


Figure 3.11: Schematic diagram of HRSG economizer

Energy entering the economizer

$$\dot{Q}_{ec,in} = \dot{m}_g c_p T_{ec,in} \quad (3.27)$$

Energy supplied by the hot gases in the economizer

$$\dot{Q}_{ec,s} = \dot{m}_g (h_{ec,in} - h_{fg,los}) \quad (3.28)$$

Energy gained by warm water in economizer

$$\dot{Q}_{ww} = \dot{m}_{ww} (h_{sw} - h_{ww}) \quad (3.29)$$

The energy exchange in economizer is supposed to satisfy the first law of thermodynamic, however, due to energy lost, the first law would not be satisfied in economizer energy exchange, thus, the energy lost can be calculated by;

$$Q_{ec,los} = (\dot{Q}_{ec,in} - \dot{Q}_{fg,los}) - (\dot{Q}_{sw} - \dot{Q}_{ww}) \quad (3.30)$$

Energy lost by the flue gases from the economizer

$$Q_{fg,los} = \dot{m}_g c_p T_{fg} \quad (3.31)$$

Total energy lost in the HRSG system is calculated by

$$Q_{HRSG,los} = Q_{ev,los} + Q_{ec,los} + Q_{fg,los} \quad (3.32)$$

Figure 3.12 shows the computer program flow chart for the HRSG system, the input parameters recorded during operation of HRSG are the mass flow rate of warm water \dot{m}_w , steam temperature T_s , warm water temperature T_w , and flue gas temperature T_{fg} . The parameters which are calculated are the steam mass flow rate \dot{m}_s and enthalpies in the evaporator and economizer. The calculated steam mass flow rate is compared with the actual mass flow rate and the results are close to the actual. However, if the results are not close to the actual value then the input and the equation must be reviewed for any mistake which might have occurred. The energy balance in the evaporator is calculated after certainties in the calculated parameters have been made, and energy losses are calculated in the evaporator. The energy balance in the economizer is carried out after calculated warm water mass flow rate is done and compared to the actual warm water mass flow rate. If the calculated warm water mass flow rate is not close to the actual value then the input and equation must be ascertain. Energy balance and the energy losses are calculated in the economizer and the total energy losses in the HRSG are then calculated.

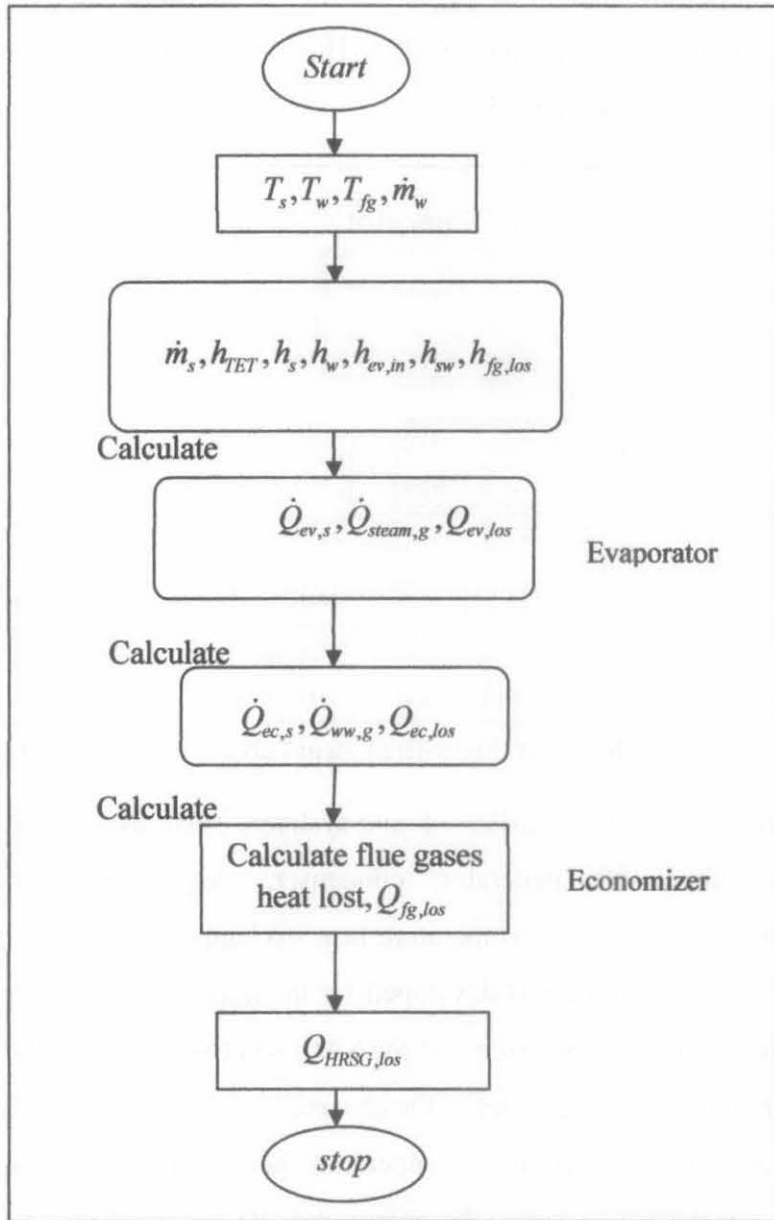


Figure 3.12: Heat recovery steam generator computer flow chart

3.5 Steam absorption chiller (SAC)

Absorption chiller is a refrigeration system which produces chilled water for air conditioning purpose. Absorption chiller uses thermal energy or gas fire as input energy to the generator. Steam is the source of heat energy to drive the generator in the absorption chiller. The source of steam is from the heat recovery steam generator (HRSG). The absorption chillers are preferable due to harmless environmental effect

and less electric consumption in their pumps, which is below 1% of their cooling capacity [76]. The performance of absorption chiller is characterized by the cooling load and the coefficient of performance [77]. The system of two stage steam fire absorption chiller is shown in Figure 3.13.

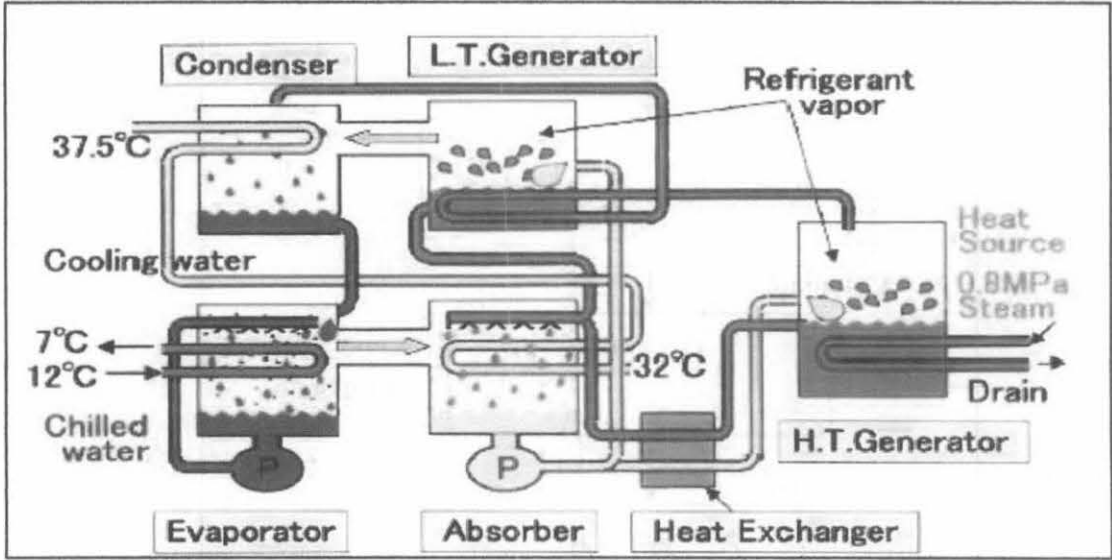


Figure 3.13: Double-effect direct-fired steam absorption chiller [10]

The steam absorption chiller consists of sub-systems, such as, high temperature generator, low temperature generator, condenser, evaporator, absorber, low temperature heat exchanger, high temperature heat exchanger, refrigerant pump, and solution pump. The energy model is developed for the main components of the SAC. The energy exchange in the sub-systems of the SAC is between Lithium Bromide and refrigerant water and the cooling water in the absorber and condenser, chilled water in the evaporator and steam in the high temperature generator. Due to inequality of energy exchange in the sub-systems, the energy models are developed to determine the energy losses and to quantify the energy in the sub-systems. The nominal and operating parameters of steam absorption chiller are shown in Table 3-3. The system of steam absorption chiller is shown in the schematic diagram of Figure 3.14. The assumption made for SAC are as follows:

1. The system is at steady state
2. Heat lost due to friction in the components are neglected
3. Refrigerant lost is neglected

Table 3-3: Operating and nominal parameters of steam absorption chiller (SAC)

Parameter	Nominal value	Operating range
Capacity, \dot{Q}_{lc}	4395.2 kJ/s	3418-4079 kJ/s
Concentrated solution, C_2	63 %	63-64 %
Concentration of diluted solution, C_1	57 %	57-58 %
Evaporating temperature, T_3	5°C	6-6.5°C
Chilled water supply temperature, T_{12}	6°C	6-7.5°C
Chilled water inlet temperature, T_{12}	13°C	13-13.5°C
Chilled water flow rate, \dot{m}_{chw}	504 m ³ h ⁻¹	503-504 m ³ h ⁻¹
Cooling water inlet temperature, T_{cwi}	28°C	28-32°C
Cooling water outlet temperature, T_2	35°C	35-40°C
Steam flow rate, \dot{m}_s	6 x 10 ³ kg/h	4.5-6.2 x 10 ³ kg/h
Steam temperature, T_{steam}	185°C	183-185°C
Steam drain temperature, T_d	85°C	60-90°C
COP	1.2	1.2-1.3

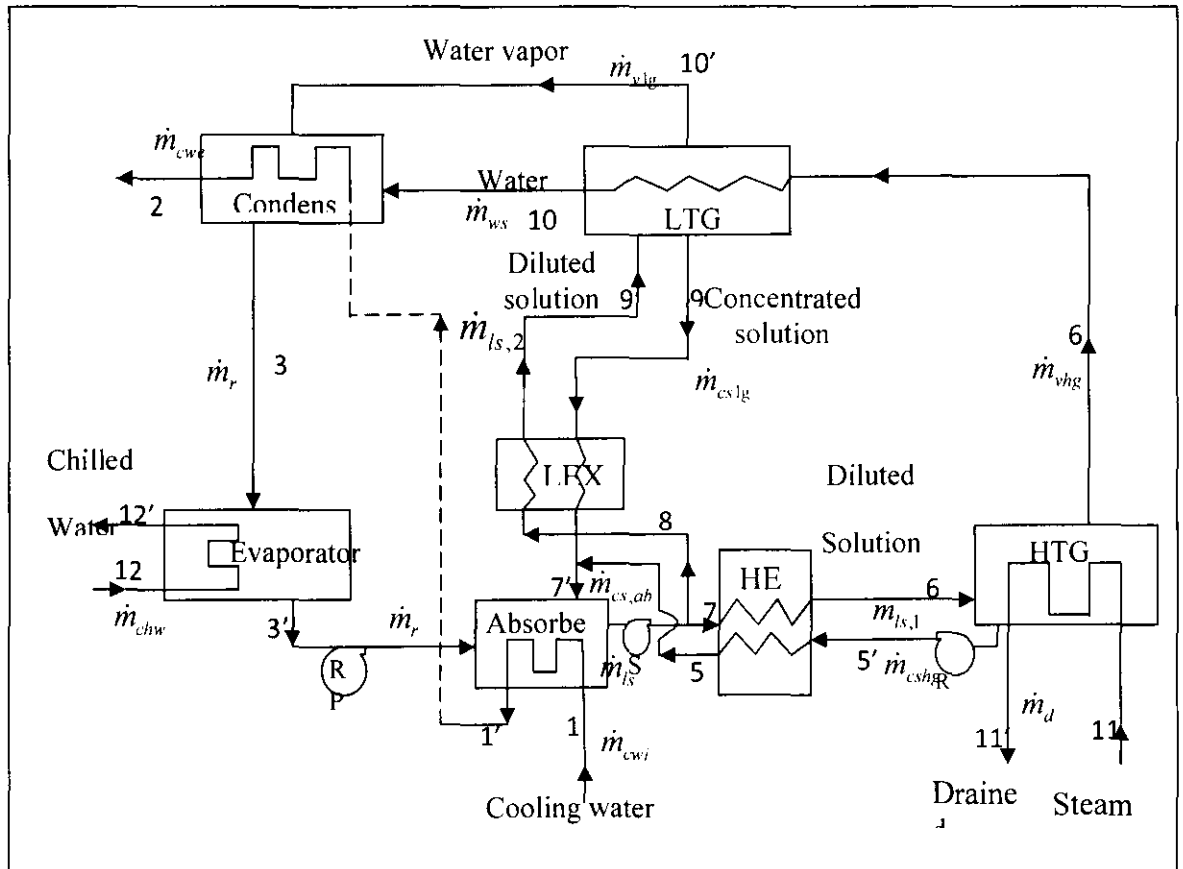


Figure 3.14: Schematic diagram of double-effect parallel-flow SAC

3.5.1 Steam absorption chiller (SAC) model

The model developed here is only for the main SAC components which are absorber, condenser, high temperature generator (HTG), and evaporator are as follows;

The refrigerant mass balance in absorber is given by;

$$\dot{m}_{ls} = \dot{m}_{cs,ab} + \dot{m}_r \quad \dot{m}_{ls} = \dot{m}_{ls,1} + \dot{m}_{ls,2} \quad (3.33)$$

$$\dot{m}_{cs,ab} = (C_1 / C_2 - C_1) \dot{m}_r \quad (3.34)$$

where C_1, C_2 are the solution concentration at absorber and high generator respectively

The mass balance in low temperature generator (LTG) is given by

$$\dot{m}_{ls,2} = \dot{m}_{vlg} + \dot{m}_{cs,lg} \quad (3.35)$$

The vapor mass exit high generator is given by

$$\dot{m}_{vhg} = 0.5 \dot{m}_r \quad (3.36)$$

The mass of solution exit low generator is given by

$$\dot{m}_{ws} = \dot{m}_{vhg} \quad (3.37)$$

The mass balance in the high generator is given by

$$\dot{m}_{vhg} = \dot{m}_{ls} - \dot{m}_{cs,hg} \quad (3.38)$$

Energy balance in the steam absorption chiller can be drawn as follows [78], [83], [86]

3.5.2 Absorber energy model

Energy rejected by cooling water in absorber;

$$\dot{Q}_{ab,cw} = \dot{m}_{cw} (h_{1'} - h_1) \quad (3.39)$$

Energy added by the refrigerant in absorber;

$$\dot{Q}_{ab,r} = \dot{m}_r h_{3'} + \dot{m}_{cs,ab} h_{7'} - \dot{m}_{ls} h_4 \quad (3.40)$$

Energy lost in absorber can be calculated by

$$\dot{Q}_{ab,los} = \dot{Q}_{ab,r} - \dot{Q}_{ab,cw} \quad (3.41)$$

3.5.3 High temperature generator (HTG) energy model

Energy gained in high temperature generator is calculated by

$$\dot{Q}_{hg} = \dot{m}_{vhg} h_6 + \dot{m}_{csg} h_5 - \dot{m}_{ls} h_6 \quad (3.42)$$

Energy added to high temperature generator by the steam

$$\dot{Q}_{hg,d} = \dot{m}_s h_{11} - \dot{m}_d h_{11} \quad (3.43)$$

Energy lost in high temperature generator

$$Q_{hg,los} = \dot{Q}_{hg} - \dot{Q}_{hg,d} \quad (3.44)$$

3.5.4 Condenser energy model

Energy added by refrigerant in condenser is calculated by

$$\dot{Q}_{cd} = \dot{m}_{vlg} h_{10'} + \dot{m}_{ws} h_{10} - \dot{m}_r h_3 \quad (3.45)$$

Energy rejected by cooling water in condenser

$$\dot{Q}_{cd,cw} = \dot{m}_{cw} (h_2 - h_1) \quad (3.46)$$

Energy lost in condenser

$$Q_{cd,los} = \dot{Q}_{cd} - \dot{Q}_{cd,cw} \quad (3.47)$$

3.5.5 Evaporator energy model

Energy absorbed by refrigerant in evaporator is calculated by

$$\dot{Q}_{lc} = \dot{m}_r (h_3 - h_2) \quad (3.48)$$

Energy rejected by chilled water in evaporator is calculated by

$$\dot{Q}_{chw} = \dot{m}_{chw} (h_{12'} - h_{12}) \quad (3.49)$$

Energy lost in evaporator;

$$Q_{ev,los} = \dot{Q}_{lc} - \dot{Q}_{chw} \quad (3.50)$$

Coefficient of performance of the SAC is calculated by

$$COP = \frac{\dot{Q}_{lc}}{\dot{Q}_{hg}} \quad (3.51)$$

Total energy lost in SAC system is determined by;

$$Q_{SAC,los} = Q_{ab,los} + Q_{hg,los} + Q_{SAC,ev,los} + Q_{cd,los} \quad (3.52)$$

Figure 3.15 shows the computer program flow chart for SAC, the input parameters are, chilled water temperature, cooling water temperature, refrigerant temperature, steam temperature, solution temperature. The enthalpies and masses are calculated for all the components in the system. The energy losses are calculated when there are energy imbalances in the components. The COP and cooling load are calculated and compared to the actual COP and cooling load and when the results are not close then input parameters and the equations must be reviewed for any mistake. The calculation is repeated with various input parameters taken from the recorded data. The certainty of the calculation is achieved by comparing the calculated results to the actual values.

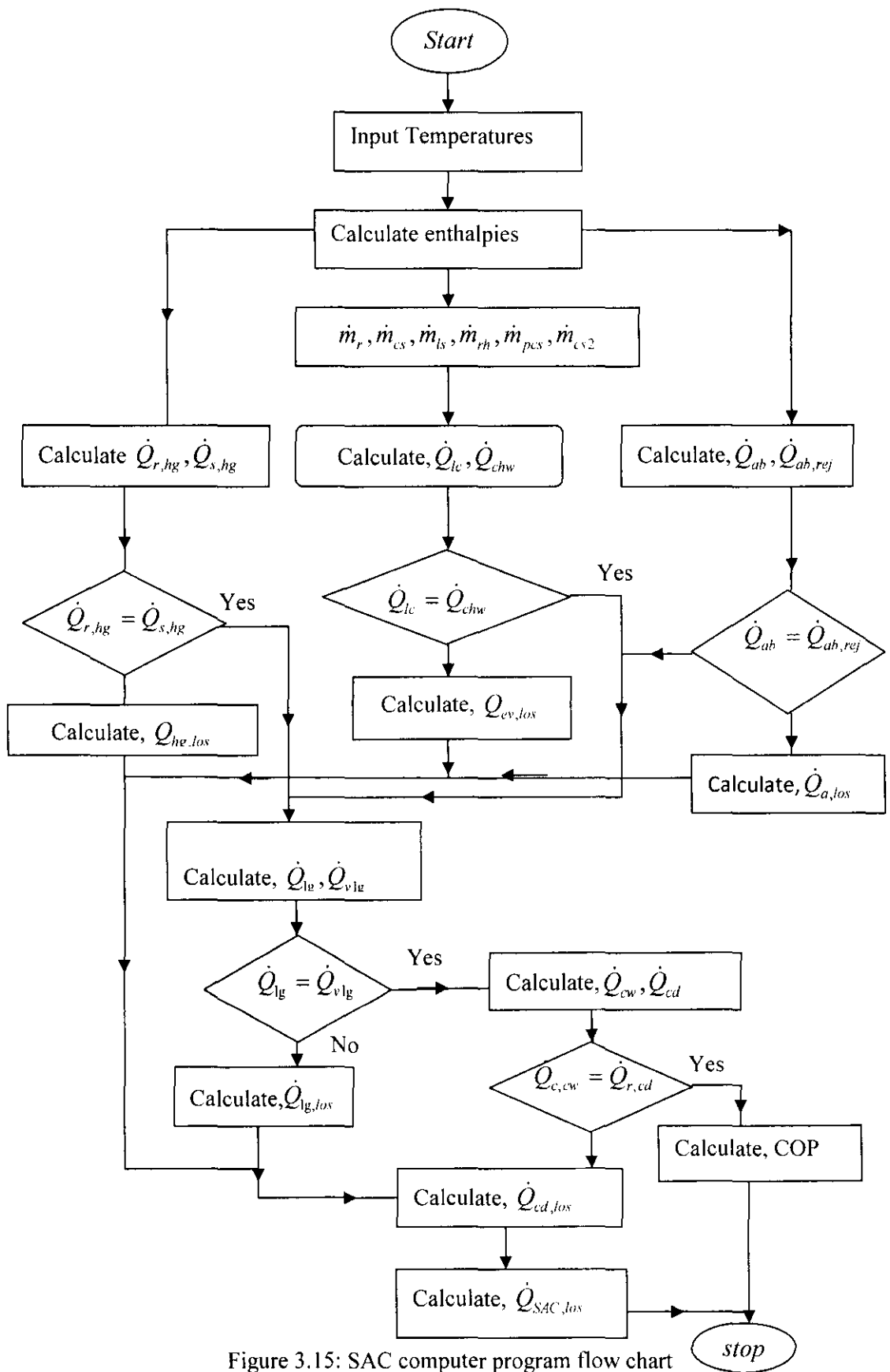


Figure 3.15: SAC computer program flow chart

3.6 Air cooled chiller (ACC)

The air cooled chiller which is also known as electric chiller, it uses electric power to drive the motor in the screw compressor. The air cooled chiller studied here has a capacity of 1143 kJ/s. The system components include screw compressor, air cooled condenser, expansion valve and evaporator. The refrigerant used is R134a, which is compressed by screw compressor and sent to air cooled condenser at high temperature and pressure, where it is condensed. The heat of condensation is rejected by cooling air. The refrigerant liquid leaves the condenser at low temperature and enters the expansion valve where the pressure and the temperature are reduced.

The refrigerant enters the evaporator at required pressure and temperature, and evaporated. Due to the heat absorbed from the circulating water the evaporator refrigerant is evaporated and on the other hand water is chilled due to heat released to the evaporator refrigerant. The evaporated refrigerant vapor is superheated at compressor suction and the cycle is repeated. Air cooled chillers are preferable because of their applicability in hot and arid regions where water sources is scarce [79]. They are preferred than water cooled chiller because of their simplicity in their installation and low maintenance costs [80].

The nominal and operating data of the air cooled chiller are shown in Table 3-4. Figure 3.16 shows the schematic cycle of air cooled chiller .The assumptions made are as follow:

1. Refrigerant mass is the same through out the system
2. The system is at steady state
3. Energy lost from expansion value is very small, neglected
4. Losses due to internal friction is neglected

Table 3-4 Operating and nominal parameters of the air cooled chiller (ACC)

Parameter	Nominal value	operating range
Capacity, $\dot{Q}_{ACC,lc}$	1143 kJ/s	879-1143 kJ/s
Chilled water temperature supply, T_{3a}	5°C	5-5.6°C
Chilled water temperature return, T_{4a}	12.7°C	12.7-13.3°C
Compressor discharge pressure, $P_{r,b}$	10.5 bar	9.8-10.5 bar
Compressor suction pressure, $P_{r,a}$	3.5 bar	----
Power of air cooled chiller, E_{comp}	<350 kW	124-295 kW
COP_{ACC}	3.5	2.3-3.7

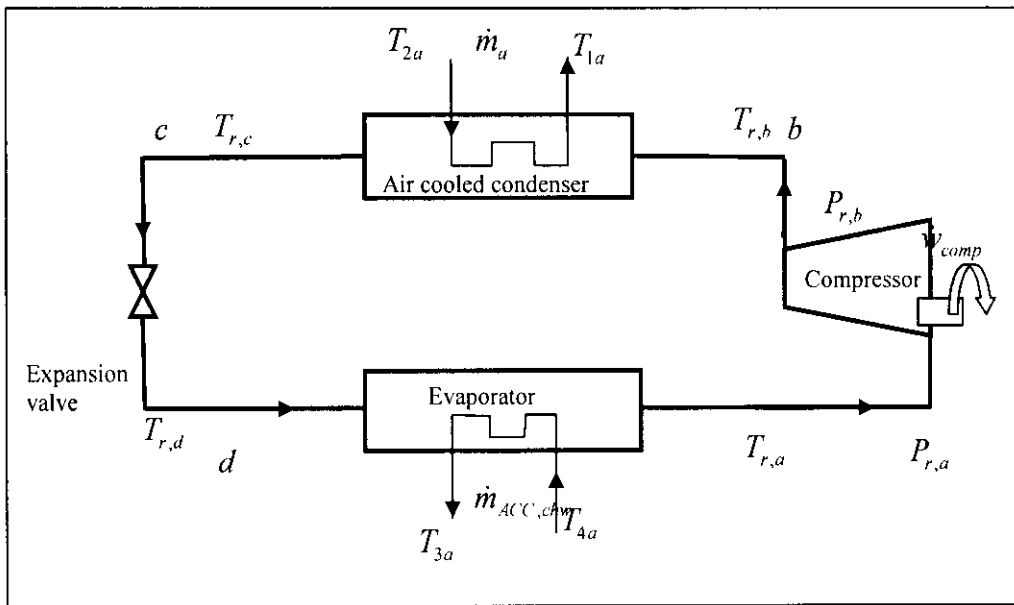


Figure 3.16: Schematic cycle of air cooled chiller

3.6.1 Air cooled condenser model

Energy rejected by air mass flow in air condenser

$$\dot{Q}_{ACC,cd} = \dot{m}_a(h_{1a} - h_{2a}) = \dot{m}_a c_p(T_{1a} - T_{2a}) \quad (3.53)$$

Energy of the refrigerant in air cooled condenser

$$\dot{Q}_{ACC,cd,r} = \dot{m}_{ACC,r}(h_{r,b} - h_{r,c}) = \dot{m}_{ACC,r} c_p(T_{r,b} - T_{r,c}) \quad (3.54)$$

Where $\dot{m}_{ACC,r}$ is the mass of refrigerant R134a and is calculated by

$$\dot{m}_{ACC,r} = \frac{V_{eff} V_d}{v_i} \quad (3.55)$$

V_{eff} is the volumetric efficiency and V_d is the volumetric displacement, is taken as $0.12 \text{ m}^3\text{s}^{-1}$ [60], because V_d is at constant speed based on the performance of the ACC at full load.

$$V_{eff} = 0.95 - 0.0125 \left[\frac{P_{r,b}}{P_{r,a}} \right] \quad (3.56)$$

Energy lost in air cooled condenser

$$Q_{ACC,cd,los} = \dot{Q}_{ACC,cd,r} - \dot{Q}_{ACC,cd} \quad (3.57)$$

3.6.2 Air cooled chiller evaporator model

Energy absorbed by refrigerant in ACC evaporator

$$\dot{Q}_{ACC,lc} = \dot{m}_{ACC,r} (h_{r,a} - h_{r,d}) = \dot{m}_{ACC,r} c_p (T_{r,a} - T_{r,d}) \quad (3.58)$$

Energy rejected by the chilled water in ACC evaporator

$$\dot{Q}_{ACC,chw} = \dot{m}_{ACC,chw} (h_{4a} - h_{3a}) = \dot{m}_{ACC,chw} c_p (T_{4a} - T_{3a}) \quad (3.59)$$

Energy lost in evaporator

$$Q_{ACC,ev,los} = \dot{Q}_{ACC,chw} - \dot{Q}_{ACC,lc} \quad (3.60)$$

3.6.3 Screw compressor model

Energy gained by the refrigerant vapor in compressor [15]

$$\dot{W}_{comp} = \frac{n}{n-1} (v_i P_{r,a}) \left(\left[\frac{P_{r,b}}{P_{r,a}} \right]^{\frac{n-1}{n}} - 1 \right) \quad (3.61)$$

Electric power input compressor is calculated by [81], [82];

$$E_{comp} = \frac{\dot{m}_{ACC,r} \dot{W}_{comp}}{\eta_i \eta_m \eta_{me}} \quad (3.62)$$

Energy lost in the screw compressor is calculated by;

$$Q_{comp,los} = E_{comp} - \dot{W}_{comp} \quad (3.63)$$

Air cooled chiller COP is calculated by;

$$COP_{ACC} = \frac{\dot{Q}_{ACC,lc}}{E_{comp}} \quad (3.64)$$

Total energy lost in air cooled chiller can be calculated by

$$Q_{ACC,los} = Q_{ACC,cd,los} + Q_{ACC,ev,los} + Q_{comp,los} \quad (3.65)$$

Figure 3.17 shows the computer program flow chart for the air cooled chiller. The operating parameters recorded during the operation of the plant are, air inlet temperature, chilled water temperature, pressure of the refrigerant, specific volume of the refrigerant, and the refrigerant temperature. The enthalpies at those various temperatures and the mass flow rate are calculated. The energy balances in the screw compressor, air cooled condenser and the evaporator are calculated. The energy losses in the components are calculated when there are energy imbalances. The total energy losses in the components are calculated after various energy losses in the components are determined. The cooling load and COP calculated and compared to the actual values recorded in the plant. The calculated cooling load and COP should be closed to the actual values, or uncertainty is check in the inputs and the equations and the calculation is repeated until the calculated values are close to the actual values. The results are then plotted and discussed based on variation in the input parameters.

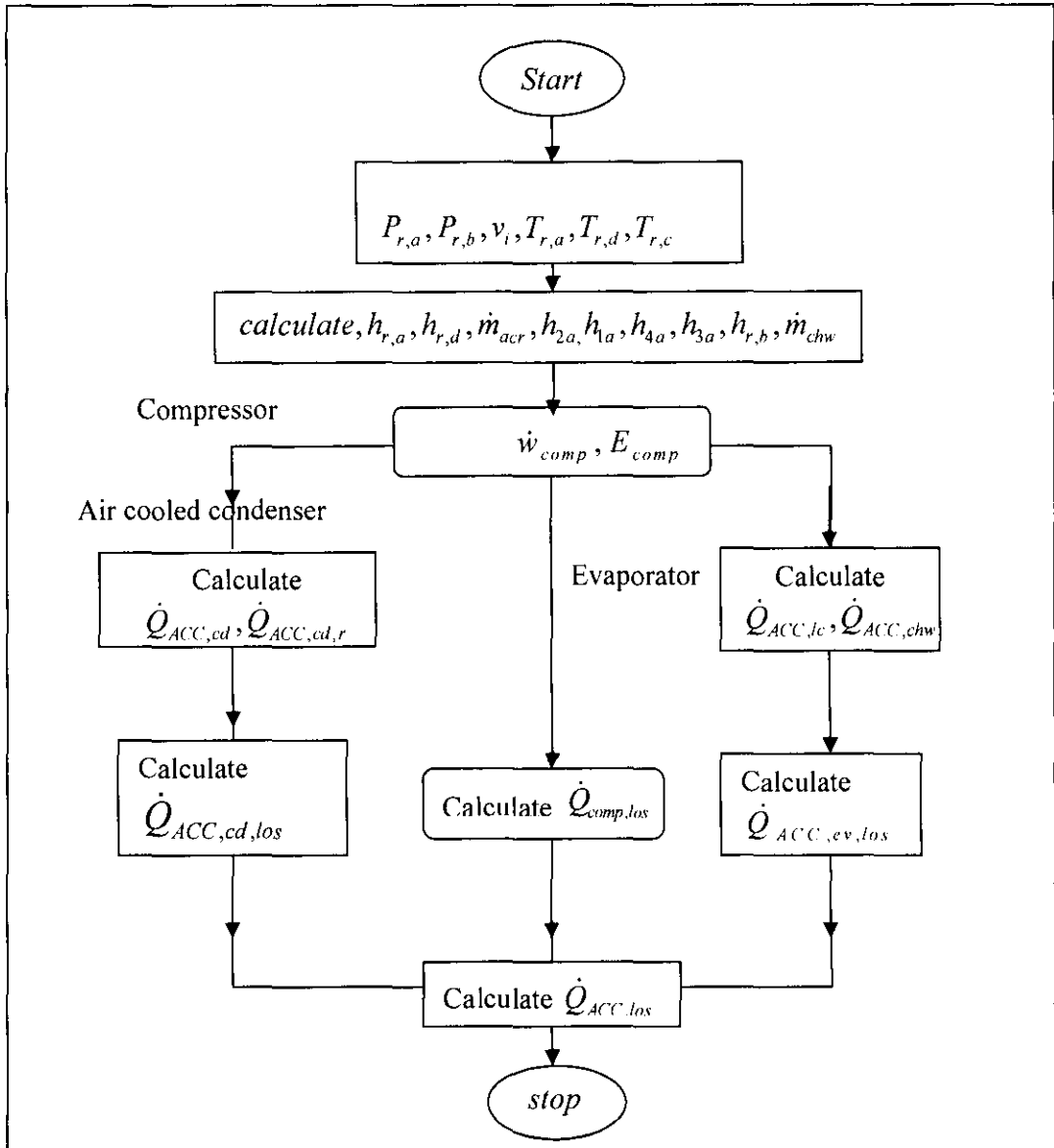


Figure 3.17: Air cooled chiller computer program flow chart

3.7 Cooling tower

A cooling tower is a cooling device to reduce warm water temperature by using air. Both heat and mass transfers take place during the water cooling process. Water that needs to be cooled is distributed in the tower by spray nozzles, splash bars, or film fill in such a way that the water surface is exposed to a large area to the atmosphere air. A fraction of water is evaporated in the cooling tower due to the less saturated moisture content in the air to that of water at the water temperature. The water vaporizes from the cooling tower due to the heat content in the warm water and as a result the portion of water outlet from the cooling tower is cold. A portion of heat energy is also

released from the water by convection. Approximately 1-3% of water is lost because of the evaporating water vapor [83]. Design improvements of cooling towers have been studied for many years both theoretical and experimental which led to better performance of the systems. With all the studies made, however, the performance of the cooling tower is not absolutely optimized without the operation of management and maintenances practices. In gas district cooling (GDC) the cooling tower type used is the induced draft wet counter-flow. Its purpose is to cool the cooling water of the steam absorption chiller.

Figure 3.18 shows the induced draft, wet counter flow cooling tower. The force draft is the application of fan in the area where air enters the tower and is forced to pass through the water fill. Warm water is supplied from the top to flow downward in counter-flow towers and air is allowed to flow upward. Due to upward flow of air, small water droplets are released and they are collected by drift eliminator, where they can be returned to fill as they are accumulated. Below the tower fill is the basin, where the cooled water is stored and returned to the thermal system. The difference between the temperature of the water entering and leaving the cooling tower is called *range*. The difference between the wet-bulb temperature of the air entering and water leaving the tower is called the *approach*. Cooling tower performance can be observed often based on the *approach* and *range* differences [84].

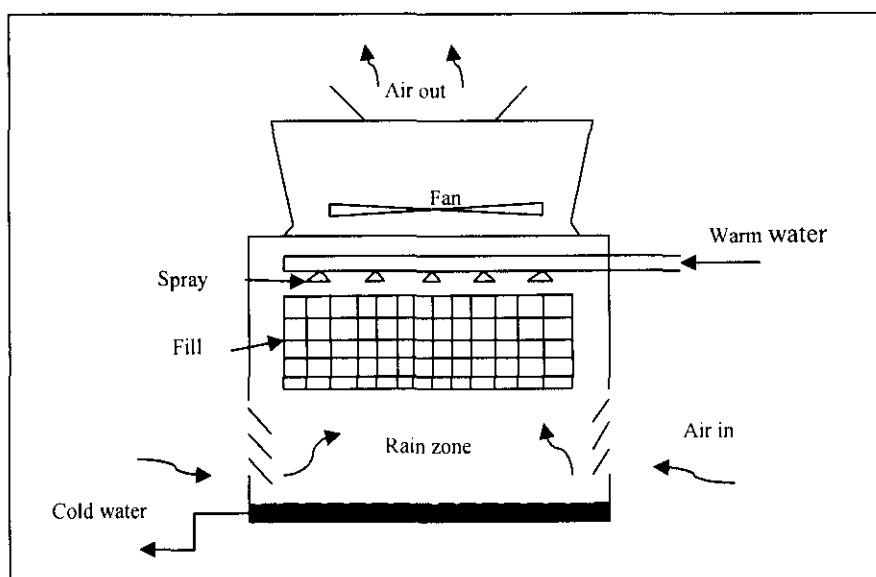


Figure 3.18: Schematic drawing of an induced draft, wet counter flow cooling tower

3.7.1 Cooling tower energy model

The model of cooling tower developed is based on cooling tower models suggested by Kroger et al. [83]. Energy balance that is found in cooling tower is due to the heat energy transfer by convection and mass of water vapor evaporating in the cooling tower which must be equal to the heat gained by air. The schematic diagram of induced draft cooling tower is shown in Figure 3.19. The analysis of the cooling tower is performed based on manufacturer data, shown in Table 3-5.

Table 3-5: Design and operating parameters of cooling tower

Parameter	Design value	Operating range
\dot{m}_w	966 m ³ /hr	
$T_{w,in}$	39.5°C	
$T_{w,o}$	32°C	
T_{wb}	28°C	24-32°C
A	15930mm×4020mm	
R	5.5	5.5-9.5

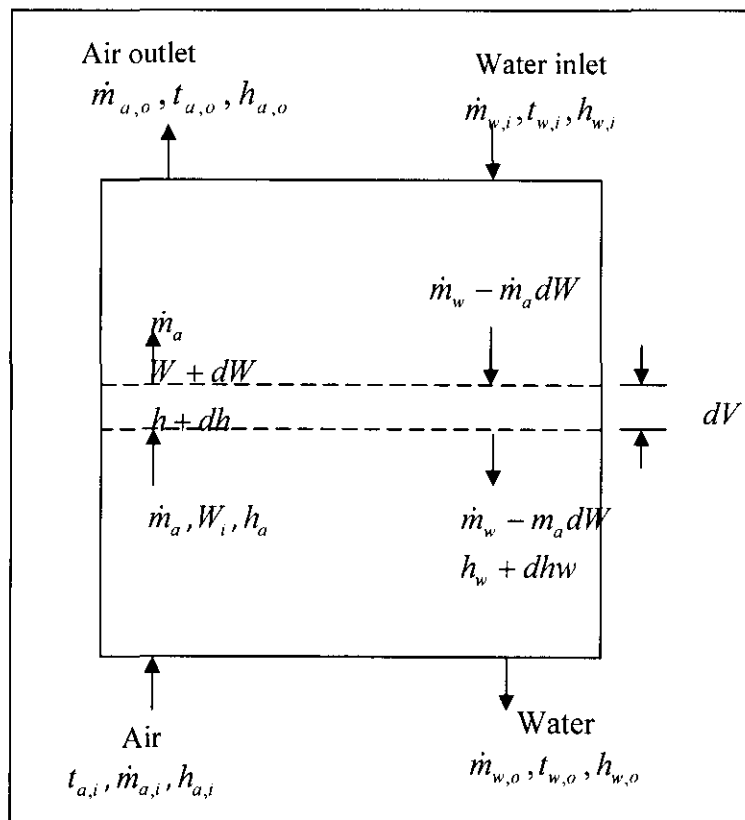


Figure 3.19: Schematic diagram of induced draft cooling tower

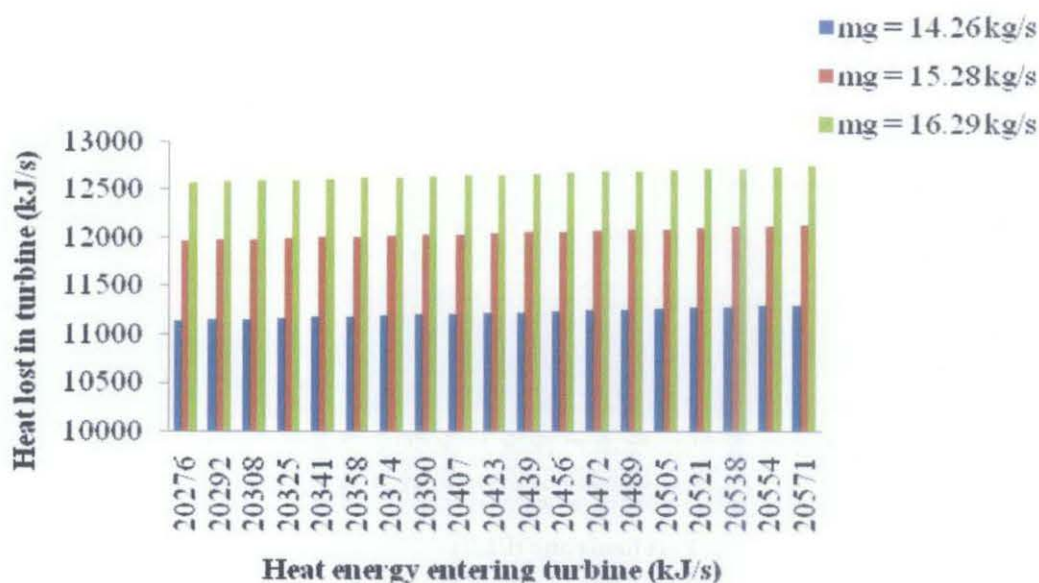


Figure 4.11: Heat energy (kJ/s) entering turbine against turbine energy lost (kJ/s)

4.2.4 Net work and part load ratio

It is customary to show the performance of a gas turbine engine at part load. Part load ratio is defined as the ratio of net work output and the nominal net work. The net work obtained in gas turbine engine is the turbine work minus the compressor work. Air compressor is one of the components in gas turbine engine which consumes most of the turbine work.

In Figure 4.12, the net work is plotted against part load ratio. Net work increases as the part load ratio increases, at minimum air mass flow rate the content of heat energy results from combustion chamber is higher at temperature which results into high net work output. Monitoring the air mass flow rate at optimum can maintain the thermal heat energy at high level. As a result the energy that can drive the turbine is high and eventually the net work is optimum. It is found that when the inlet temperature to air compressor decreases by 1 K the net work increases by 0.11%.

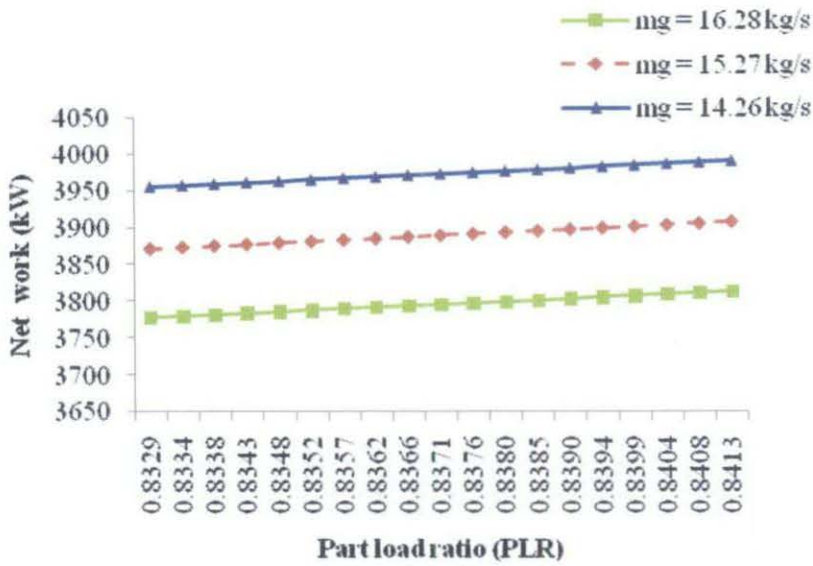


Figure 4.12: Net work (kW) against part load ratio

4.3 Results from heat recovery steam generator (HRSG) model analysis

The performance of HRSG depends on the performance of the various sub-systems such as evaporator and economizer. The energy balance in the HRSG components varies with the change of the parameters. Energy supplied to the evaporator is 38.94% at turbine exhaust temperature 728.23 K and mass flow rate of hot gases 14.26 kg/s, where 10.88% of energy supplied is gain by the steam and 28.06% is lost in the evaporator. The steam is produced at the mass flow rate of 2.24 kg/s and at steam temperature 458 K.

Energy entering the economizer is 10.21%, where the energy supplied to heat the warm water is 3.15% at warm water mass flow rate 2.69 kg/s and warm water temperature 358 K, where 7.06% of total energy in the economizer is lost. Energy lost in economizer decreases by 0.78% when the mass flow rate of warm water is increased by 0.16 kg/s. The percentage increase of energy gain by warm water in economizer is 0.84% at the same mass flow rate of warm water. In Figure 4.13 heat energy lost in the evaporator and economizer and flue gas lost are plotted. Heat supplied to the heat recovery steam generator is calculated 11.143 MW.

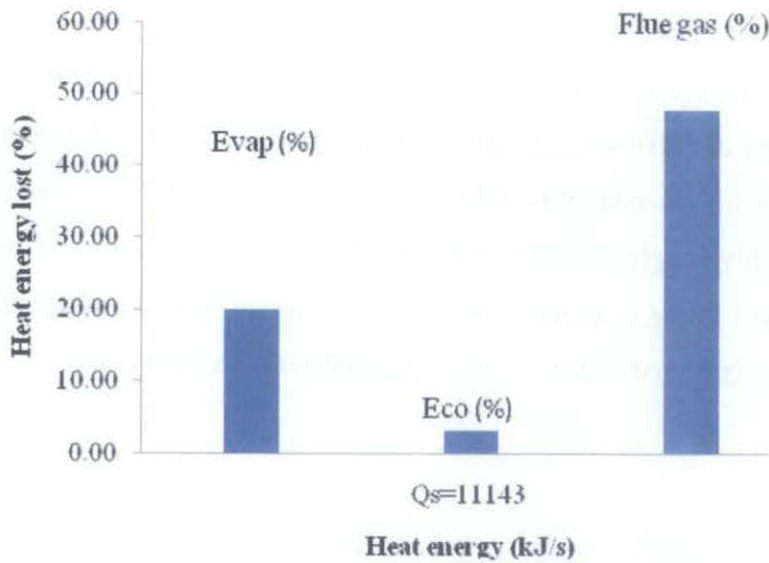


Figure 4.13: Heat energy lost (%) against heat quantity in HRSG components

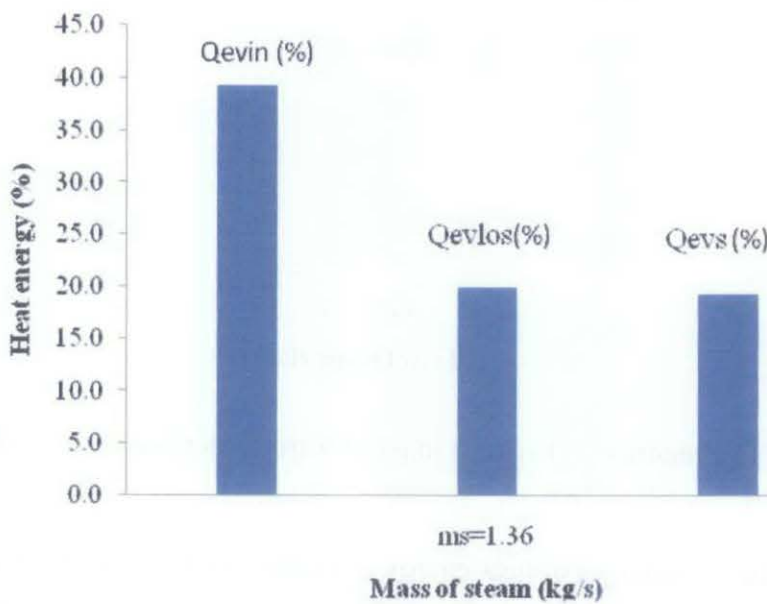


Figure 4.14: Heat energy (%) against mass of the steam (kg/s) in HRSG evaporator

In Figure 4.14 the percentages of heat in the HRSG evaporator is plotted against the steam produced at 1.36 kg/s. Heat lost in the economizer is found to be 3.15% of the total heat supplied to the economizer. The percentage of heat energy entering the HRSG evaporator is higher, the amount of heat lost in the evaporator is higher due to the imbalance of the heat gained by the steam and heat lost in the evaporator, sufficient amount of heat can be gained by the steam at sufficient mass flow rate of steam entering the evaporator. When the mass flow rate of steam is not sufficient

compared to the amount of heat energy supplied into the evaporator, heat lost in the evaporator increases, and the amount of steam produced is lower. The performance of the HRSG is optimum at sufficient amount of steam produced, when the operating parameters are optimum flow rate. When the mass flow rate of saturated water from the economizer is highly supplied to the evaporator the amount of steam produced is higher and the heat lost in the evaporator is lower, as resulted from an adequate heat exchange between the saturated water and heat supplied into the evaporator.

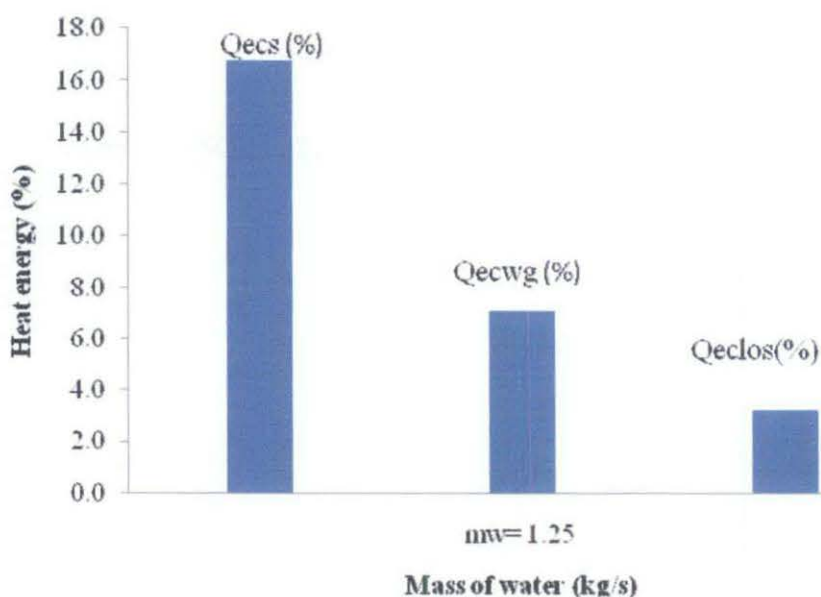


Figure 4.15: Heat energy (%) against mass of warm water (kg/s) in economizer

In Figure 4.15 the percentages of heat energy calculated in the economizer are plotted against the mass flow rate of warm water 1.25 kg/s. The quantification of heat energy in all the system are accomplished by the analytical models. The heat energy percentage supplied to the economizer is higher, but the amount of heat energy gained by the warm water supplied is not sufficiently gained by the warm water, where the remaining heat is lost to the atmosphere by the flue gases. Certainty of heat energy gained by the warm water can be accomplished by monitoring the mass flow rate of warm water entering the economizer. Supplying sufficient amount of warm water into the economizer can increase the amount of heat gained by warm water; as a result heat lost to the atmosphere by the flue gases can be minimized.

4.3.1 Heat lost in HRSG evaporator

The heat energy in the evaporator is not gained completely by the saturated water entering the evaporator. Portion of the heat in the evaporator is lost, increases as the parameters such as the saturated water mass flow rate through the evaporator are not regulated. In Figure 4.16, the heat lost and the heat gained by the steam is related, and it can be seen that heat lost decreases as the heat gained by the steam increase. The heat gained by the steam increased only when the mass flow rate of the saturated water is increase and saturated water temperature is low.

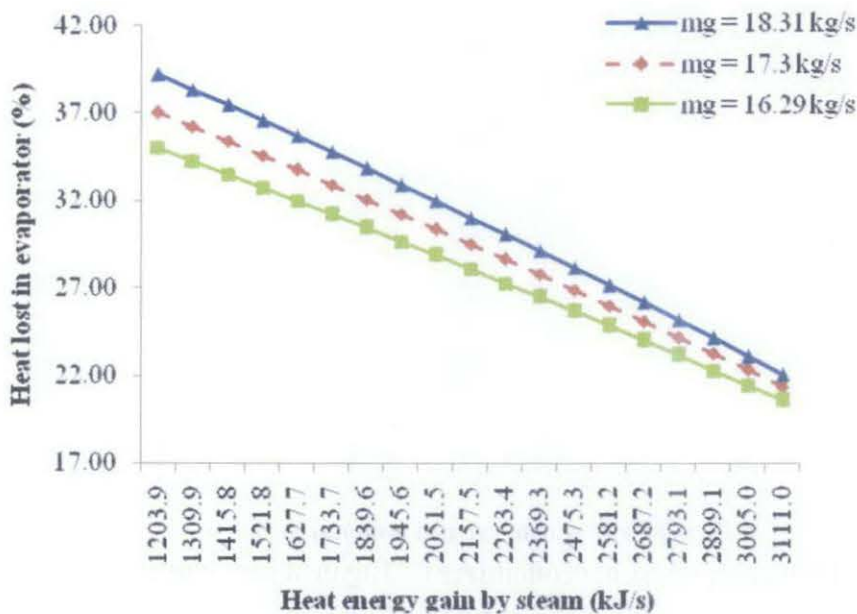


Figure 4.16: Heat energy lost in evaporator (%) against heat gained by steam (kJ/s)

4.3.2 Heat lost in HRSG economizer

In the economizer the heat leaving the evaporator is utilized to heat the warm water that will be supplied to the economizer. The main parameter that needs to be regulated in the economizer is the warm water mass flow rate flowing through the system. The warm water mass flow rate is able to be increased whenever the amount of heat entering the economizer is high. Figure 4.17, shows the relationship between the heat lost in the economizer and the heat gained by the warm water in the economizer. It can be seen that heat energy lost in the economizer decreases at high heat gained by

the warm water. When the temperature leaving the evaporator is high and the mass flow rate of warm water is low, it is found that much heat energy can not be observed by the warm water which can result into heat energy lost in the economizer. To maintain the sufficient usage of heat energy in the economizer the warm water to be heated must be supplied at sufficient rate when the heat energy is high and when the heat supplied is low the warm water supplied must be regulated at low flow rate.

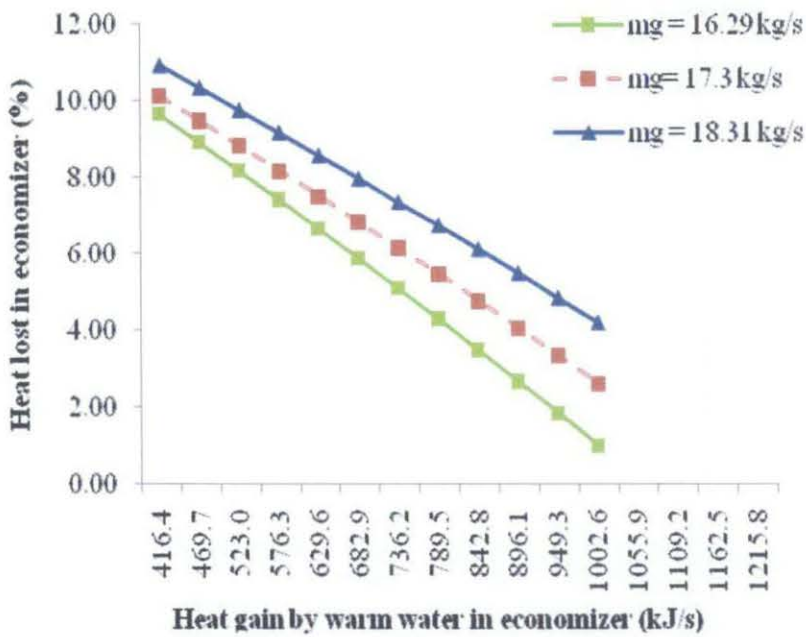


Figure 4.17: Heat energy lost in economizer (%) against heat gained by warm water (kJ/s)

4.3.3 Energy quantities in HRSG

Energy quantification for HRSG of GDC is shown in Figure 4.18. The energy in each process of the HRSG components is identified in a percentage. The energy flow into the evaporator of HRSG is quantified and energy gained by the steam and energy lost in the evaporator is identified. The remaining heat energy from the evaporator is send to the economizer where the percentage of energy gained by warm water is quantified and energy lost in the economizer. The remaining energy which is not gained by warm water can be lost into the atmosphere by the flue gases. Quantification of energy in the components of the HRSG can be useful for monitoring the performance

identification and energy losses. Energy analysis can be accomplished by considering the FoM of the thermal energy storage; FoM can be use as a guideline for energy evaluation. (FOM) is given by Wang [77]

$$FoM = \frac{\dot{Q}_{dis}}{\dot{Q}_{ch}} \quad (3.89)$$

The discharge capacity and charging capacity can be calculated by below equations

$$\dot{Q}_{dis} = \dot{m}_{chw} cp_{chw} (T_r - T_{chws}) \quad (3.90)$$

$$\dot{Q}_{ch} = \dot{m}_{chw} cp_{chw} (T_{ch} - T_{chws}) \quad (3.91)$$

Mass flow rate of chilled water is calculated by

$$\dot{m}_{chw} = V_{chw} \times \rho_{chw} \quad (3.92)$$

Where the density of the chilled water is calculated by [82]

$$\rho_{chw} = (1.49343 \times 10^{-3} - 3.7164 \times 10^{-6} T_{chw} + 7.09782 \times 10^{-9} T_{chw}^2 - 1.90321 \times 10^{-20} T_{chw}^6) \times 10^{-1}$$

The thermal energy capacity equations above can be set for calculating the energy loss, by taking the sum of the difference in the above equations

$$\sum \dot{Q}_{ch} = \sum \dot{Q}_{disch} \quad (3.93)$$

$$Q_{TES,los} = \sum \dot{Q}_{ch} - \sum \dot{Q}_{disch} \quad (3.94)$$

The energy equations above for TES are use for analysis of the system, where energy loses and balance is identified. Identification of imbalance can be the way of managing the operation of the thermal energy storage. The calculation is done based on variation of the operating parameters, so that baseline of the system can be identified on optimum performance. Figure 3.22 shows the computer program flow chart for the TES, the recorded data which are used during calculation are; return chilled water temperature, chilled water temperature, mass flow rate of chilled water, and discharge and charging load. The thermal physical properties of water are calculated namely, specific heat of water, density of water. The mass flow rate of chilled water is calculated and compared to the actual, the calculated mass flow rate of chilled water is closed to the actual value, or the calculation should be repeatedly

done meanwhile certainty in the equations and inputs are properly check. The discharge load is calculated and is compared to the actual value for certainty. The charging load is calculated after the physical properties at charging load is been calculated. The performance of the TES is evaluated by the FoM, where the FoM value is maintained at optimum value. The energy losses in the TES are determined by taking the difference between the charging and discharge load.

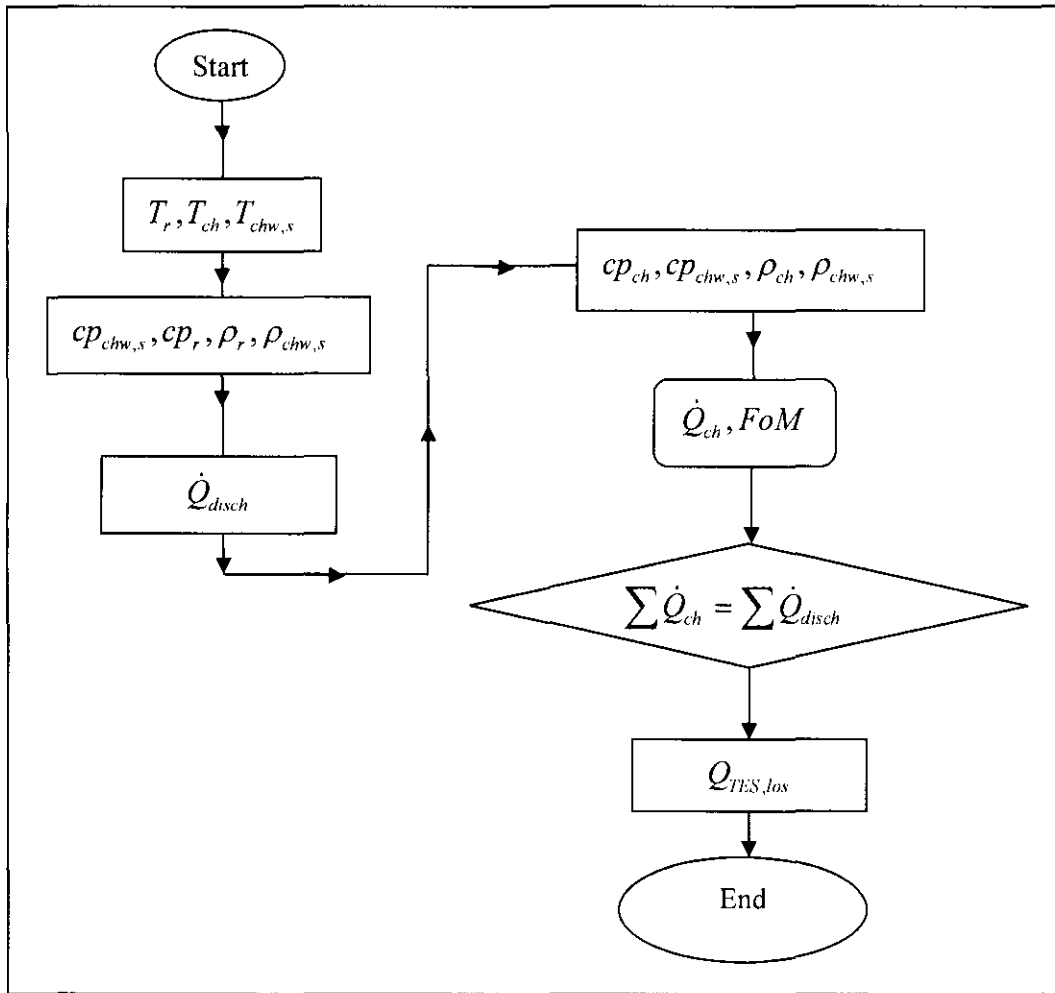


Figure 3.22: Thermal energy storage computer program flow chart

3.9 The simulation of the cogeneration plant

The input to the simulation program requires the specific parameters Table A-1 (appendix) such as the ambient air temperature T_a , compression ratio r_c , mass flow rate of air \dot{m}_a and mass flow rate of fuel \dot{m}_f . The program then solves to find other

parameters, such as specific heat at various temperatures $C_{p_a}, C_{p_{2a}}, C_{p_g}$, isentropic temperatures T_g, T_{2a}, TET and the isentropic efficiencies, η_c, η_t . The program then calculates the various energy input and output of each sub-system. Any inequalities to the first law energy balance would indicate energy losses of the sub-system. The identification of energy conservation can be acquired, and effect of the operating parameters can be managed for optimum performance of the plant. In Figure 3.23 the schematic diagram shows the whole sub-systems and the various energy in the systems.

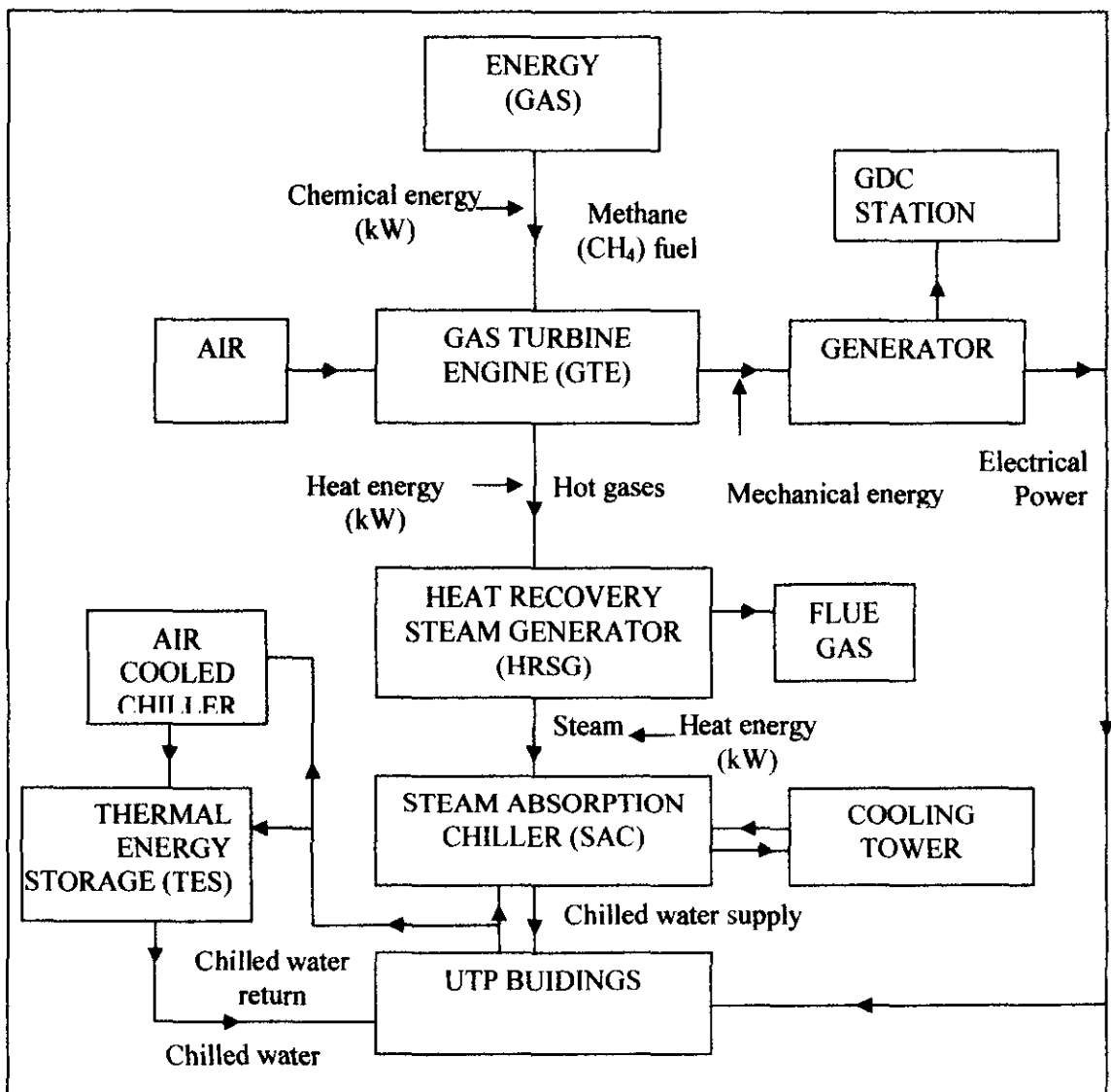


Figure 3.23: Schematic diagram for systems in GDC

CHAPTER 4

RESULTS AND VALIDATION OF THE MODELS

4.1 Validation of the models

Validation of the analytical method for energy audit of cogeneration plant (ATEAC) is performed based on the operating data collected from GDC plant. In order for the ATEAC to be effective its results must be close to the actual data collected from GDC plant. In Figure 4.1, the actual net work obtained from the records of GDC and the calculated net work from the analytical model are plotted against part load ratio.

The correlation plotted shows similarity in the trend between the actual and calculated net work. The net work increases as the part load ratio increases, the increase in the net work and the part load ratio is related to the operating parameters such as inlet air temperature, air mass flow rate and fuel flow rate. Monitoring the flow of the operating parameters at their optimum flow rate increase the net work output.

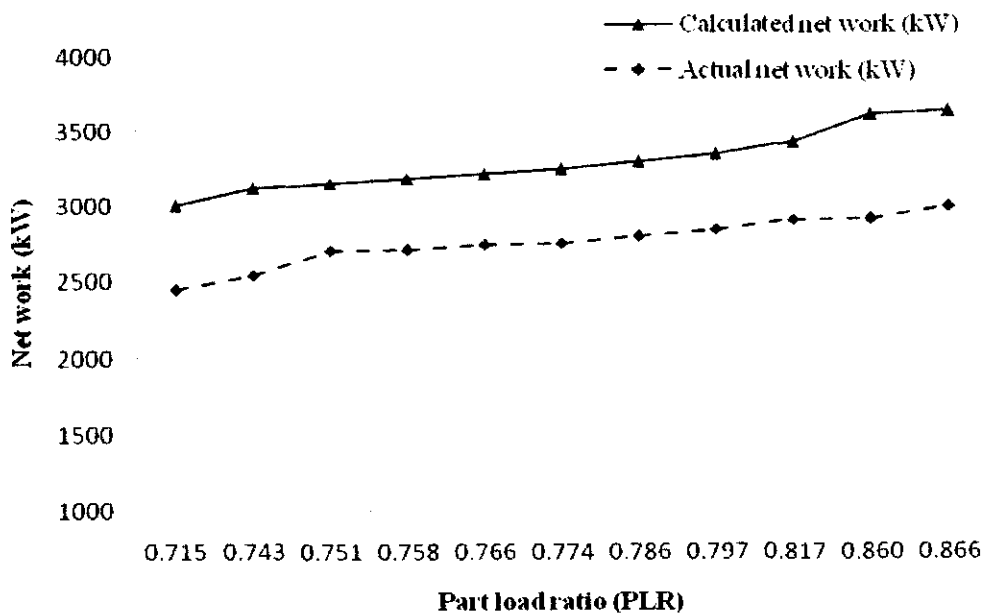


Figure 4.1: Net work (kW) against part load ratio

Validation for the HRSG model is shown in the Figure 4.2, where the steam mass flow rate is plotted against the heat gain by steam. The trend also exhibits a relationship between the calculated and the actual mass flow rate. The relationship between the actual and calculated steam mass flow rate show the same trend but the difference between the calculated and actual mass flow rate of steam is 1.8 kg/s. The calculated mass flow rate of steam increases as the supplied heat to the evaporator is increased.

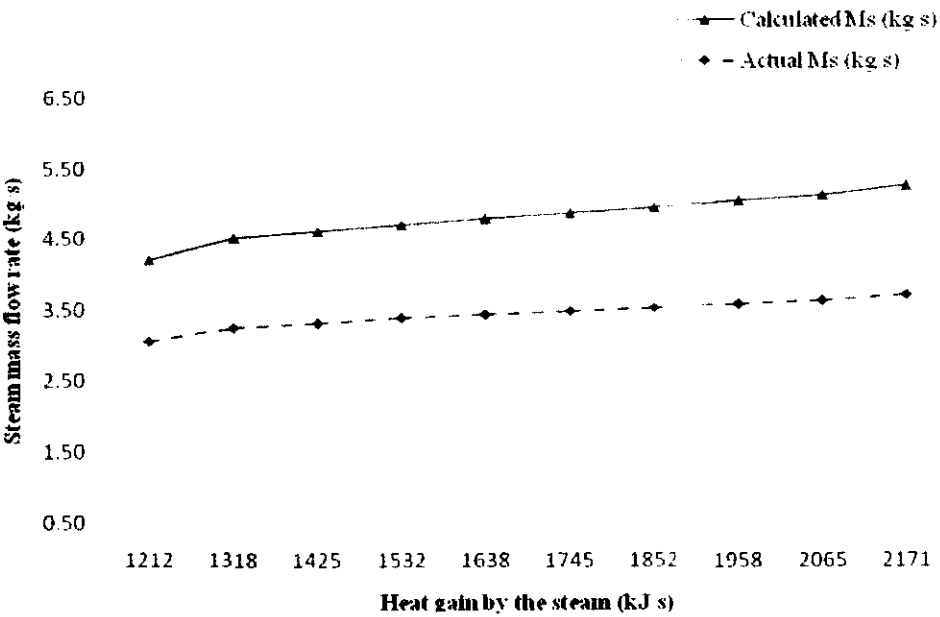


Figure 4.2: Steam mass flow rate (kg/s) against heat gained by steam (kJ/s)

Air cooled chiller validation is performed based on comparing the operating COP and the calculated COP the difference between the actual and calculated value is 0.3. The COP increases as the cooling load of the air cooled chiller is increase as shown in the Figure 4.3. The trend between the actual COP and the calculated are the same, but the difference in the calculated to the actual COP is due to ideal calculation.

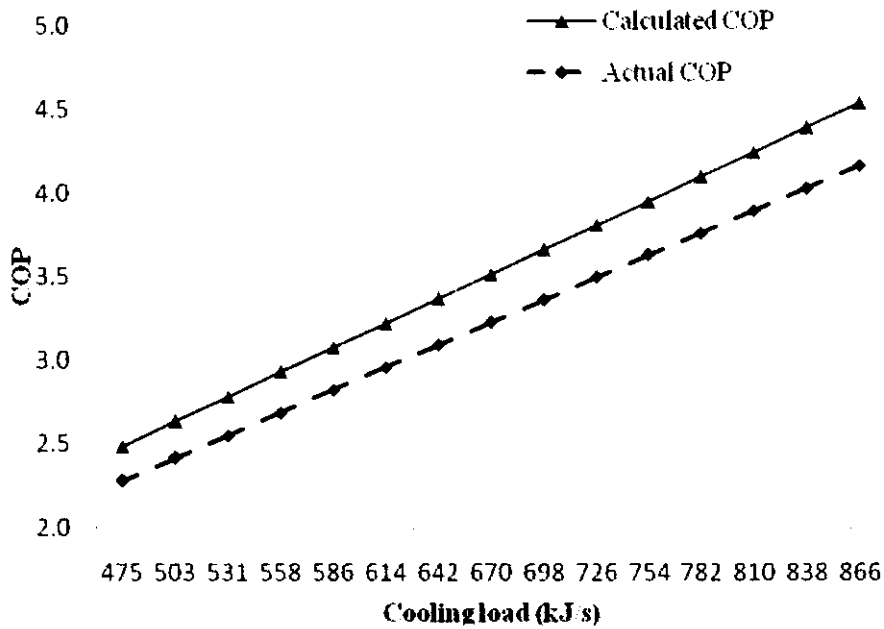


Figure 4.3: Actual and calculated COP against cooling load (kJ/s)

Validation of steam absorption chiller is performed by comparing the main operating parameters of the SAC, i.e. the cooling load and the mass flow rate of steam. The cooling load is plotted against the mass flow rate of the steam as shown in Figure 4.4. The difference between the cooling loads occurred due to specific heats calculations in the steam and chilled water.

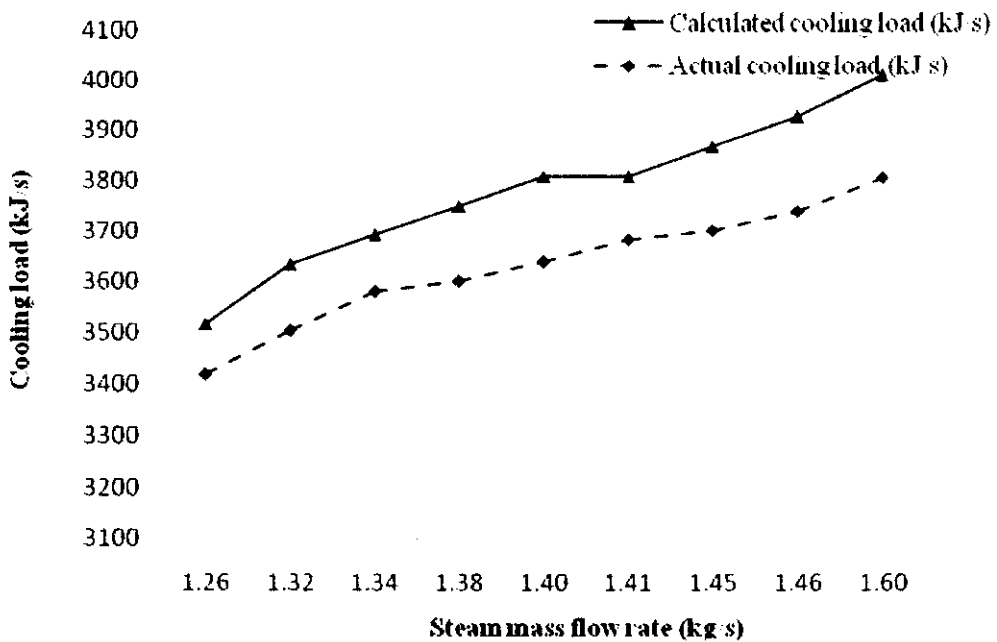


Figure 4.4: Cooling load (kJ/s) against mass flow rate of steam (kg/s)

The results of cooling tower is verified by the design data obtained from the manufacturer catalogue, as the performance of cooling tower is known by its range. The range of the tower in the manufacturer catalogue is 5.2 and the range obtained from the equation (3.74) is 5.6. The cooling tower is also characterized by Lewis factor, which is used for evaluating the performance of tower, increase in the Lewis factor indicates high performance of the tower, the value of Lewis factor is 0.9-1[11]. From the Lewis factor correlation (equation 3.82), the calculated Lewis factor is found to be 0.919-0.922 and at atmospheric pressure.

The results for thermal energy storage are validated by the actual data collected from the GDC plant. The performance of thermal energy storage is known by its Figure of Merit (FoM), which is the base on the charging and discharging of the system. The calculated and actual data of TES are shown in Table 4-1. The calculated charging and discharging load are close to the operating loads obtained from the recorded data of the thermal energy storage.

Table 4-1: Calculated parameters and actual operating parameters of the TES

No.	calculate load (kj/s)		FoM	volume m3/s	act. cooling load(kj/s)		Qlc lost	
	Qch	Qdis			Qch	Qdis	cal. (kj/s)	act. (kj/s)
1	25841.84	25785.81	1.26	0.90	25861.46	25819.27	56.03	42.19
2	24677.57	22843.66	1.13	0.82	25914.21	22872.71	1833.91	3041.49
3	26247.10	19693.06	0.98	0.73	27566.81	19701.13	6554.04	7865.68
4	28069.12	16482.41	0.81	0.65	29490.15	16480.31	11586.71	13009.85
5	28168.38	12697.32	0.70	0.56	29588.61	12696.91	15471.06	16891.70
6	30336.65	9833.69	0.54	0.48	31522.50	9859.35	20502.96	21663.15
7	33161.40	5251.68	0.38	0.37	34465.54	5263.71	27909.72	29201.83
8	35178.02	2030.01	0.28	0.32	36184.95	2032.35	33148.01	34152.60

4.2 Results from gas turbine engine model analysis

The actual performance of the gas turbine engine on the period February 2008 is shown in the Figure 4.5. It can be observed that the power output of the gas turbine engine fluctuates due to the variation of fuel flow rate to output power. For an example, when the fuel flow rate is 0.313 kg/s, the power output is 2275 kW. However, when the fuel flow rate decreases to 0.222 kg/s, power output is 3334 kW.

This show that reducing the fuel does not necessarily reduces the power but there are other factors that influenced the production of power. One possible factor is the inlet air temperature to the air compressor of the gas turbine engine. Figure 4.6 shows the relationship between the same power output as shown in Figure 4.5 to the air inlet temperature to the air compressor. The results show that the power does not increase as the inlet air reduces, hence, it doesn't reveal the real relationship of ambient temperature and net work of gas turbine engine. Hence, there are other parameters that have effects on the net work of the gas turbine. Theoretically of net work output against the ambient temperature entering the air compressor of the gas turbine engine must have a trend similar to graph shown in Figure 4.7, where the net work varies only due to the variation of ambient temperature entering air compressor. The calculated and actual parameters of gas turbine engine can be found in the Table A-2 (appendix).

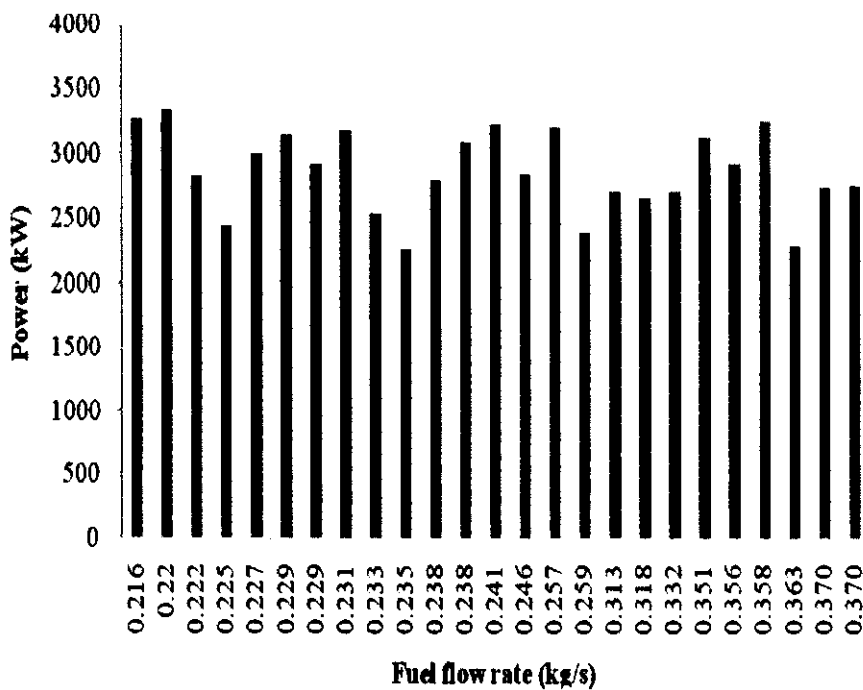


Figure 4.5: Power (kW) against fuel flow rate (kg/s)

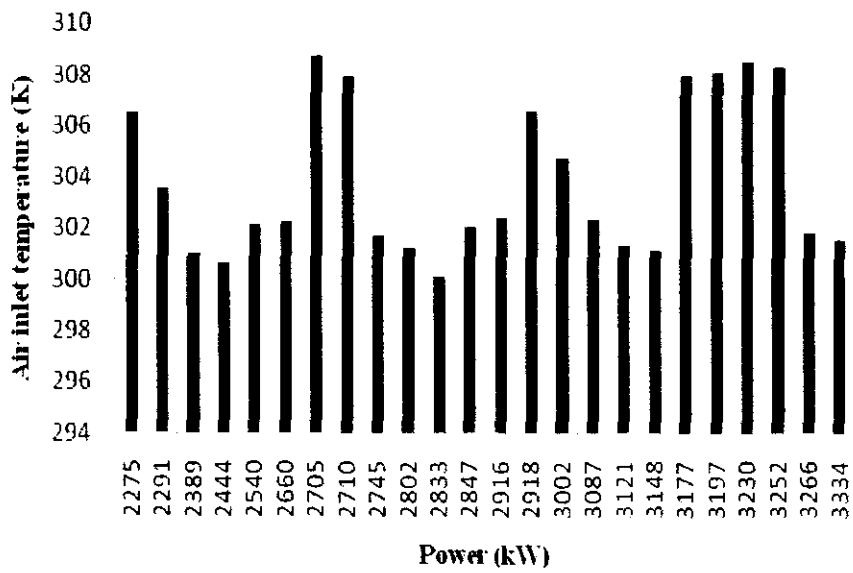


Figure 4.6: Actual power (kW) against the inlet air temperature (K)

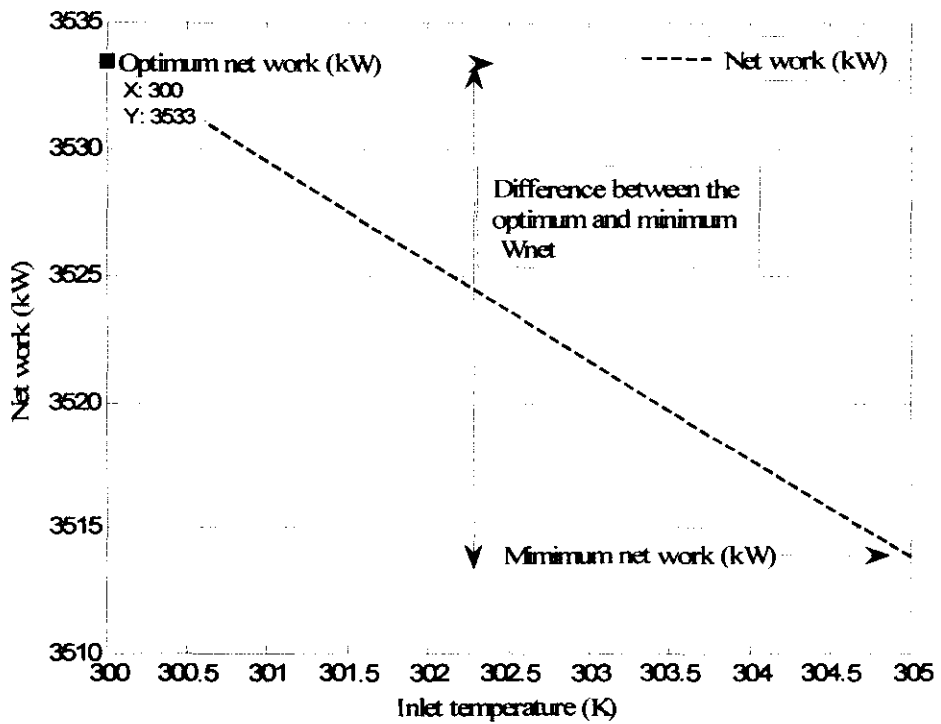


Figure 4.7: Calculated power (kW) against inlet air temperature (K) [87]

The main operating parameters that have effect on the gas turbine engine are, air mass flow rate, inlet air temperature, fuel flow rate and the compression ratio. The energy losses experienced in gas turbine engine components are shown in the Figure 4.8. These losses are obtained from the recorded data of plant and are used as inputs to the analytical models. The results from the models were compared to the actual data to determine the energy losses. From the operating data, the net work of the turbine is 3334 kW when the mass flow rate of fuel is 0.26 kg/s and mass flow rate of air is 15 kg/s, for an inlet temperature of 301.25 K. The program shows that when the inlet air temperature is at 309 K with an air mass flow rate of 14 kg/s and a mass flow rate of fuel 0.26 kg/s, an optimum net work of 3533 kW can be produced. This is an increase of 5.64% from the actual net work. When the actual net work of the gas turbine is 2902 kW at inlet temperature of 302.4 K and mas flow rate of fuel is 0.227 kg/s, it is found that the net work decreases by 17.9% from the optimum point. To maintain the perfomance of the gas turbine at optimum, the mass flow rate of air must be maintained at 14 kg/s and the fuel flow rate at 0.26 kg/s.

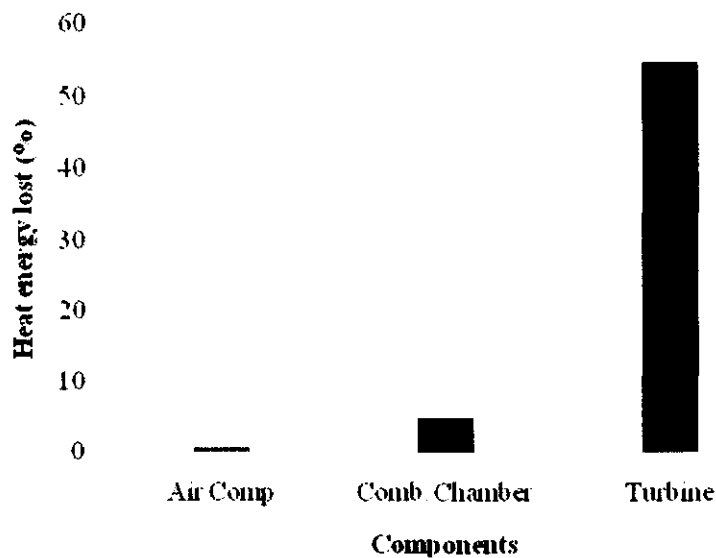


Figure 4.8: Heat energy lost (%) against gas turbine engine components

4.2.1 Energy lost in air compressor

The work input to drive the air compressor in gas turbine engine is obtained from the turbine work output. In Figure 4.9, energy lost in air compressor is plotted against the

ambient temperature, the energy losses in air compressor increase at both higher ambient temperature and air mass flow rate. Air compressor work can be minimized when the air inlet temperature and mass flow rate are minimized at low level. The energy that can be saved from air compressor is 0.77 kW, at the inlet air temperature of 304.3 K and air mass flow rate of 15 kg/s.

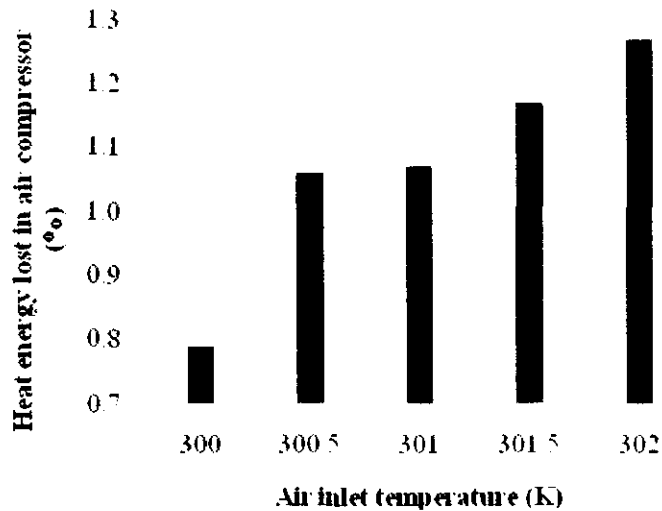


Figure 4.9: Heat energy lost (%) in air compressor against air inlet temperature (K)

4.2.2 Energy lost in combustion chamber

The energy release is due to the combustion of the fuel and the compressed air. Assuming no heat transfer through the CC, the energy leaving the CC is equal to the energy of combustion. The energy losses in the combustion chamber is found to be 5%. High mass flow rate of air can minimize the energy loss in the combustion chamber, as this would introduce more air required for combustion. The unburnt air in the combustion chamber acts as a coolant. In the Figure 4.10, the energy loss decreases as the air mass flow rate increases. Increased in the air mass flow rate reduces the temperature of the hot gases. The mass of hot gases is the result of the fuel mass flow rate and air mass flow rate burned in the combustion chamber.

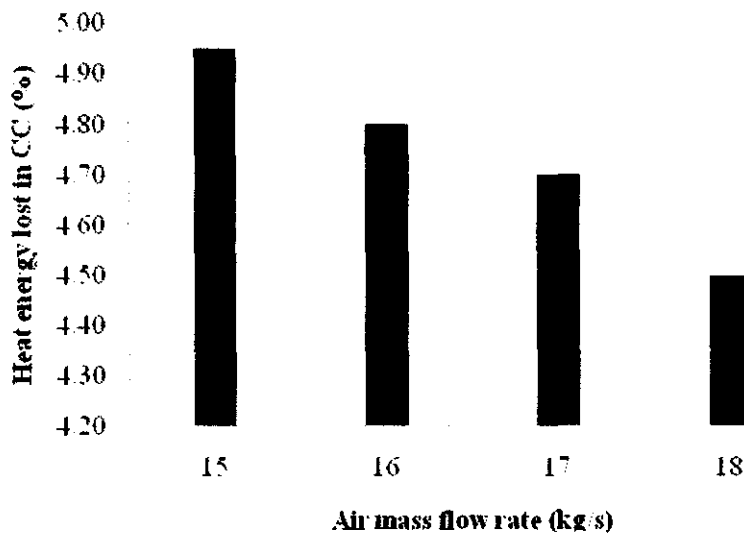


Figure 4.10: Heat energy lost in combustion chamber (%) against air mass flow rate (kg/s)

4.2.3 Heat energy lost in turbine

The performance of turbine is guided by the turbine inlet gas temperature, mass flow rate of burned gases, and the energy consumed to drive the air compressor. In Figure 4.11, the heat energy lost in the turbine is related to the heat energy entering the turbine. The heat exhaust from the turbine is considered the energy lost from the turbine, although it is use in the heat recovery steam generator. It is found that the heat energy lost from the turbine increases due to the increase of mass flow rate of hot gases. Heat energy entering the turbine is high also due to minimum air mass flow rate, where high turbine inlet temperature is acquired, as a result the high work is obtained from the turbine.

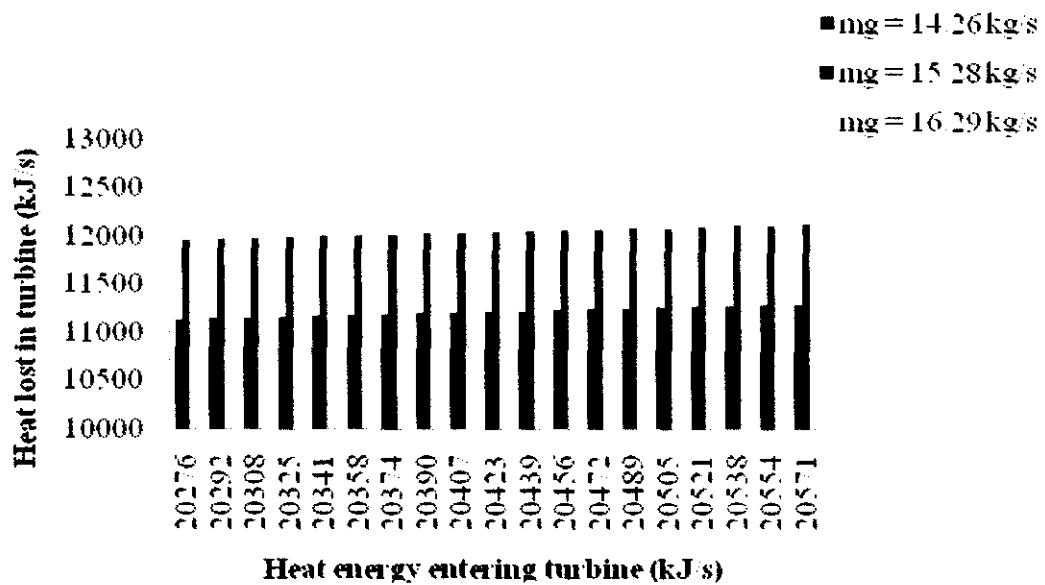


Figure 4.11: Heat energy (kJ/s) entering turbine against turbine energy lost (kJ/s)

4.2.4 Net work and part load ratio

It is customary to show the performance of a gas turbine engine at part load. Part load ratio is defined as the ratio of net work output and the nominal net work. The net work obtained in gas turbine engine is the turbine work minus the compressor work. Air compressor is one of the components in gas turbine engine which consumes most of the turbine work.

In Figure 4.12, the net work is plotted against part load ratio. Net work increases as the part load ratio increases, at minimum air mass flow rate the content of heat energy results from combustion chamber is higher at temperature which results into high net work output. Monitoring the air mass flow rate at optimum can maintain the thermal heat energy at high level. As a result the energy that can drive the turbine is high and eventually the net work is optimum. It is found that when the inlet temperature to air compressor decreases by 1 K the net work increases by 0.11%.

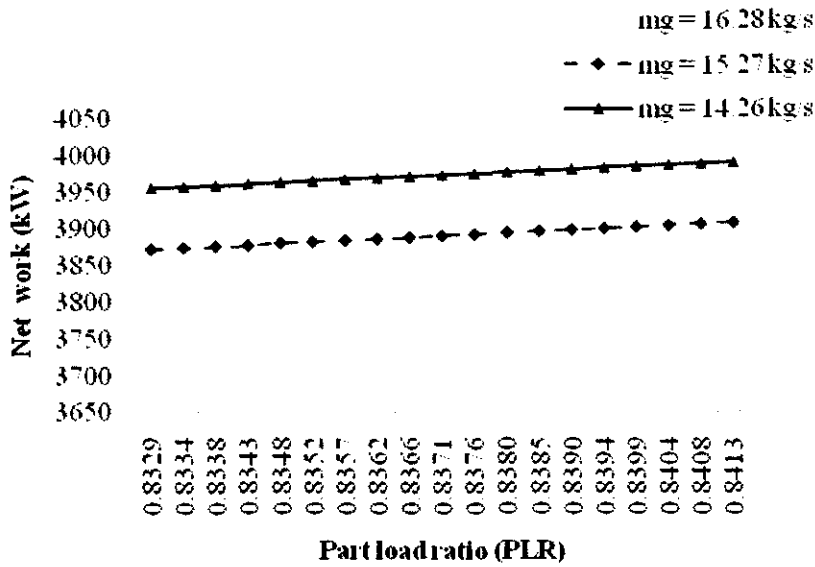


Figure 4.12: Net work (kW) against part load ratio

4.3 Results from heat recovery steam generator (HRSG) model analysis

The performance of HRSG depends on the performance of the various sub-systems such as evaporator and economizer. The energy balance in the HRSG components varies with the change of the parameters. Energy supplied to the evaporator is 38.94% at turbine exhaust temperature 728.23 K and mass flow rate of hot gases 14.26 kg/s, where 10.88% of energy supplied is gain by the steam and 28.06% is lost in the evaporator. The steam is produced at the mass flow rate of 2.24 kg/s and at steam temperature 458 K.

Energy entering the economizer is 10.21%, where the energy supplied to heat the warm water is 3.15% at warm water mass flow rate 2.69 kg/s and warm water temperature 358 K, where 7.06% of total energy in the economizer is lost. Energy lost in economizer decreases by 0.78% when the mass flow rate of warm water is increased by 0.16 kg/s. The percentage increase of energy gain by warm water in economizer is 0.84% at the same mass flow rate of warm water. In Figure 4.13 heat energy lost in the evaporator and economizer and flue gas lost are plotted. Heat supplied to the heat recovery steam generator is calculated 11.143 MW.

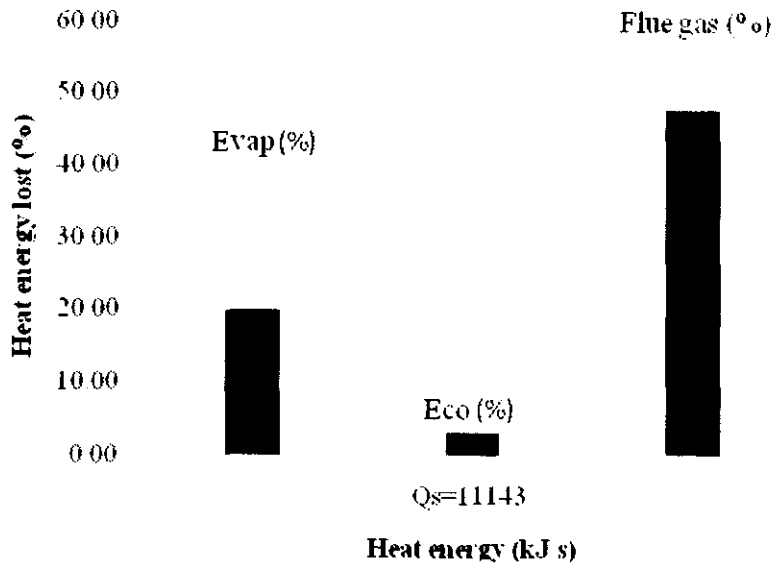


Figure 4.13: Heat energy lost (%) against heat quantity in HRSG components

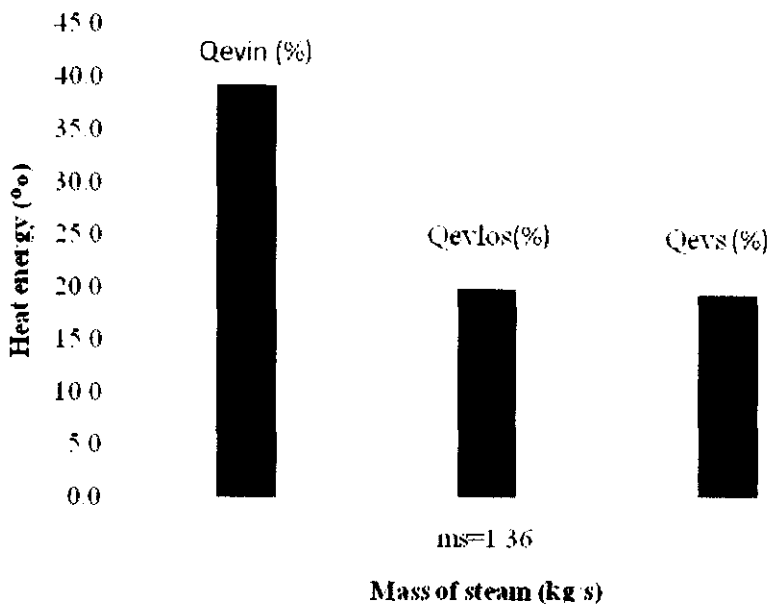


Figure 4.14: Heat energy (%) against mass of the steam (kg/s) in HRSG evaporator

In Figure 4.14 the percentages of heat in the HRSG evaporator is plotted against the steam produced at 1.36 kg/s. Heat lost in the economizer is found to be 3.15% of the total heat supplied to the economizer. The percentage of heat energy entering the HRSG evaporator is higher, the amount of heat lost in the evaporator is higher due to the imbalance of the heat gained by the steam and heat lost in the evaporator, sufficient amount of heat can be gained by the steam at sufficient mass flow rate of steam entering the evaporator. When the mass flow rate of steam is not sufficient

compared to the amount of heat energy supplied into the evaporator, heat lost in the evaporator increases, and the amount of steam produced is lower. The performance of the HRSG is optimum at sufficient amount of steam produced, when the operating parameters are optimum flow rate. When the mass flow rate of saturated water from the economizer is highly supplied to the evaporator the amount of steam produced is higher and the heat lost in the evaporator is lower, as resulted from an adequate heat exchange between the saturated water and heat supplied into the evaporator.

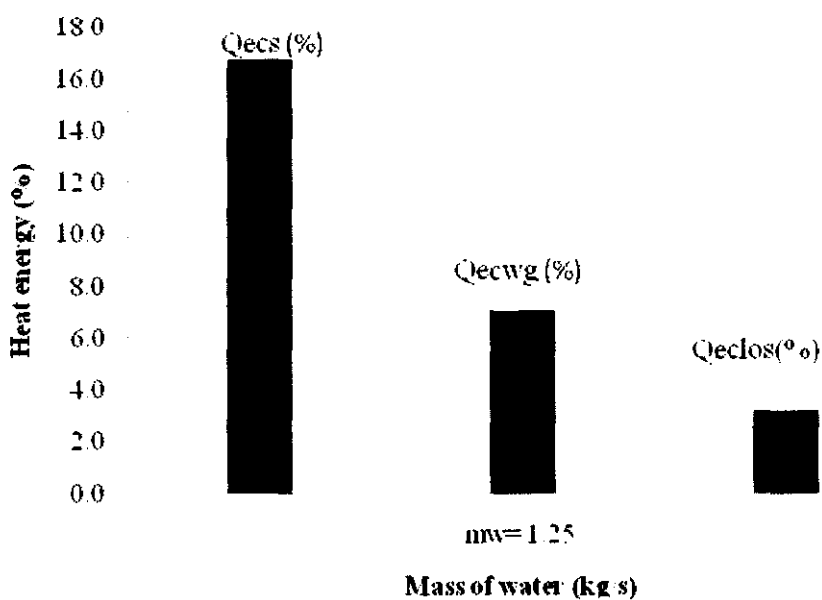


Figure 4.15: Heat energy (%) against mass of warm water (kg/s) in economizer

In Figure 4.15 the percentages of heat energy calculated in the economizer are plotted against the mass flow rate of warm water 1.25 kg/s. The quantification of heat energy in all the system are accomplished by the analytical models. The heat energy percentage supplied to the economizer is higher, but the amount of heat energy gained by the warm water supplied is not sufficiently gained by the warm water, where the remaining heat is lost to the atmosphere by the flue gases. Certainty of heat energy gained by the warm water can be accomplished by monitoring the mass flow rate of warm water entering the economizer. Supplying sufficient amount of warm water into the economizer can increase the amount of heat gained by warm water; as a result heat lost to the atmosphere by the flue gases can be minimized.

4.3.1 Heat lost in HRSG evaporator

The heat energy in the evaporator is not gained completely by the saturated water entering the evaporator. Portion of the heat in the evaporator is lost, increases as the parameters such as the saturated water mass flow rate through the evaporator are not regulated. In Figure 4.16, the heat lost and the heat gained by the steam is related, and it can be seen that heat lost decreases as the heat gained by the steam increase. The heat gained by the steam increased only when the mass flow rate of the saturated water is increase and saturated water temperature is low.

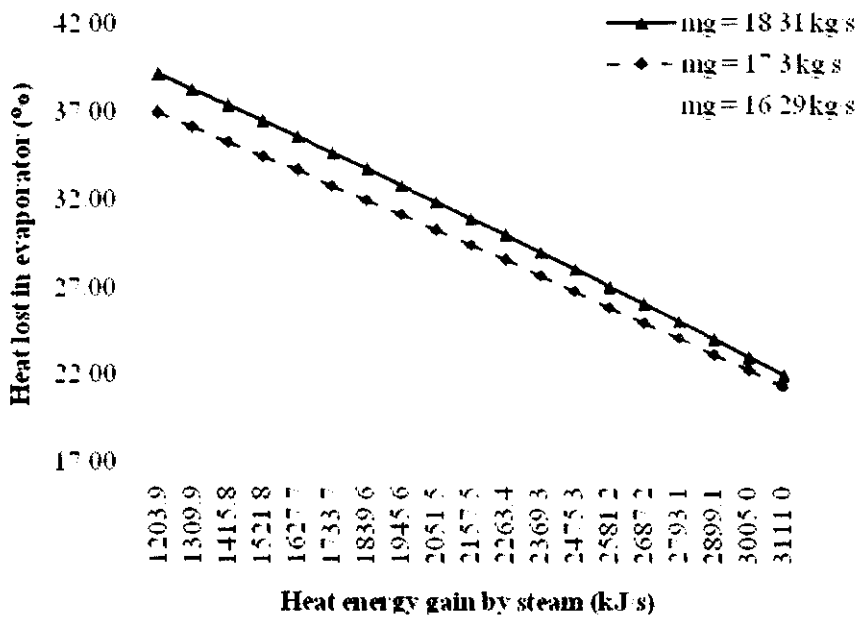


Figure 4.16: Heat energy lost in evaporator (%) against heat gained by steam (kJ/s)

4.3.2 Heat lost in HRSG economizer

In the economizer the heat leaving the evaporator is utilized to heat the warm water that will be supplied to the economizer. The main parameter that needs to be regulated in the economizer is the warm water mass flow rate flowing through the system. The warm water mass flow rate is able to be increased whenever the amount of heat entering the economizer is high. Figure 4.17, shows the relationship between the heat lost in the economizer and the heat gained by the warm water in the economizer. It can be seen that heat energy lost in the economizer decreases at high heat gained by

the warm water. When the temperature leaving the evaporator is high and the mass flow rate of warm water is low, it is found that much heat energy can not be observed by the warm water which can result into heat energy lost in the economizer. To maintain the sufficient usage of heat energy in the economizer the warm water to be heated must be supplied at sufficient rate when the heat energy is high and when the heat supplied is low the warm water supplied must be regulated at low flow rate.

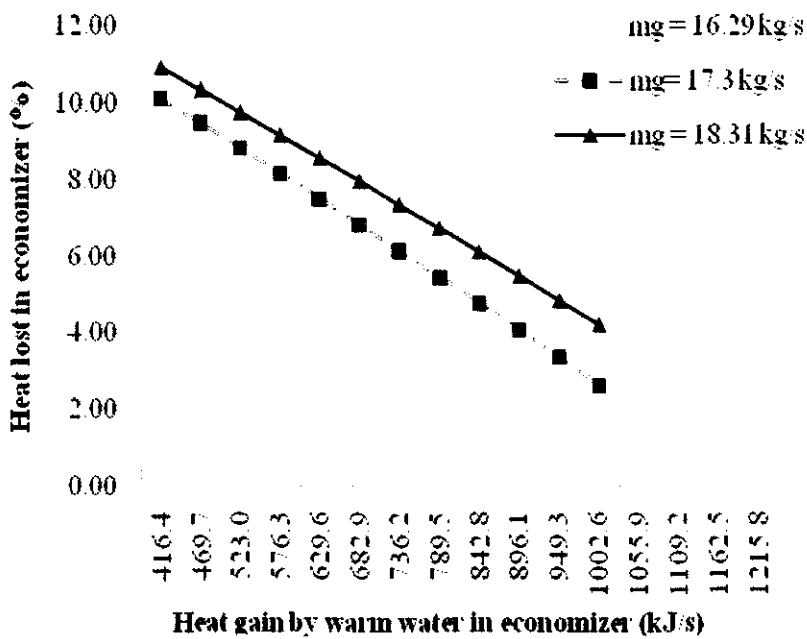


Figure 4.17: Heat energy lost in economizer (%) against heat gained by warm water (kJ/s)

4.3.3 Energy quantities in HRSG

Energy quantification for HRSG of GDC is shown in Figure 4.18. The energy in each process of the HRSG components is identified in a percentage. The energy flow into the evaporator of HRSG is quantified and energy gained by the steam and energy lost in the evaporator is identified. The remaining heat energy from the evaporator is send to the economizer where the percentage of energy gained by warm water is quantified and energy lost in the economizer. The remaining energy which is not gained by warm water can be lost into the atmosphere by the flue gases. Quantification of energy in the components of the HRSG can be useful for monitoring the performance

of the system at optimum level, where energy losses can be minimized to upgrade the operation of the system. Identification of energy quantities in the systems can be the technique of energy management of the cogeneration plant.

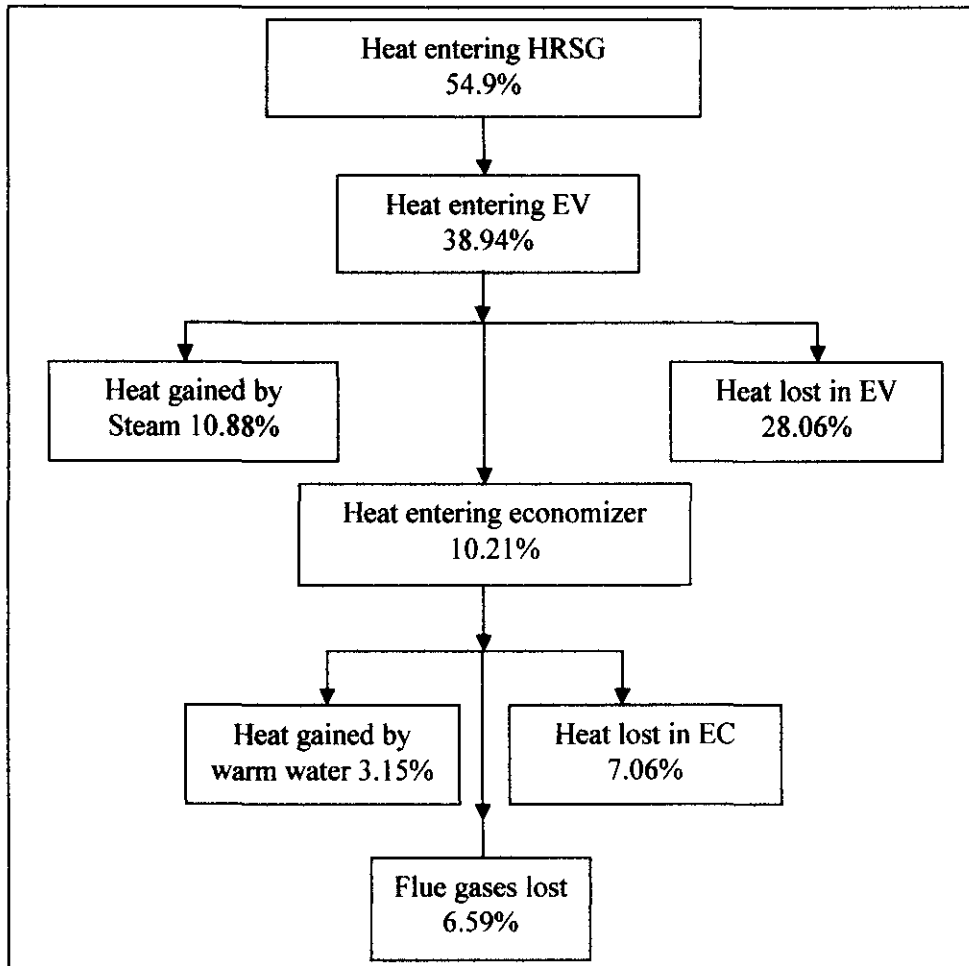


Figure 4.18: Heat energy quantities in the HRSG

4.4 Results from steam absorption chiller (SAC) model analysis

The performance of steam absorption chiller (SAC) is characterized by its cooling load and COP. Variation of the chilled water entering the evaporator, steam mass flow rate entering the high generator and the cooling water entering the absorber and the condenser identify energy lost when the mass flow rate is not balanced with the refrigerant mass. Energy exchanges in SAC involved heat rejection in absorber and condenser which is equal to the heat gain by the cooling water. Due to the energy losses in the absorber and the condenser; the total heat to be rejected is not equal to

the heat gained by the cooling water in the absorber and condenser. The energy lost in the absorber is found to be 17.78% at the cooling water mass flow rate 210 kg/s and refrigerant mass flow rate 2.03 kg/s and in the condenser the energy lost is 25.8% of the total energy lost in the SAC system.

Energy lost in the evaporator is found to be 4.49% at cooling load 3310 kW and chilled water mass flow rate 144.5 kg/s and in the high temperature generator the energy lost is 51.35% at steam mass flow rate 9.03 kg/s. Energy balance of the SAC is the total heat supplied by the high temperature generator and evaporator which must be equal to the total heat sink in the absorber and condenser. The energy in SAC is not balanced and the difference is 2.72-3.07 kJ/s; which is the imbalance energy in the whole system of SAC at the optimum operation. The coefficient of performance of the SAC is calculated 1.13 and is compared to the actual coefficient of performance which is 1.12.

4.4.1 Heat lost in SAC components

The percentage of heat losses in the steam absorption chiller components are shown in Figure 4.19. High heat energy is lost in the high generator of SAC as the source of heat energy is generated in the high generator. To reduce the heat losses in the steam absorption chiller the mass flow rate of the chilled water and the cooling water must be regulated. The heat energy balance of the SAC is the heat energy supplied by the evaporator and generator which must be equal to the heat energy rejected by the absorber and condenser.

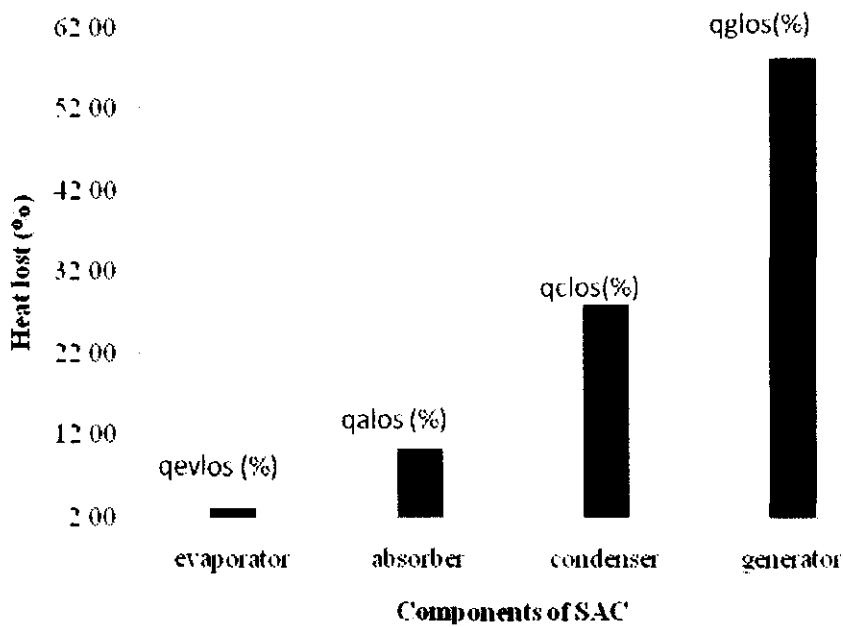


Figure 4.19: Heat lost (%) against the components of SAC

The performance of the absorber and condenser in SAC is optimum when they reject sufficient heat content required from the system. It is found that the heat rejection in absorber is higher compared to condenser as shown in Figure 4.20. High heat is rejected in absorber due to cooling water supplied to absorber first and then the cooling water leaving the absorber is sent to condenser.

The water leaving the absorber is already heated by the heat in the absorber. By using the water leaving the absorber to reject heat in condenser, the amount of heat rejected is low. Due to minimum heat rejection in condenser, heat lost content is high as shown in Figure 4.21. To increase heat rejection in condenser the mass flow rate of cooling water must be increased, as a result the content of heat rejection can be at high rate.

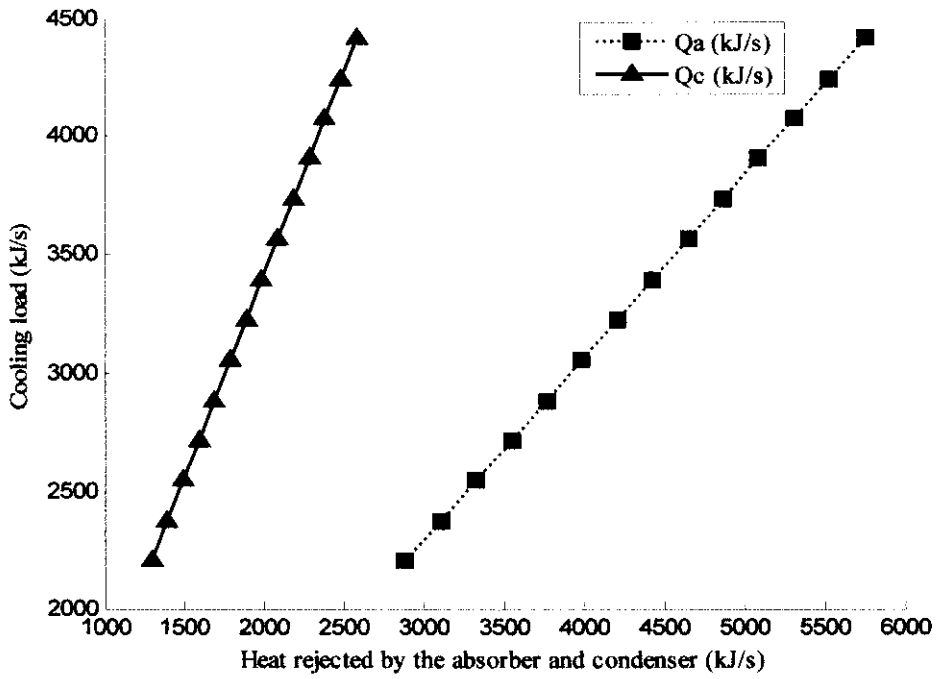


Figure 4.20: Heat rejected by condenser and absorber (kJ/s) against cooling load (kJ/s)

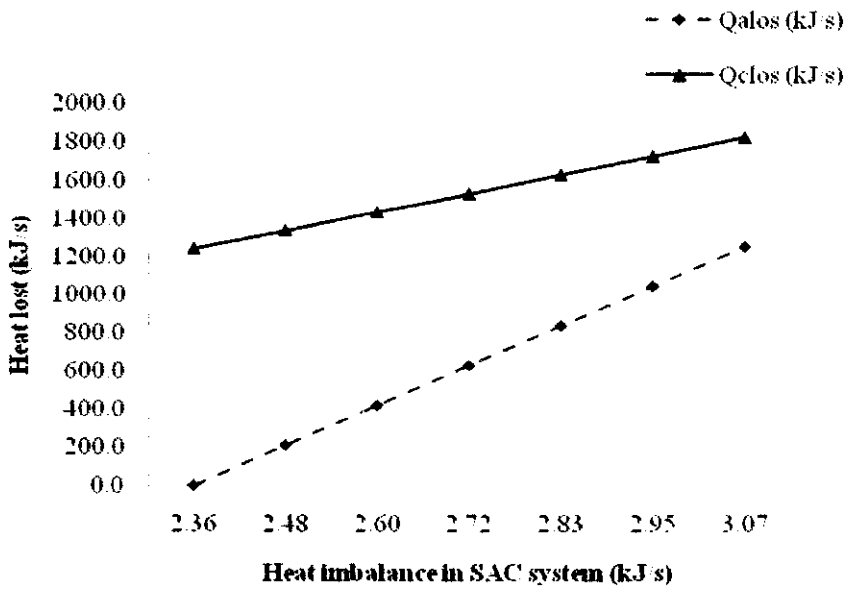


Figure 4.21: Heat energy lost (kJ/s) in condenser and absorber against heat imbalance in SAC system (kJ/s)

Increasing the refrigerant mass flow rate increases the heat absorption by the refrigerant and as a result the heat lost inside the component can be minimized. The refrigerant mass flow rate must relate to the steam mass flow rate in high generator and mass flow rate of cooling water in condenser and absorber.

Figure 4.22 shows the heat lost in high generator and condenser, the main two components that experience high heat lost. Higher heat lost can occur in high generator because the exchange of heat supplied and the refrigerant mass flow rate in high generator is not complete. Hence the refrigerant which is to be vaporized in the high generator is not sufficient for the amount of heat supplied. Heat lost in the components can be minimized when the balance of heat and mass is accomplished in the components.

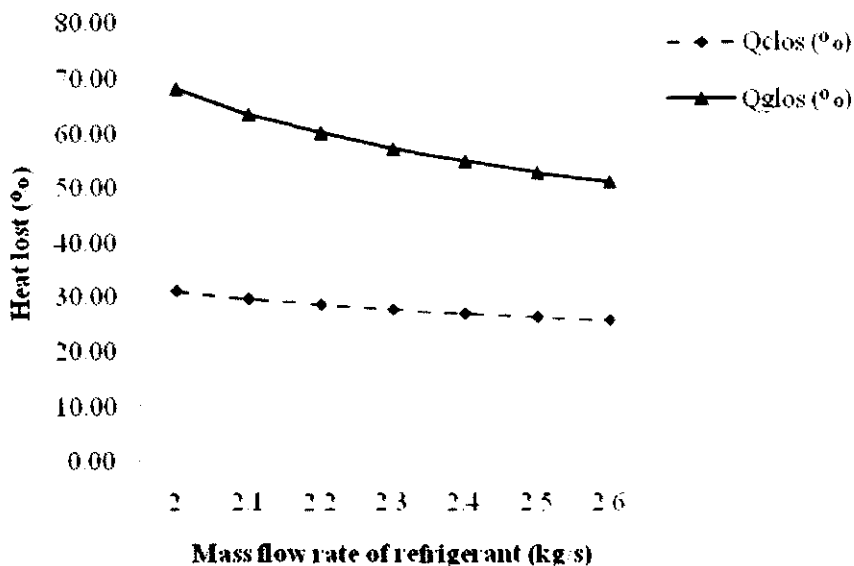


Figure 4.22: Heat energy lost (kJ/s) against mass flow rate of the refrigerant (kg/s)

Heat balance in absorber and evaporator of SAC can be seen in Figure 4.23, as it is shown the heat lost in the components increases as the heat balance between the components of the SAC is increasing. The main issue in the SAC system is to balance the heat energy, maintaining the heat balance can increased the performance of the system. Comparing the percentage of heat lost in the absorber and evaporator, the heat lost in the absorber is higher compared to heat lost in the evaporator, due to sufficient

amount of heat is sent to the absorber to be rejected to the cooling water. To ascertain sufficient rejection of heat to the cooling water in the absorber, the cooling mass flow rate should be at higher flow rate and the temperature of the cooling water should be at lower temperature.

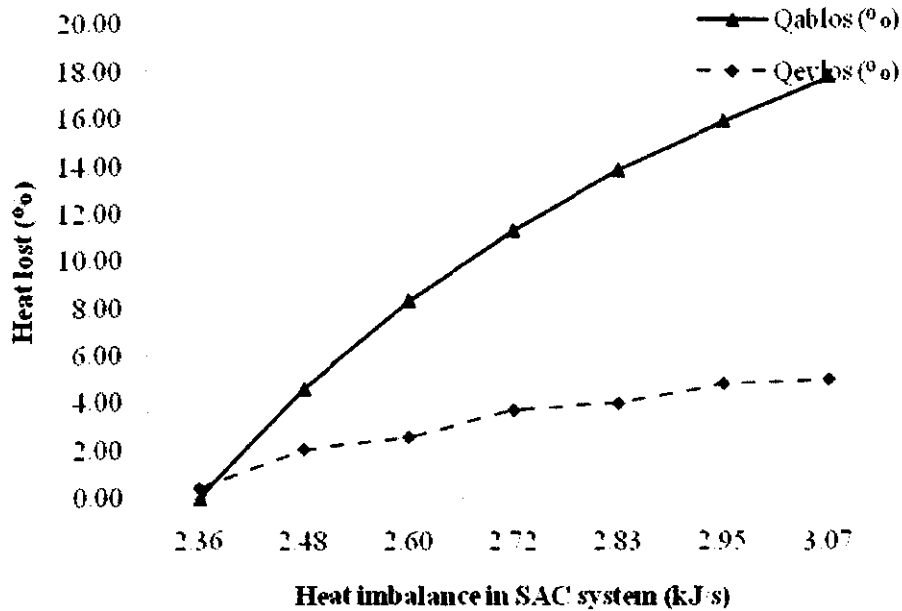


Figure 4.23: Heat energy lost (%) against heat imbalance in SAC (kJ/s)

4.5 Results from air cooled chiller (ACC) model analysis

There are three places where potential energy losses occur. First is in the condenser where the un-rejected energy is 54.1% of the total heat energy in ACC. Energy which is un-rejected in the air cooled condenser increases when the air mass flow rate increases by 0.1% and at increasing air inlet temperature of 1-1.5 K. Second component is the evaporator where the energy lost is 16.5% of the total energy lost in the ACC. When the mass flow rate of chilled water is increased by 0.02% the energy lost in the evaporator is reduced by 1.7%. The third component in the air cooled chiller is the screw compressor where the amount of energy lost is 3.5%.

The energy exchange in ACC evaporator is heat supplied by the chilled water to evaporator which is equal to the heat gain by the refrigerant and heat lost in the evaporator. Heat energy exchange in air cooled condenser is the heat supplied by the working refrigerant, which is equal to the heat rejected from the air cooled condenser

and heat lost inside air cooled condenser. In compressor energy balance is the power used by the compressor which must be equal to heat energy gained by the refrigerant vapor and energy losses. Energy lost in air cooled chiller condenser can be decreased by 5.74-7.3% when the inlet air temperature is decreased by 1-1.5 K.

4.5.1 Heat lost in ACC components

Heat losses in the ACC components are shown in the Figure 4.24, the maximum heat lost is found in air cooled condenser. Air cooled condenser is a component which rejects the total heat from the air cooled chiller. Heat removed from the evaporator and compressor of the air cooled chiller is to be sent to air cooled condenser where it is rejected to the surrounding. Heat energy lost in air cooled condenser occurs when the supplied air mass flow rate to cold the air cooled condenser is high and the air inlet temperature is high. The amount of heat energy lost in evaporator is high when the chilled water mass flow rate is high compared to the mass flow rate of the refrigerant in the evaporator.

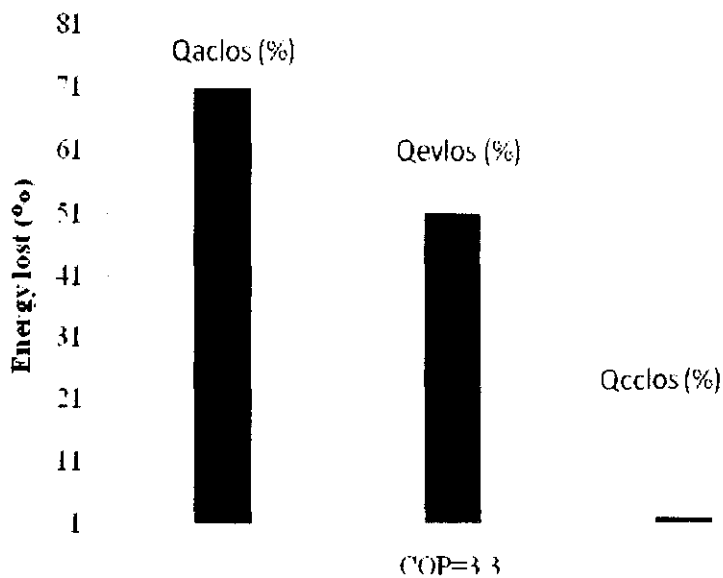


Figure 4.24: Heat energy lost (%) against COP

4.5.2 Heat lost in ACC condenser

The performance of air cooled condenser in the ACC can be controlled by two parameters which are the air inlet temperature and air mass flow rate entering the air cooled condenser. Increased in air mass flow rate and air inlet temperature can increased the heat losses inside the air cooled condenser as shown in Figure 4.25. The decreased of heat losses is simply because the air is at high temperature which can not removed sufficient heat energy to the surrounding. Increase in air mass flow rate is vital at lower air inlet temperature when sufficient heat can be rejected to the surrounding due to sufficient air mass flow rate at low air inlet temperature. The percentage of heat lost in the air cooled condenser can be reduced by controlling air mass flow rate and air inlet temperature.



Figure 4.25: Heat energy lost (%) in air cooled condenser against air inlet temperature (K)

In Figure 4.26 the heat lost in the air cooled condenser is graphed against the heat removed from the the air cooled condenser. The heat remove from the air cooled condenser decreases when the heat energy lost inside the condenser increases. The heat lost inside the condenser increased because the air inlet temperature is high. Air inlet temperature is one of the parameter which can be monitored inorder to acquire the optimum performance of air cooled condenser. At higher temperature of the air

inlet temperature to air cooled condenser the cooling of the air cooled condenser can not be adequately, due to higher temperature of the air inlet. As a result the amount of rejected heat in the air cooled condenser can not be sufficiently accomplished and the unrejected heat in the air cooled condenser increases. Air cooled condenser is the main component in the air cooled chiller to be working at the optimum performance, so that the COP of air cooled chiller can be at optimum. The main operating parameters of the air cooled condenser, which can be monitored are the mass flow rate of air and air inlet temperature. Monitoring the main parameters in air cooled condenser at optimum flow, the performance of the air cooled condenser can be optimized.

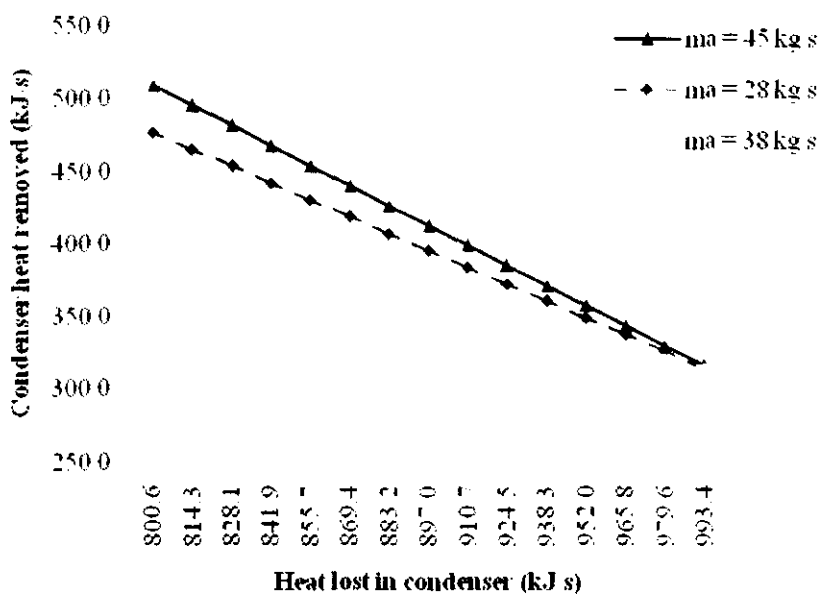


Figure 4.26: Heat energy lost in air cooled condenser (kJ/s) against heat removed (kJ/s)

4.5.3 ACC evaporator performance and heat losses

The main parameters of air cooled chiller performance are the coefficient of performance and the cooling load. As plotted in Figure 4.27, the cooling load increases as the COP is increased. The main parameter that control both the COP and cooling load is the mass flow rate of the chilled water entering the evaporator. To acquire the optimum cooling load, the mass flow of chilled water rate must be regulated. As a result the amount of the refrigerant can evaporate the sufficient chilled

water entering evaporator, which can minimize the heat losses in the evaporator. The optimum performance of the air cooled evaporator can be regulated to achieve the higher performance by balancing the heat energy and mass flow rate of the refrigerant and chilled water. Heat supplied by the chilled water returned to the evaporator is to be equalized by the heat observed by the refrigerant for evaporation; hence, heat lost in the evaporator is minimized.

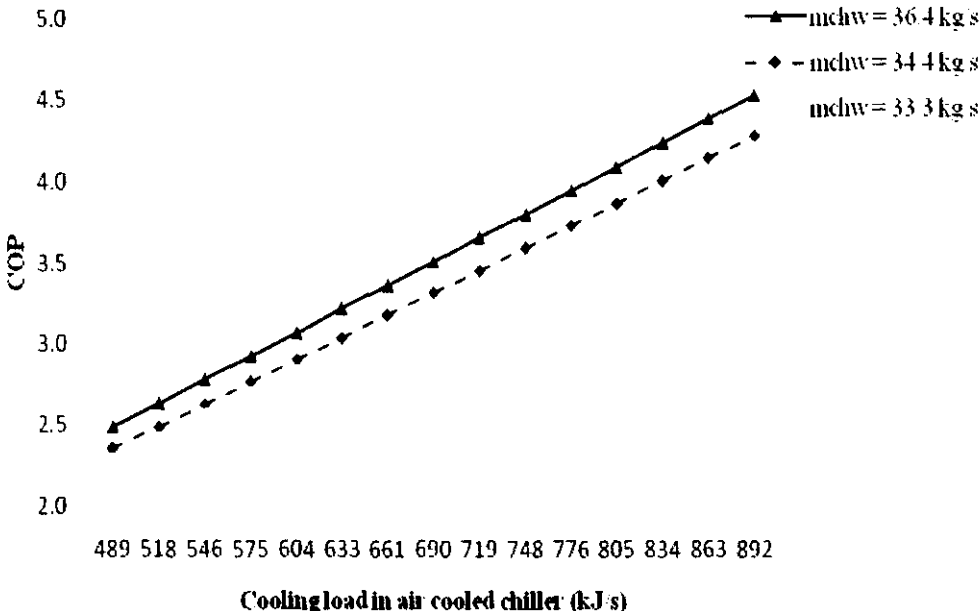


Figure 4.27: Cooling load (kJ/s) against the COP

Cooling load is plotted against the COP in the air cooled chiller as shown in Figure 4.28 and Figure 4.29. The increased in heat losses in the evaporator can minimized the coefficient of performance of the air cooled chiller. The heat losses occur in the evaporator is simply because of heat imbalance between the refrigerant and the chilled water entering the evaporator. The imbalance of the heat energy in the SAC evaporator can be regulated by tuning the operating parameters. Chilled water mass flow rate can be significant parameter which can be controlled to monitor the performance of the SAC evaporator at optimum.

Evaporation occurs in the SAC evaporator as a result of heat exchange between the mass flow rate of return chilled water and the refrigerant. At higher flow rate of return chilled the heat lost in the evaporator is lower due to an adequate heat exchange

between the return chilled water and the refrigerant. When the mass flow rate of return chilled water is lower compared to the refrigerant flow then the heat exchange between the two fluid, heat imbalances can be observed in the evaporator and the amount of heat lost in the evaporator increases.

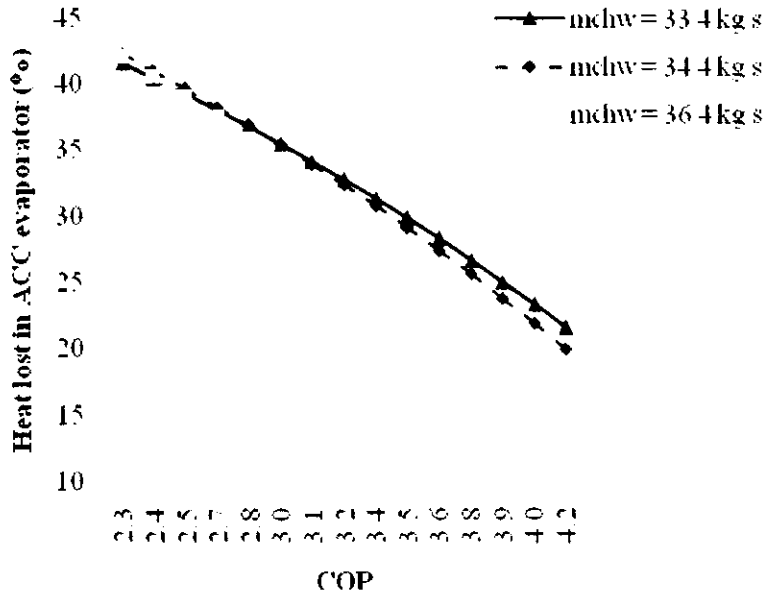


Figure 4.28: Heat energy lost (kJ/s) in ACC evaporator against COP

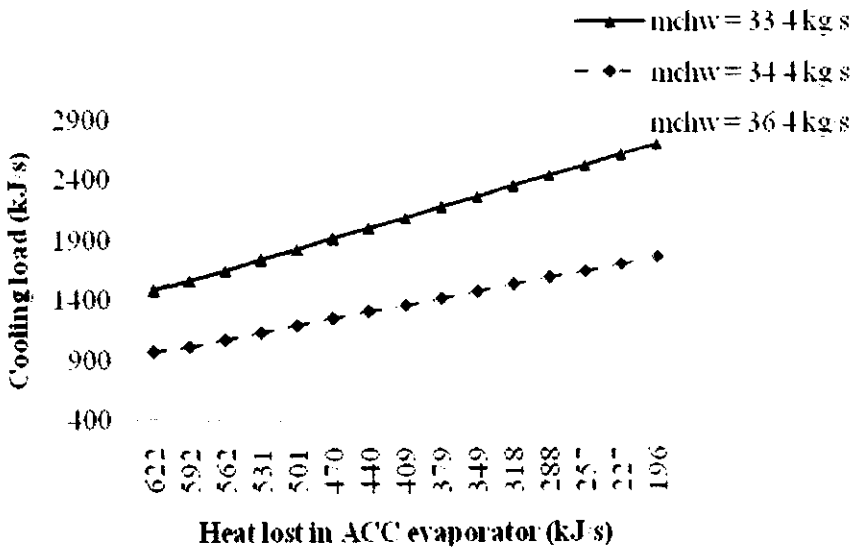


Figure 4.29: Heat energy lost (kJ/s) in ACC evaporator against cooling load (kJ/s)

4.6 Results from cooling tower model analysis

The cooling tower installed in the GDC is used for cooling the warm water from the absorption chiller. The quantity of heat removal from the warm water that comes from the absorption chiller must be equal to the heat removal by the mass evaporation and convection heat transfer. The tower performance can be high when the heat removed from the warm water is sufficient, and maintaining the loss of water by evaporative mass at minimum. The performance of the cooling tower in this work is analyzed base on the heat quantity expel from the tower by the evaporative mass and convection heat transfer. The parameters considered are the air mass flow rate, Lewis factor, thermal ratio of the tower, humidity ratio.

The effect of the parameters mentioned have shown their effect on the heat lost due to evaporated mass of water and convection heat transfered. The operating performance of cooling tower is at efficient performance when the cold water temperature leaving the tower obtained the design condition. Heat lost from the tower by mass of evaporation, convection heat transfer, and total heat is shown in Figure 4.30. It shows that high difference of heat lost is due to convection heat transfer compared to mass evaporation. Heat lost by convection heat is depending on the heat transfer coefficient. It is found that heat lost by convection is at maximum water mass flow rate. At the mass flow rate of water 240-268.33 kg/s and air mass flow rate 37.4-37.8 kg/s the heat lost due to mass evaporation is 0.83-1.25 J/s and heat lost due to convection heat transfer range from 15.35-15.80 J/s when the dry bulb temperature is 300.15 K and wet bulb temperature is 297.15 K.

The heat losses for cooling the warm water are mainly due convection heat transfer which is the most effective. About 94.6% of heat is rejected by convection heat transfer and the remaining which is 5.4% is by mass evaporation, neglecting the loss due to drift losses. In the cooling tower the energy lost by evaporated mass can be decreased by 1.01-1.5% when the inlet air temperature is reduced by 1-1.5 K.

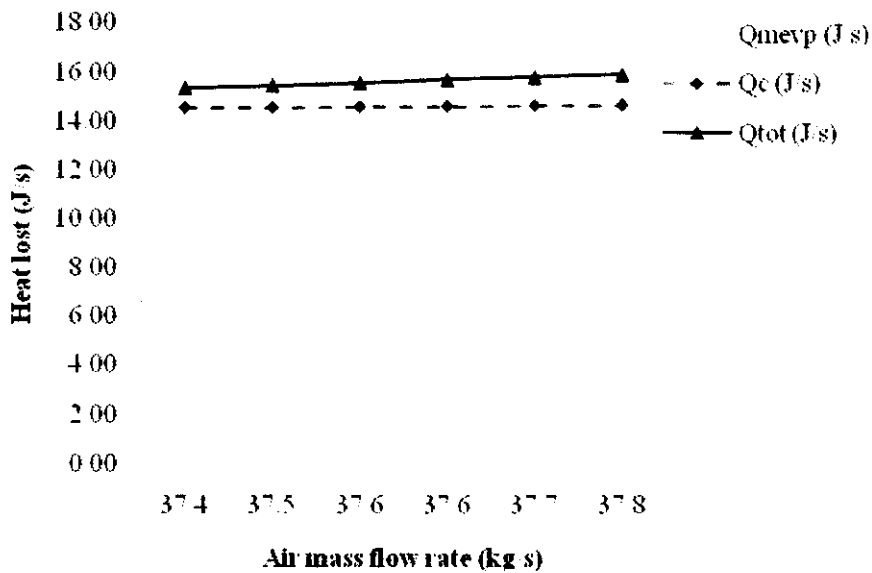


Figure 4.30: Heat energy lost (J/s) against air mass flow rate (kg/s)

The effect of relative humidity on heat transfer due to convection in the cooling tower is related in Figure 4.31, the quantity of heat lost increases at low relative humidity. High relative humidity in the air decreases the lost due to convection, which happens due to moisture content in the air flow rate, at high humidity the air moisture content is high and the cooling capacity of air is high. The heat lost due to convection heat transfer can be control at air mass flow rate, as increase in flow rate of air can increase the mass of evaporation lost, which eventually decreases the water quantity.

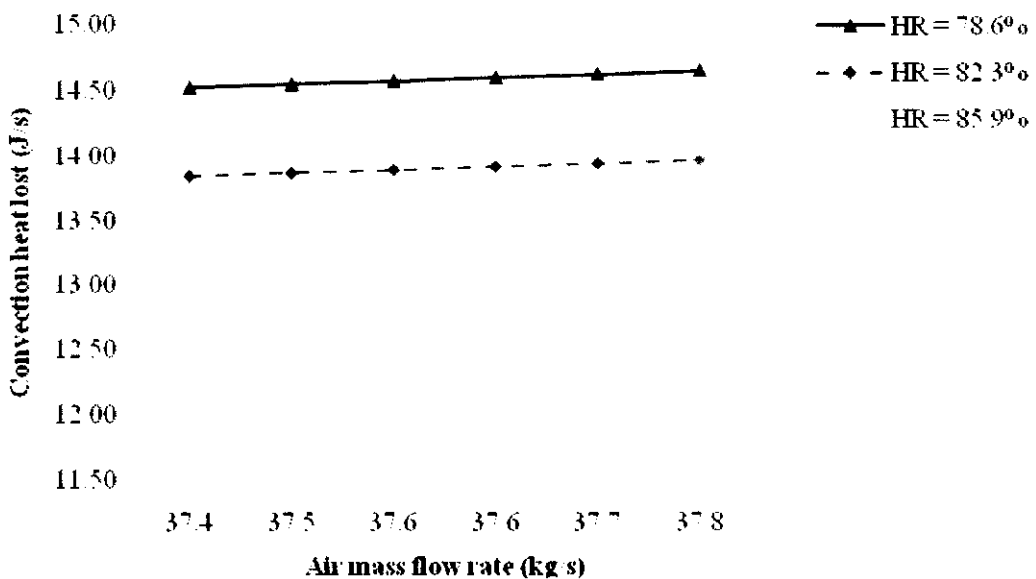


Figure 4.31: Convection heat lost (J/s) against air mass flow rate (kg/s)

The performance of cooling tower can be characterized by its thermal ratio. In the Figure 4.32, thermal ratio of the cooling tower is evaluated based on the heat lost by evaporation and the evaporated mass. It is found that the thermal ratio of the tower is lower when the heat lost by evaporative mass is increased.

The thermal ratio of the tower depends on the temperature difference between the inlet water entering tower and the wet bulb temperature. One effective temperature that determines the optimum performance of the tower is cold water temperature. Lower temperature of the cold water would give optimum performance of the tower; however, the mass of evaporation must be limited at design point. At the wet bulb temperature 297.15-300.15 K and water inlet temperature range 312.65-313.1 K and outlet water temperature is ranged 305.7-306 K, the thermal ratio found is 0.46-0.6

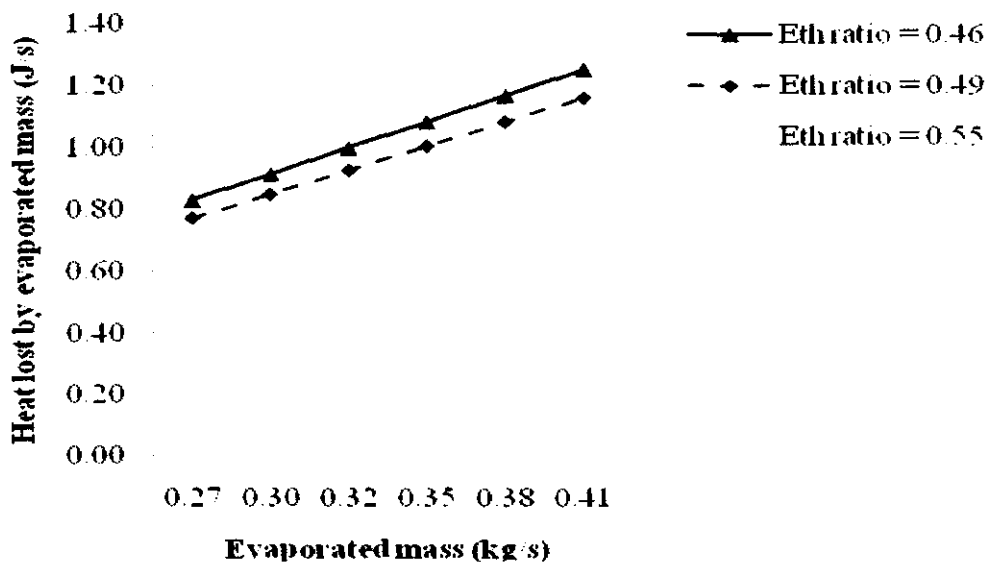


Figure 4.32: Heat energy lost by evaporation (J/s) against evaporated mass (kg/s)

Considering the Lewis factor in cooling tower heat losses as shown in Figure 4.33, the Lewis factor is high when the heat lost due to mass evaporation is increased. Increase in the evaporative mass can decrease the mass of cool water outlet the tower. One effective parameter to manage the mass flow rate of evaporative mass is the air mass flow rate.

High flow rate of air mass flow rate increases the losses due to evaporation. The evaporative mass flow rate calculated at mass flow rate of water 240-268.33 kg/s is range 0.27-0.41 kg/s based on the actual data where Lewis factor obtained is 0.9217 and heat lost due to evaporative mass is ranging from 5.41-7.9%.

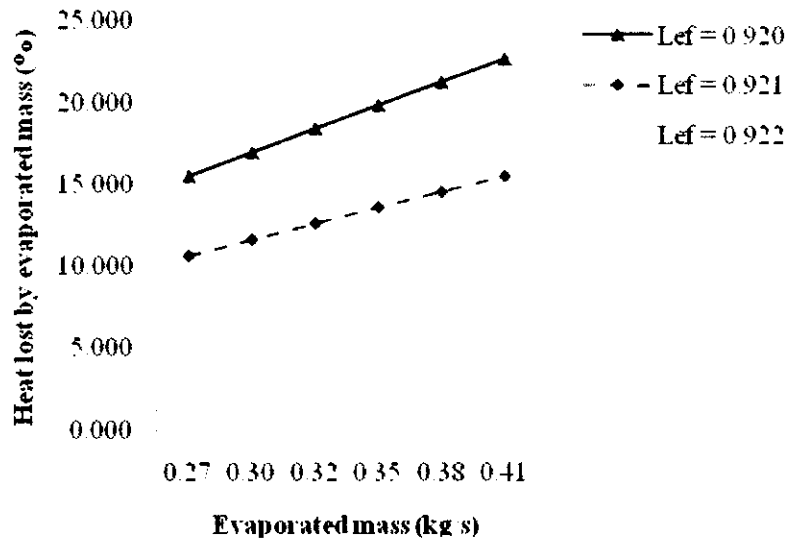


Figure 4.33: Heat energy lost by evaporated mass against evaporated mass (kg/s)

The heat lost due to convection heat transfer in cooling tower is affected by heat transfer coefficient. Increase in heat transfer coefficient increases the heat lost by convection heat transfer. Heat lost due to convection heat transfer calculated is ranged from 12.4-14.5 Watt when the mass flow rate of air is range 37.4-37.8 kg/s with interval of 0.1 kg/s the coefficient of heat transfer is range from 675-719 W/m² k, Figure 4.34 shows the relationship between convection heat lost and air mass flow rate.

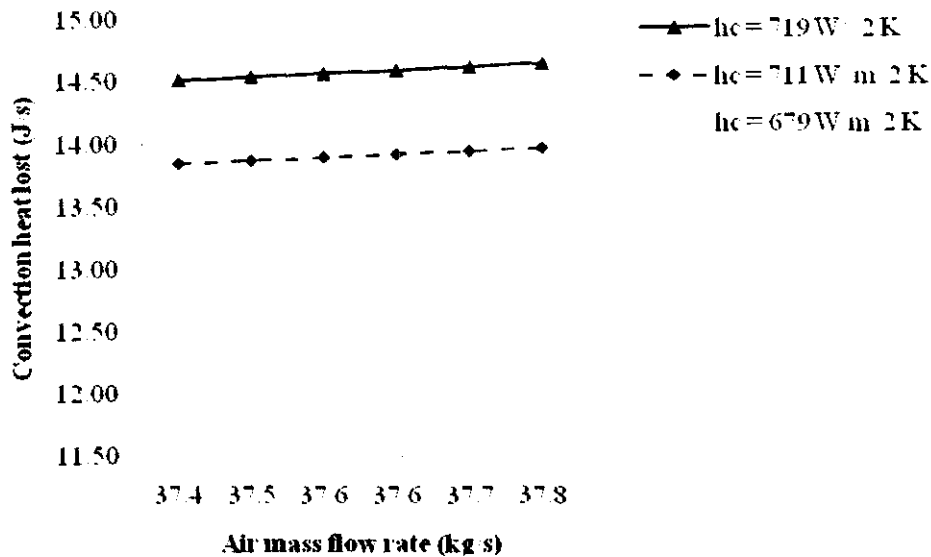


Figure 4.34: Convection heat lost (J/s) against air mass flow rate (kg/s)

4.7 Results from thermal energy storage (TES) model analysis

Energy balance in the thermal energy storage is accomplished based on the cooling load during charging and discharging period. The losses which take place in thermal energy storage are due to time gap and imbalance of the cooling capacity between the off-peak period and on-peak period. The time gap is the difference between the charging time and discharging time of the TES. Balance in charging and discharging capacity of the TES can result to optimum operation of the system.

To maintain the performance of the TES for energy audit approach, the management of the thermal energy storage can be undertaken by analyzing the discharge and charge capacity during on-peak and off-peak period respectively. One of the parameters that can ascertain the optimum performance of the thermal energy storage is the Figure of Merit (FoM). High value of FoM means the performance of the thermal energy storage is optimum. Figure 4.35 shows the actual performance of the thermal energy storage at both charging and discharging based on the actual data recorded from the thermal energy storage of the GDC.

The TES is operating on peak when the demand of the cooling load for the space cooling is high. The cooling load demand is high during day period as day time is mostly the working hours in the buildings. The TES at night periods stores the chilled water that can be used during the on-peak period.

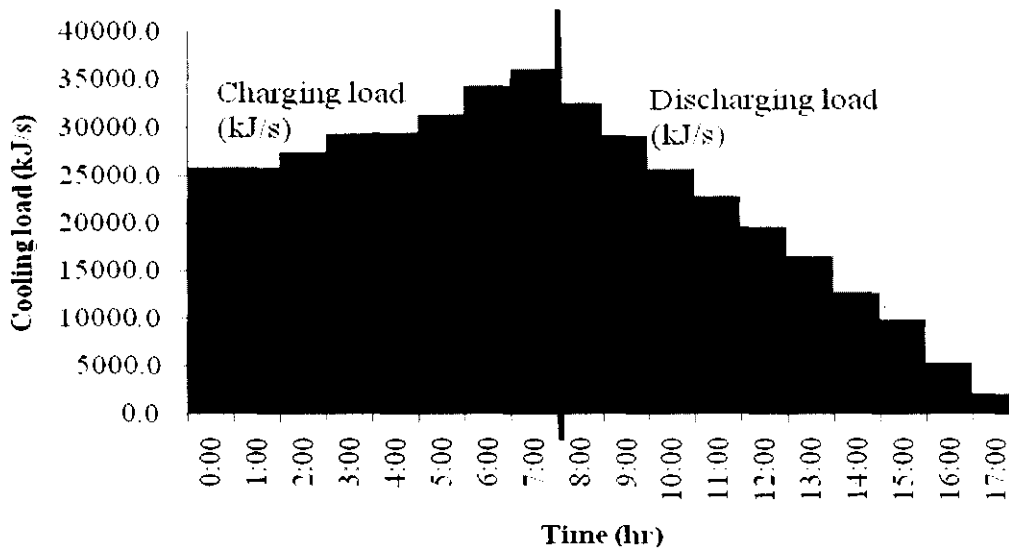


Figure 4.35: Actual cooling load of TES (kJ/s) against time (hr)

4.7.1 Cooling load lost in TES

The FoM depends on the discharge rate of chilled water supplied to the customer. At optimum discharge rate of chilled water the FoM increases. Increase in FoM indicates that the losses of cooling load in the TES is minimum. The cooling load losses increase in the TES at high temperature of the return chilled water, to the thermal energy storage. This is because the heat in the return chilled water temperature is observed by the chilled water stored in the TES. Figure 4.36 shows the cooling load lost percentage against the FoM, minimum percentage of cooling load lost results into high FoM. 5-22.4% of cooling load is lost in the thermal energy storage at the FoM 0.38-0.9. The high value of FoM is 1.12. To maintained the performance of TES the cooling load storage must be discharge at optimum rate, that can safisties the Figure of merit value of 0.9-1.12, which can identify optimum operation of thermal energy storage.

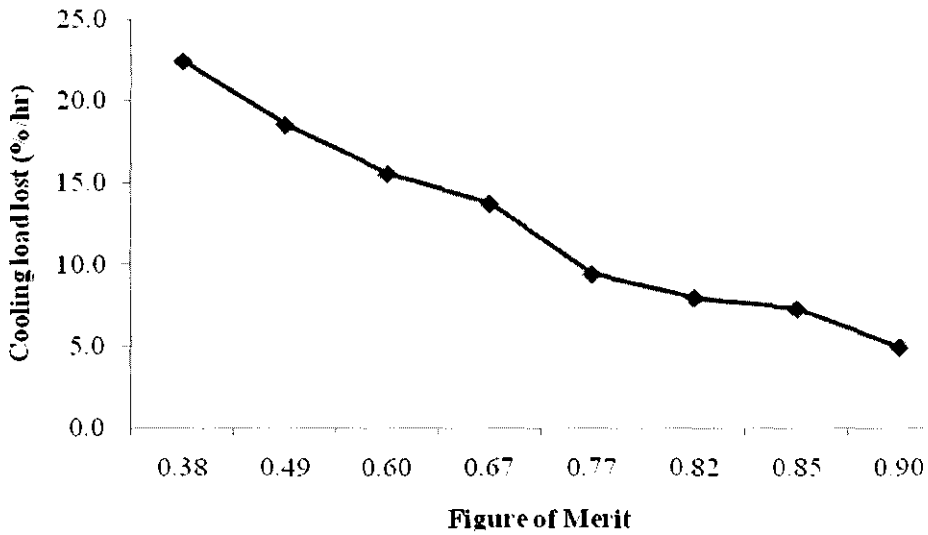


Figure 4.36: Cooling load lost (% /hr) against Figure of Merit (FoM)

4.7.2 Effect of returned chilled water on discharge load in TES

Figure 4.37 shows the relationship between the discharge load (kW) against the returned chilled water temperature (K), the effective parameter that can lead to high performance of the thermal energy storage is the returned chilled water temperature. To reduce the effect of the returned chilled water on the cooling load, the discharge rate must be increase as the returned temperature increases, to ascertain maximum used of stored load in the TES.

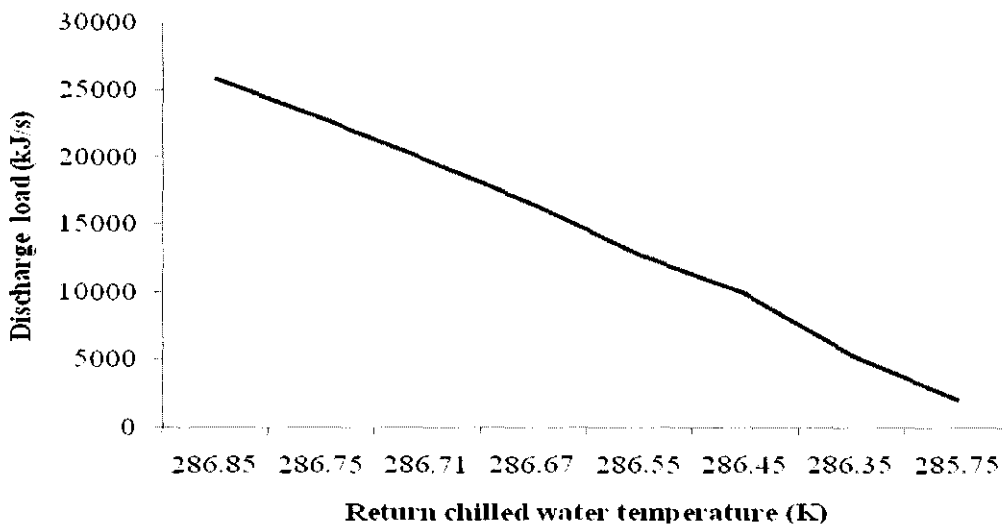


Figure 4.37: Discharge load (kJ/s) against return chilled water temperature (K)

4.8 The overall analysis of GDC plant

The overall analysis for all the systems in GDC plant is accomplished by plotting the effective operating parameters in all the systems. The operating parameters that are most effective in gas turbine system are the turbine inlet temperature (TIT), air inlet temperature, mass flow rate of air. These parameters can affect the energy flow in the gas turbine system at their un-optimized flow rate. Figure 4.38 shows the effect of turbine inlet temperature to the energy loss in the gas turbine engine. It is found that energy loss in the gas turbine engine can increase as the turbine inlet temperature is increased, the turbine inlet temperature can be regulated by controlling the mass flow rate of air and air inlet temperature. Regulating the air mass flow rate at optimum flow rate can result in to an optimum turbine inlet temperature. Decrease in air inlet temperature to air compressor can minimize the air compressor work as a result the net work output increases.

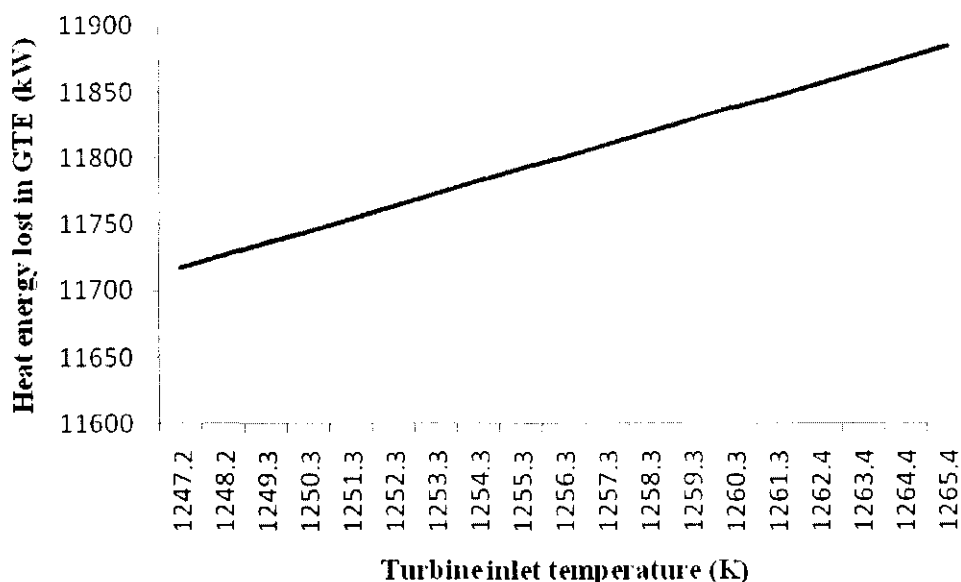


Figure 4.38: Heat energy lost in GTE (kW) against turbine inlet temperature (K)

Figure 3.49 shows the relationship between the heat gain by the steam in HRSG and the turbine inlet temperature. It can be seen that increase in the turbine inlet temperature can result in an increase in heat gain by the steam in the HRSG. Heat gain by the steam can be effective at the parameter optimum flow rate such as saturated water entering evaporator of HRSG. The parameters that are to be regulated at optimum flow rate in the HRSG are the mass flow rate of warm water and saturated

water in the steam drum. The flow rate of the warm water can be regulated in such a way it can be high at higher flow rate of heat energy into the HRSG economizer. The source of energy into the HRSG is from the gas turbine engine, the energy such as turbine inlet temperature at higher level can be advantageous to the HRSG.

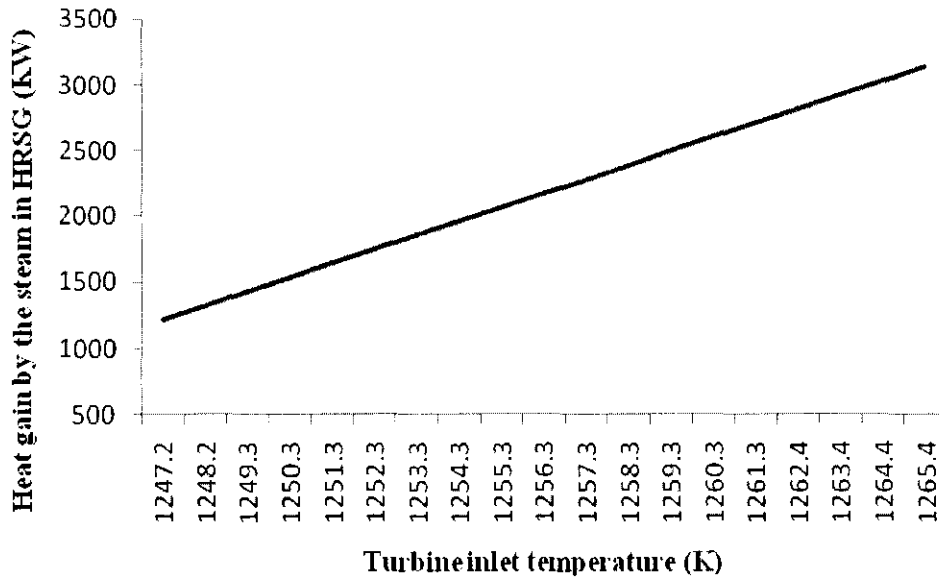


Figure 4.39: Heat gain by the steam in HRSG (kW) against turbine inlet temperature (K)

Figure 4.40 shows the correlation between the turbine inlet temperature and the mass flow rate of steam. Steam mass flow rate is the source of energy to the steam absorption chiller and the mass flow rate of steam increase as the turbine inlet temperature. Turbine inlet temperature is effective to the steam mass produced because the turbine inlet temperature is the source of energy from the turbine to the HRSG. Turbine inlet temperature is effective in gas turbine engine, HRSG and SAC. Higher net work in gas turbine engine can be achieved at optimum value of the turbine inlet temperature. At higher temperature of turbine inlet temperature the exhaust energy from the turbine is higher as a result the energy required for the HRSG is maximum and the output such as steam produced is higher. Steam is the source of energy to the absorption chiller and it can show significant effect on the performance of the SAC.

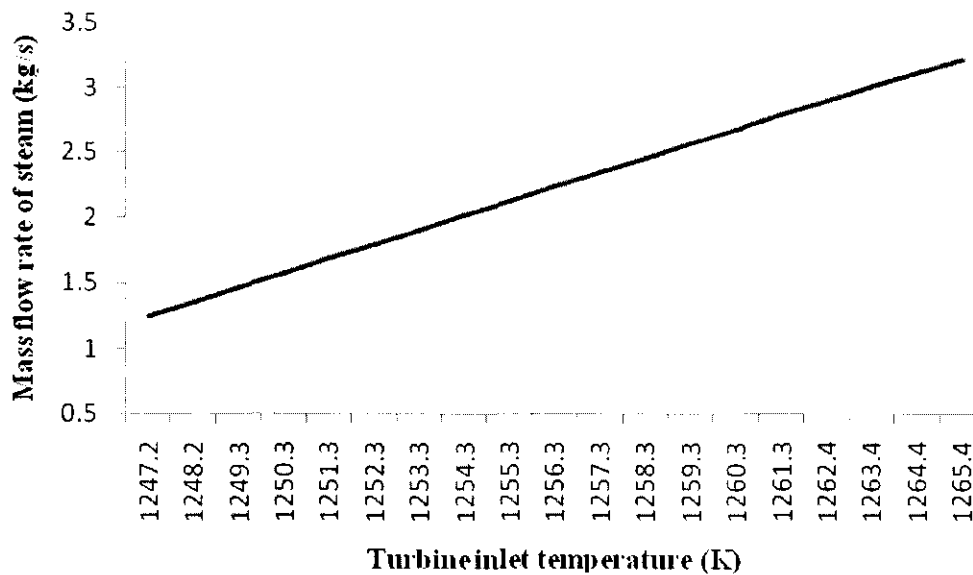


Figure 4.40: Mass flow rate of steam in HRSG (kg/s) against turbine inlet temperature (K)

Figure 4.41 shows the relationship between the cooling load in steam absorption chiller and the mass flow rate of steam. Mass flow rate of steam is the source of energy into the steam absorption chiller. It is found that increase in the mass flow rate of steam increases the cooling load in steam absorption chiller. The mass flow rate of steam can be increased when the parameters in the HRSG are adjusted at their optimum flow rate. When the operating parameters in the HRSG are regulated at their optimum flow rate the energy losses can be minimized.

The cooling load in the steam absorption chiller can be at its optimum level when the energy input is at optimum and the energy losses in the steam absorption chiller is minimize. The energy losses in the steam absorption chiller can be minimized by monitoring the optimum flow of the working fluid. The working fluids in the steam absorption chiller are the chilled water, refrigerant and the solutions.

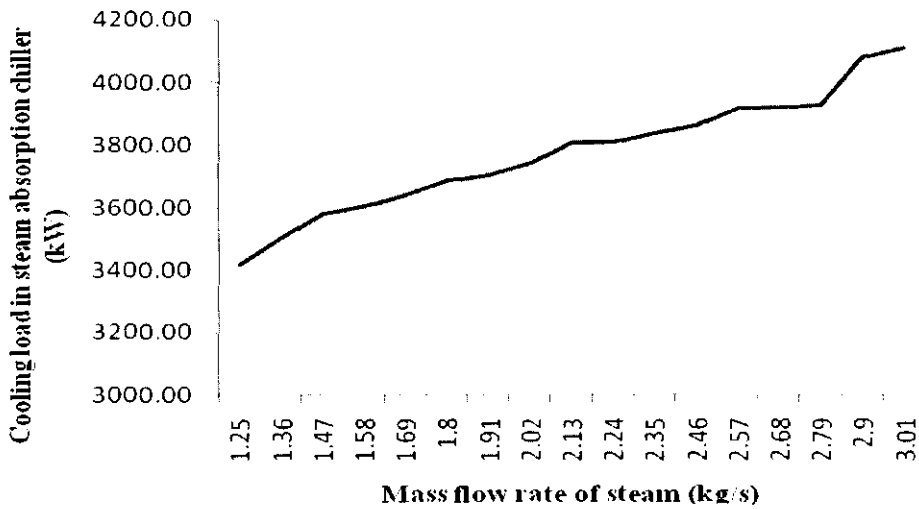


Figure 4.41: Cooling load in SAC (kW) against mass flow rate of steam (kg/s)

Figure 4.42 shows the correlation between the parameters in the air cooled chiller namely, air inlet temperature and un-rejected heat in air cooled condenser. Air inlet temperature has a significant effect on the performance of air cooled condenser. Air as being used for cooling in air cooled chiller condenser. It is found that increase in air inlet temperature increases the un-rejected heat in the air cooled condenser. The un-rejected heat shows performance degradation of the air cooled chiller, its quantity in air cooled condenser can be decreased by reducing the air inlet temperature and increasing the mass flow rate of air. At higher mass flow rate of air into air cooled condenser the heat energy can be rejected at higher level.

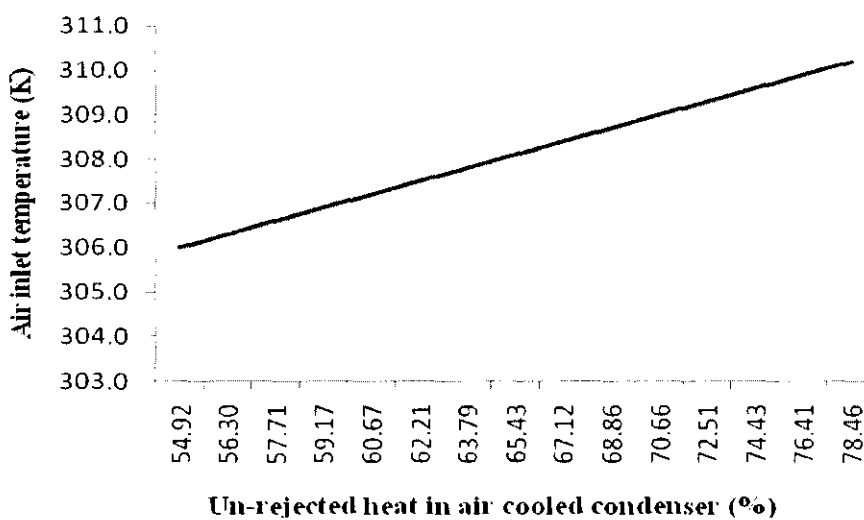


Figure 4.42: Air inlet temperature (K) against un-rejected heat in air cooled condenser (%)

Figure 4.43 shows the relationship between the parameters of the TES namely, chilled water mass flow rate and charging load. The charging load in the thermal storage tank is the main operating parameter in the performance of the TES. Increase in charging load of the TES shows the higher storage of the energy, where the stored energy can be of more importance at the peak load. Charging load increases as the chilled water mass flow rate entering the TES increases as plotted in the figure below. The chilled water flow rate is supplied by the air cooled chiller, optimizing the performance of the air cooled chiller; it can produce the required chilled water for the TES storage. At optimum chilled water flow rate to the TES the storage energy can be at optimum level. The performance of TES can be optimized when the charging load and the discharge load are equalized, where energy losses in the TES is minimize at lower level.

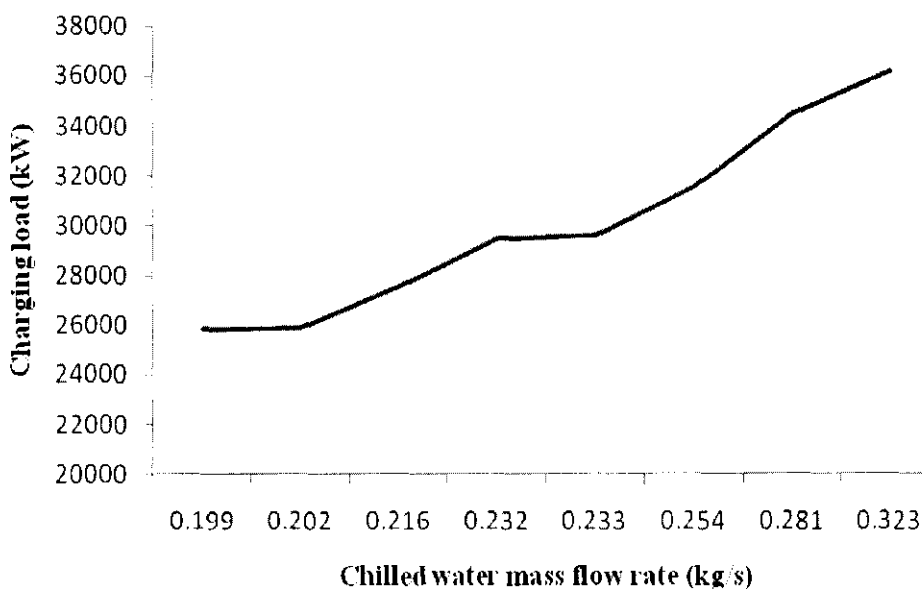


Figure 4.43: TES Charging load (kW) against chilled water mass flow rate (kg/s)

Figure 4.44 shows the correlation between the operating parameters of cooling tower namely, wet bulb temperature and heat rejected by the cooling tower. Wet bulb temperature shows significant effect on the performance of cooling tower. Decreased in wet bulb temperature can result into higher performance of the cooling tower and increase in the heat energy rejected by the cooling tower. The wet bulb temperature can be most effective at low flow rate of warm water entering the cooling tower.

Another parameter in cooling tower is the mass flow rate of air. At higher mass flow rate of air the performance of the cooling tower can be optimized, where higher heat energy can be rejected by the cooling tower. The performance of the cooling tower can be regulated based on the operating data, when the wet bulb temperature is at lower level, the operation of the air blowers in the cooling tower can be reduced to decrease the electrical consumption.

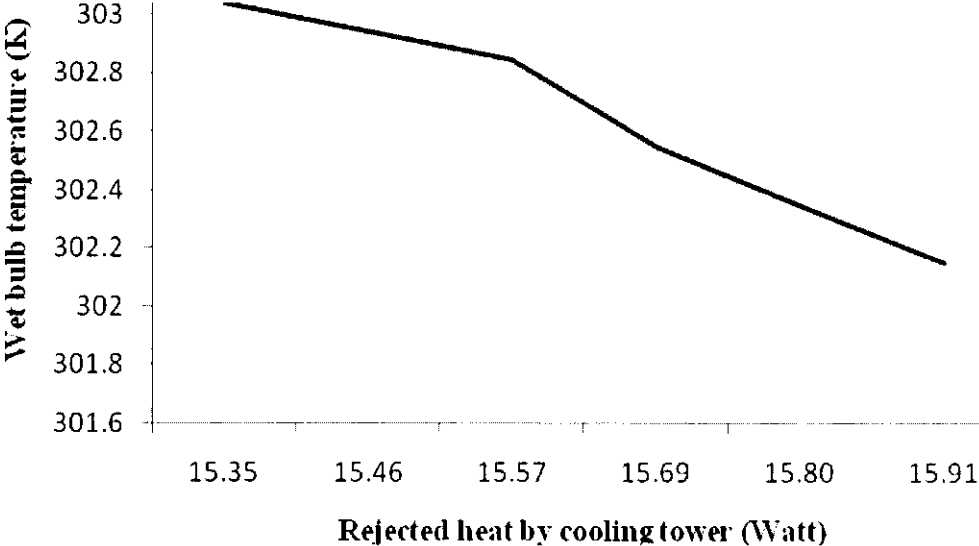


Figure 4.44: Warm water temperature (K) against rejected heat by cooling tower (Watt)

CONCLUSIONS AND FUTURE WORK

5.1 Conclusions

The methodology applied in this research shows that an analytical method for energy audit of a cogeneration plant can be an easy analytical tool for finding energy conservation and energy losses in the components of the cogeneration plant. Based on variation of the operating parameters, the energy quantities and energy losses are determined for the components of the cogeneration plant. The equipment models written in the computer program show relatively close trends to the actual data collected from the GDC plant. The results obtained from the energy analysis show that, operation of the plant can be maintained at optimum when continuous energy audit is performed. It is found that energy imbalance degrades the performance of the components in the cogeneration plant. It is also shown that non-optimized operating parameters contributed to the degradation of the plant performance due to increase in energy losses and misuses.

5.2 Gas turbine engine and HRSG

The energy lost in the combustion chamber of the gas turbine is approximately 5% of total heat energy lost in the engine at the optimum operation of the gas turbine engine. Increase in the heat lost in the combustion chamber decreases the part load ratio and as a result decreases the net work. Air compressor work consumption from the turbine is 27.9% of the turbine inlet heat energy, the work of air compressor can be reduced by 1.1% of the turbine work if the inlet air temperature is increased to 305 K instead of at 298 K.

The percentages of energy losses in the turbine and the component of HRSG are list as follow;

1. The exhaust energy lost from the turbine is 54.9% of the turbine inlet heat energy, and Energy consumed by the turbine is 45.1% of the turbine inlet energy.
2. Energy supplied to the evaporator for steam production is 39.94% of the total energy entering the HRSG. A percentage of 10.88% of that energy is gained by the steam while 28.06% is lost in the evaporator.
3. Increase in mass flow rate of steam by 0.11 kg/s increase the energy gained by the steam by 0.92% and decreases the lost energy in the evaporator by 0.88%.
4. Energy supplied to the economizer is 10.21%, and energy gained by warm water is 3.15% of the energy entering the economizer. Energy lost in the economizer is 7.06% of the total energy entering economizer while energy lost by the flue gases is 6.59%
5. Increasing the mass flow rate of warm water by 0.16 kg/s decreases the energy lost in economizer by 0.78% by increasing the warm water energy gain by 0.84%.

5.3 Steam absorption chiller (SAC)

The performance of the SAC is characterized by the cooling load and the COP. To maintain the optimum performance of the SAC its energy balance must be regulated during operation. It is found that energy losses and imbalance can decreased the performance of the SAC. In the components of SAC the heat rejected by the absorber is high compare to heat rejected by the condenser. The heat rejected by the absorber is 61-69.6% while the heat rejected by the condenser is 10.17-11.5%. Energy losses in the components of SAC result to degradation of COP and cooling load, hence, the performance of the SAC degrades. The percentage of energy lost in high temperature generator is found 51.35 % and in condenser is 25.8 % while energy lost in absorber is found to be 0.01-17.78%. The minimum energy lost in SAC is in the evaporator which is 0.44-4.9%.

5.4 Air cooled chiller (ACC)

The performance of air cooled chiller can be monitored by analysis of the energy quantities in the ACC components. The energy misuses and losses in the air cooled condenser, evaporator and screw compressor can be regulated by the analytical tool developed. The energy losses that occur in the components of the ACC can be minimized by controlling the parameters. In air cooled condenser energy losses can be minimized by increasing the mass flow rate of air and the temperature of air entering the air cooled condenser. The un-rejected heat in the air cooled condenser is 54.1% at air mass flow rate of 45 kg/s. In the evaporator heat released at chilled water flow rate of 36.4 kg/s is found 16.5% of total heat released in air cooled chiller. In the screw compressor the heat energy lost is 1.87-3.5% of the total heat energy lost in air cooled chiller. The analytical model is able to quantify energy quantities in the air cooled chiller. It can be applicable for energy audit and management of the air cooled chiller. In the air cooled chiller condenser the energy un-rejected can be decreased by 5.74-7.3% when the inlet air temperature is decreased by 1-1.5 K

5.5 Cooling tower

The performance of cooling tower can be optimum when the energy losses are controlled. The analytical tool used for detail energy audit of cooling tower shows that the performance of the cooling tower can be regulated to be optimum by identifying the energy quantities by both mass evaporation and by convection. The energy lost in cooling tower is 5.41-7.9% by evaporative mass of the total heat energy lost in the cooling tower. The heat energy lost in the cooling tower by convection heat transfer is 92-94.6% of the total heat energy lost in the cooling tower. Energy lost in cooling tower is remarkable by convection heat transfer, and it can be concluded that performance of cooling tower can be maintained by controlling the heat transfer by convection. To identify the performance of the cooling tower by the heat energy lost, it can be done by the analytical model developed.

5.6 Thermal energy storage (TES)

The performance of thermal energy storage is analyzed by the analytical tool developed. It is found that the regulation of the thermal energy storage can be monitored by the analytical tool. The discharge and charge capacities and the Figure of merit (FoM) of the thermal energy storage can be calculated. The tool can be used for calculation of the operating parameters and based on the optimum range identified; the operation of the thermal energy storage can be maintained. The cooling load lost in TES is found to be 5-22.4% and the FoM is 0.38-0.9. The analytical tool can be used as a tool for energy audit and management of TES due to its capability of identifying energy lost and FoM of the thermal energy storage. The optimum operation of TES can be at optimum FoM 0.9 where energy lost can be 5%, because increase in FoM shows better performance of the TES, hence the optimum value calculated at high performance is 0.9.

5.7 Future work

An improved mathematical model for the design and analysis of a cogeneration plant can be proposed for optimization purpose based on considering minimum heat energy losses by inclusion of the following factors:

1. Internal friction
2. Lubrication losses
3. Heat transfer losses
4. Control systems

APPENDIX

PUBLICATIONS

1. Yongo, P. W., Abdul Karim, Z. A. Development of Analytical Model for Energy Audit of Cogeneration Plant. 2nd Engineering Conference on Sustainable Engineering Infrastructure Development and Management (ENCON2008-Abs190), Kuching, Sarawak, Malaysia. 2008
2. Yongo, P. W., Abdul Karim, Z. A. Development of Analytical Models for Energy Audit of Refrigeration Systems. The 4th International Conference on Cooling and Heating Technologies (ICCHT2008-KOCEN081420), Jinhae City, Korea. 2008

Table A-1: Operating parameters of the gas turbine engine

Power (kW)	T_1 (K)	m_f (kg/s)
3266	306.55	0.257
3334	303.55	0.259
2833	301.05	0.238
2444	300.65	0.222
3002	302.15	0.241
3148	302.25	0.351
2916	308.75	0.235
3177	307.95	0.370
2540	301.75	0.225
2275	301.25	0.313
2802	300.15	0.238
3087	302.05	0.246
3230	302.45	0.363
2847	306.65	0.231
3197	304.75	0.356
2389	302.35	0.216
2710	301.35	0.332
2660	301.15	0.229
2705	308.05	0.227
3121	308.15	0.358
2918	308.55	0.229
3252	308.35	0.370
2291	301.85	0.216
2745	301.55	0.318

Table A-2: Calculated and operating parameters of the gas turbine engine

m_f (kg/s)	m_a (kg/s)	T_a (deg)	cal wnet	act wnet (kW)	$w_{c,los}$ (%)	CC_{los} (%)	$w_{t,los}$ (%)
0.22	13.5	27	2291	2291	0.24	4.975	54.912
0.22	13.83	27.5	2389	2387	0.30	4.973	54.913
0.22	14	27.9	2444	2441	0.36	4.972	54.914
0.22	15.15	28	2540	2539	0.42	4.970	54.913
0.23	15.34	28.1	2660	2659	0.48	4.969	54.914
0.23	15.35	28.2	2705	2705	0.54	4.967	54.912
0.23	15.53	28.4	2710	2710	0.60	4.966	54.913
0.23	15.6	28.6	2745	2745	0.66	4.965	54.914
0.23	16.56	28.7	2754	2753	0.72	4.963	54.913
0.23	16.7	28.9	2802	2806	0.77	4.962	54.914
0.24	16.8	29	2833	2830	0.83	4.961	54.915
0.24	16.82	29.1	2847	2846	0.89	4.959	54.913
0.24	17.1	29.2	2916	2914	0.95	4.958	54.914
0.25	17.3	29.3	2918	2918	1.01	4.957	54.912
0.26	18.1	30.4	3002	3002	1.07	4.955	54.913
0.26	18.43	31.6	3087	3087	1.13	4.954	54.914

REFERENCES

- [1] P. Karunakaran. Industrial Energy Audit Guidelines. A Handbook for Energy Auditors, Pusat Tenaga Malaysia, 2003
- [2] S. F. Robert. An Exergy Diagnostic Methodology for Energy Management in Manufacturing, Oklahoma State University, PhD. Thesis. USA, 2006
- [3] B. A. Qureshi, S. M. Zubair. (2006). A complete model of wet cooling towers with fouling in fills. Applied Thermal Engineering. [online]. Vol. 26. pp. 1982-1989. Available: www.sciencedirect.com
- [4] A. Thumann. Plant Engineers and Managers Guide to Energy Conservation. Eighth Edition. The Fairmount Press. Lilburn, USA, 2001,
- [5] E. Tahsin, V. Ari. (2005, July). Energy audit and recovery for dry type cement rotary Kiln systems. Energy Conversion and Management. [online]. Vol. 46. pp 551-562. Available: www.sciencedirect.com
- [6] A. Thumann, W. J. Younger. Handbook of Energy Audits. Sixth Edition. The Fairmount Press. Lilburn, USA, 2003
- [7] S. M. Bhatt. (1999, Feb.). Energy audit case studies I-steam systems. Applied Thermal Engineering. [online]. Vol. 20. pp 285-296. Available: www.sciencedirect.com
- [8] S. M. Bhatt. (2000). Energy audit case studies II-air conditioning (cooling) systems. Applied Thermal Engineering. [online]. Vol. 20. pp. 297-307. Available: www.sciencedirect.com
- [9] C. Beggs. Energy Management Supply and Conservation. Published, Elsevier Science and Technology Books. USA, 2002
- [10] D. Y. Goswami, F. Kreith. Energy Management and Conservation Handbook. Published. CRC Press. Taylor and Francis Group. USA, 2007
- [11] J. L. Silveira, C. E. Tuna. (2004, Aug.). Thermo-economic analysis method for optimization of combined heat and power systems-part II. Progress in Energy and Combustion Science. [online]. Vol. 30. pp. 673-678. Available: www.sciencedirect.com
- [12] C. Casarosa, F. Donatini, A. Franco. (2004, Italy). Thermo-economic optimization of heat recovery steam generators operating parameters for combined plants. Energy. [online]. Vol. 29. pp 389-414. Available: www.sciencedirect.com
- [13] X. Q. Kong, R. Z. Wang, X. H. Huang. (2004, Aug.) Energy optimization model for a CCHP system with available gas turbines. Applied Thermal Engineering. [online]. Vol. 25. pp 377-391, 2004. Available: www.sciencedirect.com
- [14] A. M. Bassily. (2005, Feb.). Modeling numerical, optimization, and irreversibility of reduction of a dual-pressure reheat combined cycle. Applied Energy. [online]. Vol. 81. pp 127-151. Available: www.sciencedirect.com

- [15] F. W. Yu, K. T. Chan. (2006). Advanced control of heat rejection air flow for improving the coefficient of performance of air-cooled chillers. *Applied Thermal Engineering*. [online]. Vol. 26. pp 97-110. Available: www.sciencedirect.com
- [16] K. T. Chan, F. W. Yu. (2005). Thermodynamic-behavior model for air-cooled screw chillers with a variable set-point condensing temperature. *Applied Energy*. [online]. Vol. 83. pp 265–279. Available: www.sciencedirect.com
- [17] F. W. Yu, K. T. Chan. (2006). Improved condenser design and condenser–fan operation for air-cooled chillers. *Applied Energy*. [online]. Vol. 83. pp 628-648. Available: www.sciencedirect.com
- [18] N. Sessaiah, K. G. Subrata, R. K. Sabhoo, Kr. S. Sarangi. (2006, July). Mathematical modeling of the working cycle of oil injected rotary twin screw compressor. *Applied Thermal Engineering*. [online]. Vol. 27. pp 145-155. Available: www.sciencedirect.com
- [19] J. U. Khan, B. A. Qureshi, S. M. Zubair. (2003, April). A comprehensive design and performance evaluation study of counter flow wet cooling towers. *International Journal of Refrigeration*. [online]. Vol. 27. pp 914-923. Available: www.sciencedirect.com
- [20] G. Y. Jin, W. J. Cai, L. Lu, E. L. Lee, A. Chiang. (2007, Sept.). A simplified modeling of mechanical cooling tower for control and optimization of HVAC systems. *Energy Conservation and Management*. [online]. Vol. 48. pp 355-365. Available: www.sciencedirect.com
- [21] J. Facao, A. Oliveira. (2004, April). Heat and mass transfer correlation for design of small indirect contact cooling towers. *Applied Thermal Engineering*. [online]. Vol. 24. pp 1969-1978. Available: www.sciencedirect.com
- [22] W. Zalewski, P. A. Gryglaszewski, (1997) Mathematical model of heat and mass transfer processes in evaporative fluid coolers. *Chemical Engineering and Processing*. [online]. Vol. 36. pp 271-280. Available: www.sciencedirect.com
- [23] M. S. Soylemez. (2004, Feb.). On the optimum performance of forced draft counter flow cooling towers. *Energy Conservation and Management*. [online]. Vol. 45. pp 2335-2341. Available: www.sciencedirect.com
- [24] P. Stabat, D. Marchio. (2004). Simplified model for indirect contact evaporative cooling tower behavior. *Applied Energy*. [online]. Vol. 78. pp 433-357. available: www.sciencedirect.com
- [25] P. Naphon. (2005, June). Study on the heat transfer characteristic of an evaporative cooling tower. *International Communications in Heat and Mass Transfer*. [online]. Vol.32. pp 1066-1074. Available: www.sciencedirect.com
- [26] N. Williamson, S. Armfield, M. Behnia. (2008, May). Numerical simulation of flow in a natural draft wet cooling tower-the effect of radial thermo-fluid fields. *Applied Thermal Engineering*. [online]. Vol. 28. pp.178-189. Available: www.sciencedirect.com
- [27] A. H. W. Lee, Jones, W. Jerold. (1996). Modeling of an ice-on-coil thermal energy storage system. *Energy Conservation and Management*. [online]. Vol. 37. No .10. pp. 1493-1507. Available: www.sciencedirect.com

- [28] C. Chaichana, W. W. S. Charters, L. Aye. (2001, April). An ice thermal storage computer model. *Applied Thermal Engineering*. [online]. Vol. 21. pp. 1769-1778. Available: www.sciencedirect.com
- [29] B. Yimer, M. Adami. (1997). Parametric study of phase change thermal energy storage systems for space application. *Energy Conservation and Management*. [online]. Vol. 38. No.3 pp. 253-262. Available: www.sciencedirect.com
- [30] D. MacPhee, I. Dincer. (2008). Thermal modeling of a packed bed thermal energy storage system during charging. *Applied Thermal Engineering*. [online]. Available: www.sciencedirect.com
- [31] V. Badescu. (2004, April). Optimal operation of thermal energy storage units based on stratified and fully mixed water tanks. *Applied Thermal Engineering*. [online]. Vol. 24. pp 2101-2116. Available: www.sciencedirect.com
- [32] M. Mostafavi, A. Alaktiwi, B. Anew. (1998, Nov.). Thermodynamic analysis of combined open-cycle-twin-shaft gas turbine (Brayton cycle) and exhaust gas operated absorption refrigeration unit. *Applied Thermal Engineering*. [online]. Vol. 18. pp. 847-856. Available: www.sciencedirect.com
- [33] R. Chacartegui, J. F. Espadafor, S. T. Sanchez. (2008, April). Analysis of combustion turbine inlet air cooling systems applied to an operating cogeneration power plant. *Energy Conservation Management*. [online]. Vol. 49. pp. 2130-2141. Available: www.sciencedirect.com
- [34] M. M. Alhazmy, Y. S. H. Najjar. (2004, Sept). Augmentation of gas turbine performance using air coolers. *Applied Thermal Engineering*. [online]. Vol. 24. pp 415-429. Available: www.sciencedirect.com
- [35] S. Khurana, B. Bangan, U. Gaitonde. (2001, Nov.). Energy balance and cogeneration for a cement plant. *Applied Thermal Engineering*. [online]. Vol. 22. pp. 485-494. Available: www.sciencedirect.com
- [36] V. Manuel, L. R. Jose, (2000, Nov.). Optimization of heat recovery steam generators for combined cycle gas turbine power plants. *Applied Thermal Engineering*. [online]. Vol. 21. pp 1149-1159. Available: www.sciencedirect.com
- [37] C. J. Bucher, B. V. Reddy. (2007, Jan.). Second analysis of a waste heat recovery based power generation system, *International Journal of Heat and Mass Transfer*. [online]. Vol. 50. pp 2355-2363. Available: www.sciencedirect.com
- [38] B. Zaporowski, R. Szczerbowski. (2003, Jan.). Energy analysis of technological systems of natural gas fired combined heat and power plants. *Applied Energy*. [online]. Vol. 75. pp 43-50. Available: www.directscience.com
- [39] T. S. Kim, D. K. Lee, S. T. Ro. (1999, Sept.). Analysis of thermal stress evolution in the steam drum during start-up of a heat recovery steam generator. *Applied Thermal Engineering*. [online]. Vol. 20. pp 977-992. Available: www.sciencedirect.com

- [40] S. Boonnasa, P. Namprakai, T. Muangnapoh. (2006, Oct.). Performance improvement of the combined cycle power plant by intake air cooling using an absorption chiller. *Energy*. [online] Vol. 31. pp 2036-2046. Available: www.sciencedirect.com
- [41] Y. Sanjay, S. Onkar, B. N. Prasad. (2007, Mar.). Energy and exergy analysis of steam cooled reheat gas-steam combined cycle. *Applied Energy Engineering*. [online]. Vol. 27. pp 2779-2790. Available: www.sciencedirect.com
- [42] S. H. N. Yousef, A. S. Alghamdi, M. H. Al-Beiruty. (2004, Jan.). Comparative performance of combined gas turbine systems under three different blade cooling schemes. *Applied Thermal Engineering*. [online]. Vol. 24. pp 1919-1934. Available: www.sciencedirect.com
- [43] F. J. Wang, J. S. Chiou. (2004, May.). Integration of steam injection and inlet air cooling for a gas turbine generation system. *Energy Conservation and Management*. [online]. Vol. 45. pp 15-26. Available: www.sciencedirect.com
- [44] S. K. Tong, T. R. Sung. (1995, Feb.). Effect of control modes and turbine cooling on the part load performance in the gas turbine cogeneration system. *Heat Recovery System and CHP*. [online]. Vol. 15. pp 281-291. Available: www.sciencedirect.com
- [45] P. Akber, J. Sanjeev. (1995). Combined cycle heat recovery steam generators optimum capabilities and selection criteria. *Heat Recovery System and CHP*. [online]. Vol. 15. pp 147-154. Available: www.sciencedirect.com
- [46] B. V. Reddy, G. Ramkiran, K. A. Kumar, P. K. Nag. (2001, Sept.). Second law analysis of a waste heat recovery steam generator. *International Journal of Heat and Mass Transfer*. [online]. Vol. 45. pp 1807-1814. Available: www.sciencedirect.com
- [47] A. M. Bassily. (2001, May). Effects of evaporative inlet and after cooling on the recuperated gas turbine cycle. *Energy*. [online]. Vol. 21. pp 1875-1890. Available: www.sciencedirect.com
- [48] A. Franco, A. Russo. (2001, Oct.). Combined cycle plant efficiency increase based on the optimization of the heat recovery steam generator operating parameters. *International Journal of Thermal Science*. [online]. Vol. 41. pp 843-859. Available: www.sciencedirect.com
- [49] N. Zhang, C. Ruixian. (2002). Analytical solutions and typical characteristics of part-load performances of single shaft gas turbine and its cogeneration. *Energy Conservation and Management*. [online]. Vol. 43. pp 1323-1337. Available: www.sciencedirect.com
- [50] O. B. Omar. (1999). Gas turbine performance improvements. *Applied Energy*. [online]. Vol. 64. pp 263-273. Available: www.sciencedirect.com
- [51] J. P. Bedecarats, F. Strub. (2008, June). Gas turbine performance increase using an air cooler with a phase change energy storage. *Applied Thermal Engineering*. [online]. Available: www.sciencedirect.com
- [52] G. P. Xu, Y. Q. Dai. (1997, April). Theoretical analysis and optimization of a double-effect parallel flow-type absorption chiller. *Applied Thermal Engineering*. [online]. Vol. 17. pp 157-170. Available: www.sciencedirect.com

- [53] G. P. Xu, Y. Q. Dai., K. W. Tou, C. P. Tso, (1996, Jan.). Theoretical analysis and optimization of series-flow-type absorption chiller. *Applied Thermal Engineering*. [online]. Vol. 16. pp 975-987. Available: www.sciencedirect.com
- [54] R. Tozer, A. Syed, G. Maidmen. (2005, Mar.). Extended temperature–entropy (T–s) diagrams for aqueous lithium bromide absorption refrigeration cycles. *International Journal of Refrigeration*. [online]. Vol. 28. pp 689–697. Available: www.sciencedirect.com
- [55] M. B. Arun, M. P. Maiya, S. S. Murthy. (2001, Dec.). Performance comparison of double effect parallel-flow and series flow water-lithium bromide absorption systems. *Applied Thermal Engineering*. [online]. Vol. 21. pp 1273-1279. Available: www.sciencedirect.com
- [56] G. A. Florides, S. A. Kalogirou, S. A. Tassou, L. C. Wrobel. (2003). Design and construction of a LiBr-water absorption machine. *Energy Conservation and Management*. [online]. Vol. 44. pp. 2483-2508. Available: www.sciencedirect.com
- [57] H. T. Chua, H. K. Toh, A. Malek, K. C. Ng, K. Srinivasan. (2000). Improved thermodynamic property fields of LiBr-water solution. *International Journal of Refrigeration*. [online]. Vol. 23. pp. 412-429. Available: www.sciencedirect.com
- [58] F. W. Yu, K. T. Chan. (2004). Advanced control of condensing temperature for enhancing the operating efficiency of air-cooled chillers. *Building and Environment*. [online]. Vol. 40. pp 727-737. Available: www.sciencedirect.com
- [59] K. T. Chan, F. W. Yu. (2002). Applying condensing-temperature control in air-cooled reciprocating water chillers for energy efficiency. *Applied Energy*. [online]. Vol. 72. pp 565-581. Available: www.sciencedirect.com
- [60] F. W. Yu, K. T. Chan (2008). Improved energy performance of air cooled centrifugal chillers with variable chilled water flow. *Energy Conservation. and management*. [online]. Vol. 49. pp 1595-1611. Available: www.sciencedirect.com
- [61] F. W. Yu, K. T. Chan (2007). Optimizing condenser fan control for air-cooled centrifugal chillers. *International Journal of Thermal Sciences*. [online]. Vol. 47. pp 942–953. Available: www.sciencedirect.com
- [62] F. W. Yu, K. T. Chan (2005). Tune up of the set point of condensing temperature for more Energy efficient air cooled chillers. *Energy Conservation and Management*. [online]. Vol. 47. pp 2499–2514. Available: www.sciencedirect.com
- [63] J. C. Kloppers, D. G. Kroger. (2005, Nov.). A critical investigation into the heat and mass transfer analysis of counter flow wet cooling towers. *International Journal of Heat and Mass transfer*. [online]. Vol. 48. pp 765-777. Available: www.sciencedirect.com
- [64] M. P. Maiya. (1995). Analysis of modified counter flow cooling towers. *Heat recovery systems and CHP*. [online]. Vol. 15. pp 293-303. Available: www.sciencedirect.com
- [65] J. U. Khan, M. Yaqub, S. M. Zubair. (2003). Performance characteristics of counter flow wet cooling towers. *Energy Conservation and Management*. [online]. Vol. 44. pp 2073-2091. Available: www.sciencedirect.com

- [66] F. Bosnjakovic, K. F. Knoche. (1998). Pinch analysis for cooling towers. *Energy Conservation Management*. [online]. Vol. 39. pp 1745-1752. Available: www.sciencedirect.com
- [67] J. C. Kloppers, D. G. Kroger. (2005, April). The Lewis factor and its influence on the performance prediction of wet-cooling towers. *International Journal of Thermal Sciences*. [online]. Vol. 44. pp. 879-884. Available: www.sciencedirect.com
- [68] M. Lemouari, M. Boumanza, I. M. Mujtaba. (2007, Oct.). Thermal performances investigation of a wet cooling tower. *Applied Thermal Engineering*. [online]. Vol. 27. pp.902-909. Available: www.sciencedirect.com
- [69] T. Maungnoi, W. Asvapoositkul, S. Wongwises. (2007, Oct.). An exergy analysis on the performance of a counter-flow wet cooling tower. *Applied Thermal Engineering*. [online]. Vol. 27. pp.910-917. Available: www.sciencedirect.com
- [70] R. Domanski, G. Fellah. (1998, April). Thermo-economic analysis of sensible heat, thermal energy storage systems. *Applied Thermal Engineering*. [online]. Vol. 18. No. 8. pp. 693-704. Available: www.sciencedirect.com
- [71] E. M. Alawadhi. (2008). Numerical analysis of a cool-thermal storage system with a thermal conductivity enhancer operating under a freezing condition. *Energy*. [online]. Vol. 33. pp 796–803. Available: www.sciencedirect.com
- [72] P. Neil. *Combined Heating, Cooling and Power Handbook, Technology and Approach to Energy Conservation, Resource Optimization*. Published, The Fairmount Press. Lilburn, USA, 2002
- [73] M. P. Boyce. *Gas Turbine Engineering Handbook*. Second Edition. Gulf Publishing Company Houston. USA, 2001
- [74] M. P. Boyce. *Gas Turbine Engineering Handbook*. Third Edition. Gulf Publishing Company Houston. USA, 2001
- [75] W. F. Stoeker. *Design of Thermal Systems*. Third Edition. McGraw Hill Publish. USA, 1976
- [76] J. M. Gordon, K. N. Choon. (1995, Oct.). A general thermodynamic model for absorption chillers, theory and experiment. *Heat Recovery Systems & CHP*. [online].Vol. 15. pp 73-83. Available: www.sciencedirect.com
- [77] S. K. Wang. *Handbook of Air Conditioning and Refrigeration*. Second Edition. Professional Publication, McGraw-Hill. New York, 1993
- [78] C. P. Arora. *Refrigeration and Air Conditioning*. Second Edition. Tata McGraw-Hill Publishing. USA, 2001
- [79] F. W. Yu, K. T. Chan. (2005). Modeling of the coefficient of performance of an air-cooled screw chiller with variable speed condenser fans. *Building and Environment*. [online]. Vol. 41 pp 407–417. Available: www.sciencedirect.com
- [80] L. Fu, G. Ding, Z. Su, G. Zhao. (2002). Steady state simulation of crew liquid chillers. *Applied Thermal Engineering*. [online]. Vol. 22. pp 1731-1748. Available: www.sciencedirect.com

- [81] F. C. McQuiston, J. D. Parker, J. D. Spittler. HVAC analysis and design. Sixth edition. Argosy publishing. Hamilton, USA, 2005
- [82] W. P. Jones. Air Conditioning Engineering. Fourth Edition. London, Great Britain, 1994
- [83] D. G. Kroger. Air-cooled Heat Exchangers and Cooling Tower. PennWell, Tulsa, Oklahoma, 2004
- [84] W. F. Stoecker, J. W. Jones. Refrigeration and Air Conditioning. Second Edition. McGraw-Hill Publishing. USA, 1982
- [85] A. Thumann, P. Mehta. Handbook of Energy Engineering. Fifth Edition. The Fairmount Press. Lilburn, USA, 2001
- [86] A. Y Cengel, A. M. Boles. Thermodynamics, An Engineering Approach. Sixth Edition. McGraw Hill Publish. USA, 2007
- [87] T. Giampaolo. The Gas Turbine Handbook, Principle and Practice. Second Edition. Publisher, the Fairmount Press. USA, 2002